PREPARATION AND CHARACTERIZATION OF WOUND DRESSING CONTACT LAYER

A Thesis Submitted to
the Graduate School of Engineering and Science of
Izmir Institute of Technology
in Partial Fulfillment of the Requirements for the Degree of

DOCTOR OF PHILOSOPHY

in Bioengineering

by
İpek ERDOĞAN

July 2015
İZMİR

We approve the thesis of **İpek ERDOĞAN**

Examining Committee Members:

Prof. Dr. Oğuz BAYRAKTAR
Department of Chemical Engineering, Ege University

Assoc. Prof. Dr. Ali ÇAĞIR
Department of Chemistry, Izmir Institute of Technology

Assist. Prof. Dr. Mehmet ATEŞ
Institute of Health Sciences, Dokuz Eylül University

Assist. Prof. Dr. Ayşegül BATIGÜN
Department of Chemical Engineering, Izmir Institute of Technology

Assist. Prof. Dr. Uğur TÜRKAN
Department of Biomedical Engineering, Gediz University

28 July 2015

Prof. Dr. Oğuz BAYRAKTAR
Supervisor, Department of
Chemical Engineering
Ege University

Prof. Dr. Atay ATABEY
Co-Supervisor, Department of
Plastic and Reconstructive Surgery
Dokuz Eylul University

Assoc. Prof. Dr. Güldemet BAŞAL
Co-Supervisor, Department of
Textile Engineering
Ege University

Prof. Dr. Volga BULMUŞ
Head of the Department of
Biotechnology and Bioengineering

Prof. Dr. Bilge KARAÇALI
Dean of the Graduated School of
Engineering and Sciences

ACKNOWLEDGMENTS

Firstly, I would like to express my deep and sincere gratitude to my advisor Prof. Dr. Oğuz BAYRAKTAR for his suggestions, guidance, encouragement and support throughout my Ph.D. study. I also would like to thank him for his generosity for providing materials and laboratory facilities.

I warmly express my special thanks to my co-workers, Mehmet Emin USLU, Ceren SÜNGÜÇ, Özge TÜNCEL ÇERİK, Sedef TAMBURACI, Seda GÜNEŞ, Esra AYDINLIOĞLU and Damla TAYKOZ for their support, help, patience and friendship.

I want to express special thanks to my family for their love, encouragement, patience and support during my education.

ABSTRACT

PREPARATION AND CHARACTERIZATION OF WOUND DRESSING CONTACT LAYER

Wound dressings provide therapeutic and protective features and promotes natural healing process when applied to a wound area. Being non-toxic and immunologically inert, natural biopolymers have potential in fabrication of wound dressings. Growth factors and antibiotics can also be used in functionalization of wound dressings as well as plant extracts. Olive leaf extract has gained attraction due to its dual antimicrobial and antioxidant effect. By clearing pathogenic microorganisms and scavenging against increased amount of reactive oxygen species in the wound area, it has high potential in wound healing. In this study, olive leaf extract incorporated zein fibers were prepared as a model of wound dressing contact layer. In this regard, crude olive leaf extract was fractionated and characterized in terms of antioxidant capacity, total phenol content and antimicrobial activity. Crude extract and its fractions were also subjected to wound scratch assay in the presence of hydrogen peroxide. Oleuropein, as the most abundant component in crude extract, was found to promote cell migration better and close the wound area at a higher rate than other components. On the other hand, crude olive leaf extract exhibited higher percentage of wound closure than its fractions within the same time period, which may be attributed to synergistic effect of unidentified phenolics. Crude olive leaf extract also provided crosslinking effect when incorporated into zein fibers, as well as promoting cell spreading behaviour.

ÖZET

YARA ÖRTÜSÜ TEMAS YÜZEYİ HAZIRLANMASI VE KARAKTERİZASYONU

Yara örtüleri terapötik ve koruyucu özelliklere sahip olup, yara bölgesine uygulandığında doğal iyileşme sürecini destekleyici görev yapmaktadırlar. Toksik olmamaları ve immunolojik bir reaksiyon yaratmamaları bakımından doğal polimerlerin yara örtüsü olarak kullanım potansiyelleri bulunmaktadır. Yara örtülerinin fonksiyonel hale getirilmesinde büyüme faktörleri ve antibiyotiklerin yanısıra bitki özütleri de kullanılmaktadır. Zeytin yaprağı özütü sahip olduğu ikili antimikrobiyal ve antioksidan etkisi sayesinde ilgi görmektedir. Yara bölgesindeki patojen mikroorganizmaların temizlenmesi ve artan miktardaki reaktif oksijen türlerinin süpürülmesinde rol oynaması nedeniyle yara iyileşmesinde önemli bir potansiyele sahiptir. Bu çalışmanın içeriğini bir yara örtüsü temas yüzeyi modeli olarak zeytin yaprağı özütü içerikli zein fiberlerinin hazırlanması oluşturmaktadır. Bu bağlamda, ham zeytin yaprağı özütü fraksiyonlanmış ve antioksidan kapasite, toplam fenol içeriği ve antimikrobiyal aktivitesi bakımından karakterize edilmiştir. Ham özüt ve fraksiyonları hidrojen peroksit varlığında yara modeli oluşturma çalışmalarında da kullanılmışlardır. Ham özüt içerisinde en yüksek miktarda bulunan oleuropeinin hücre göçünü en iyi destekleyen bileşen olduğu ve diğer bileşenlere oranla yara kapanmasını hızlandırdığı ortaya çıkarılmıştır. Diğer taraftan fraksiyonlanmamış ham özütün fraksiyonlarla karşılaştırıldığında hücre göçünü hızlandırdığı ve aynı zaman diliminde daha yüksek oranda yara kapanmasını sağladığı gözlenmiştir. Bu durumun özüt içinde bulunan tanımlanmamış fenolik bileşiklerin sinerjik etki göstermesine bağlı olduğu düşünülmektedir. Ham zeytin yaprağı özütü aynı zamanda zein fiberlere eklendiği zaman çapraz bağlama etkisi sağlamakta ve hücre yayılımına imkan sağlamaktadır.

TABLE OF CONTENTS

LIST OF FIGURES

Figure **Page**

LIST OF TABLES

Table **Page**

CHAPTER 1

INTRODUCTION

Wound dressing is the material that provides therapeutic and protective features when applied to a wound area. These key features also explain the function of wound dressing as promoting natural healing process. Throughout the years, people applied folk medicines like crude plant herbs, animal fat, honey, gums of the trees to heal their wounds and the development in this area has now reached to tissue engineered scaffolds and wound dressing contact layer materials which skin substitute can also be used to refer. Biocompatilibity, uniform composition and functionalization by active molecules to promote cell proliferation in order to accelarate healing, determine the efficiency in utilization of a skin substitute (Schneider et al., 2009). Challenge among various materials formed by natural and synthetic compounds focuses on question of biocompatibility, mechanical property and biofunctionalization. The material itself should be non-toxic to cells in wound area and should not cause immunogenicity, in this aspect natural biopolymers have more potential to be used in fabrication of wound dressing. Functionalization property can be gained by incorporation of growth factors, antimicrobial and antioxidant agents.

Wound area is exposed to circulatory ischemia and reperfusion, referring inadequate oxygen delivery to wound area and sudden blood flow after a period of ischemia. Presence of highly concentrated bacteria in wound area induce leukocyte migration because of inflammation and increase in amount of proteases and oxidative enzymes. Oxidative enzymes specifically causes death of bacteria but they can not work efficiently because of topical anemia and resulting hypoxia, so bacteria proliferate by using non-vital tissue as nutrient source. Wound healing process is ceased by prevention of cell migration required for wound closure due to high protease activity and degredation of extracellular matrix. The most common bacteria has been found as *Staphylococcus aureus* and *Pseudomonas aeruginosa* in chronic leg ulcers. *Streptococcus* species, *Proteus* species, *Escherichia coli*, *Klebsiella* and *Citrobacter* species are also the most common isolates in pressure ulcers (O'Meara et al., 2000). In reperfusion period, sudden flow of blood to wound area results in inflammation and oxidative damage through the induction of oxidative stress rather than restoration of

normal function. Wound dressing fabricated by natural biopolymers and functionalized by a compound having double effect as antioxidant and antimicrobial activity can be a suggestion to healing issue of wounds. In this study, the objective is to fabricate wound dressing contact layer by using natural biopolymer, zein and functionalize this material by olive leaf extract.

Zein, has been used in the food industry as a coating material (Shukla and Cheryan, 2001) which was also shown as a carrier to protect drugs from stomach acid in form of microsphere (Mathiowitz et al., 1993). Zein possesses the additional benefits of being renewable and biodegradable. Zein microspheres have also been investigated for use as carriers to protect drugs from stomach acid. Dong et al. (2004) reported that zein films exhibited very good ability to proliferate both human liver cells and murine fibroblast cells. These findings suggested that zein was a promising biomaterial with good biocompatibility.

It is known that olive leaf (*Olea europaea*) has been used as folk medicine in Mediteranean coasts of Europe for hundreds of years. Visioli et al. (1998) has shown that olive leaf is a free radical scavenger, besides its antioxidant property due to its composition of phenolic compounds such as oleuropein and hydroxytyrosol. Olive leaf may have therapeutic potential in cancer, heart diseases, atherosclerosis, rheumatoid arthritis and neurodegenerative diseases related with oxidative stress due to increase in reactive oxygen species. Markin et al. (2003) also performed a study revealing that olive leaf has antimicrobial and antifungal activity. This combined antimicrobial effect may be beneficial in preventing opportunistic infections after long term usage of antibiotics. Olive leaf has antimicrobial effect against resistance species such as *Klebsiella* and *Pseudomonas*, besides *Escherichia coli* and *Candida Albicans.* By means of this, olive leaf clears pathogenic microorganisms as having antimicrobial effect and have scavenging activity against increased amount of reactive oxygen species so prevents cytotoxicity. Owing to its antioxidant and antimicrobial properties, olive leaf extract has potential to provide wound healing.

Fabrication of zein fibers by electrospinning and biofunctionalization the fibers by olive leaf extract is the main objective of this study. Electrospinning conditions and blending ratios of zein were optimized to obtain high mechanical properties and enlarged surface area to provide optimum material transport and enhanced cell spread. Olive leaf extract was incorporated to functionalize the fibers owing to its antimicrobial and antioxidant properties. Release properties of the material and sustainability of

extract efficiency in terms of antimicrobial, antioxidant properties and amount of polyphenolic compounds were also investigated by mimicking the wound area in flow-cell conditions besides cytotoxicity analysis and cell spread observation through the dressing material. Investigation of wound healing properties of olive leaf extract was also aimed during the study, in order to reveal its potential in cell migration. Crude extract was fractionated and analysed by means of composition and scavenging capacity against oxidative stress. Cytotoxic profile and wound healing properties were also investigated in order to determine if the effect was fraction specific or synergy of the fractions played a role in its wound healing potential.

CHAPTER 2

LITERATURE REVIEW

2.1 Wound stages and wound dressings

2.1.1 Skin components

A wound can be described as a defect or a break in the skin, resulting from physical or thermal damage or as a result of the presence of an underlying medical or physiological condition.

Skin, as being the largest and most highly complex organ in the human body, corresponds to one-tenth of the body mass and has a surface area of 1.5–2 m^2. Skin has role in providing thermal regulation, preventing dehydration by evaporative water loss and acts as a barrier against chemical and infectious agents (Balasubramani et al., 2001). It is composed of three layers as epidermis, dermis and hypodermis. Epidermis is made up of cells and thick enough to provide vital barrier which has a continuous process of proliferation, maturation and death of cells. This layer is divided into strata composed of keratinocytes in different maturation stages. Dermis strengthens the skin by collagen fibers, which is woven with elastin fibers, proteoglycans, glycosoaminoglycans (GAGs) dominantly hyaluronic acid and dermatan sulfate with some chondroitin-6-sulphate and heparin sulphate, fibronectin and other components that constitutes extracellular matrix (ECM) (Ramos-Silva and Castro, 2002, Matthews et al., 2002). Complexity of this environment influence phenotypic and other cellular behavior by providing indirect and direct informational signaling cues for cellular organization, survival and function. Fibroblasts are distributed through ECM, adhering to collagen fibers, blood and lymph vessels and nerve endings. Any significant loss of dermis layer distorts the skin by producing a scar tissue. There is also hypodermis, lying beneath the dermis layer and composed of adipose tissue that has role in mechanical and thermal insulation (Ramos-Silva and Castro, 2002).

2.1.2 Wound healing process

Damage of a part of skin has critical consequences due to its large area. According to the Wound Healing Society, a wound is the result of disruption of normal anatomic structure and function (Boateng et al., 2008). Wound healing involves different cell types and their response to environmental signals through informational signaling cues driven by matrix components aforementioned. Cells synthesize necessary proteins for proliferation and migration in a phased manner (Balasubramani et al., 2001).

Wound repair has three stages as inflammation, new tissue formation, and remodelling (Gurtner et al., 2008). Inflammation occurs immediately after tissue damage as the first stage, immune system is alarmed to prevent blood and body fluid losses, to remove non-vital tissues and prevent infection. Platelet plug and fibrin matrix structure together forms a scaffold for infiltrating cells, haemostasis is achieved.

New tissue formation is the second stage of wound repair and occurs 2-10 days after injury. Cellular proliferation and migration are dominant at this stage. Firstly keratinocytes migrate over the injury site and new blood vessels are formed termed as angiogenesis. Fibrin matrix formed at the first stage is replaced by capillaries associated with fibroblasts and macrophages. This layer functions as a substrate for keratinocyte migration which restore epitelium and regain its barrier property at later stages. Vascular endothelial growth factor and fibroblast growth factor 2 are positive regulators of angiogenesis. Fibroblasts are differentiated into myoblasts which are contractile and close the wound by bringing the edges together by producing extracellular matrix together with fibroblasts.

Remodelling is the last and longest step in wound healing that begins after 2 or 3 weeks of injury. During the stage, most of the endothelial cells, macrophages and myofibroblasts undergo apoptosis, while leaving behind a few cells and pieces of extracellular matrix proteins. Epithelial-mesenchymal interactions continue to regulate skin integrity with the aid of additional feedback loops. During a year, fibroblasts, macrophages and endothelial cells secrete matrix metalloproteinases to strengthen the repaired tissue by remodelling acellular matrix composed of collagen type I (Figure 2.1)

Wounds can be classified as acute or chronic wounds due to repair process. Acute wounds arise from external factors such as friction, cuts, burns and chemical injuries. Chronic wounds fail to heal because of repeated tissue insults or underlying

physiological conditions such as diabetes and malignancies, persistent infections. They are divided into three main categories as pressure sores, diabetic ulcers and venous ulcers, also a small group which involves ulcers developed due to ischemia-local anaemia (Mustoe T, 2004). During wound healing process, cellular and matrix components act together to reestablish the integrity of damaged tissue and regenerate epidermis. Fibroblasts distributed through ECM contribute to wound healing process by secreting collagenase and other proteases to remodel collagen located inside (Ramos-Silva and Castro, 2002). Closure of the wound by epitelial cells is the most important step in healing as it protects underlying tissue by the epidermal barrier formation. Normal wound healing begins with controlled proliferation and migration of keratinocytes from the wound edge. This process is followed by proliferation of dermal fibroblasts in the neighborhood of the wound. The reason for chronic wounds in pathological conditions, such as diabetes, arises from absence of reepitalization (Schneider et al., 2009). This problem leads to non-healing wounds. Chronic wounds especially diabetic ulcers are also characterized by their tendency to to become heavily colonized with bacterial, and sometimes fungal, organisms termed as bioburden or bacterial burden (Falanga, 2004). Combination of bacteria attract leukocytes to wound area and result in a high-protease, high-oxidant environment (Mustoe T, 2004). Oxidant-producing enzymes are specific for bacteria killing but their activity is proportional to amount of oxygen in the wound area. Because these enzymes cannot work in case of ischemia and resulting hypoxia, bacterial count arises using the protein extrude and nonviable tissues as nutrient. High protease activity as a result of leukocyte migration degrades extracellular matrix and prevents wound closure by inhibiting cell migration. The most common bacteria has been found as *Staphylococcus aureus* and *Pseudomonas aeruginosa* in chronic leg ulcers. *Streptococcus* species, *Proteus* species, *Escherichia coli, Klebsiella* and *Citrobacter* species are also the most common isolates in pressure ulcers (O'Meara et al., 2000).

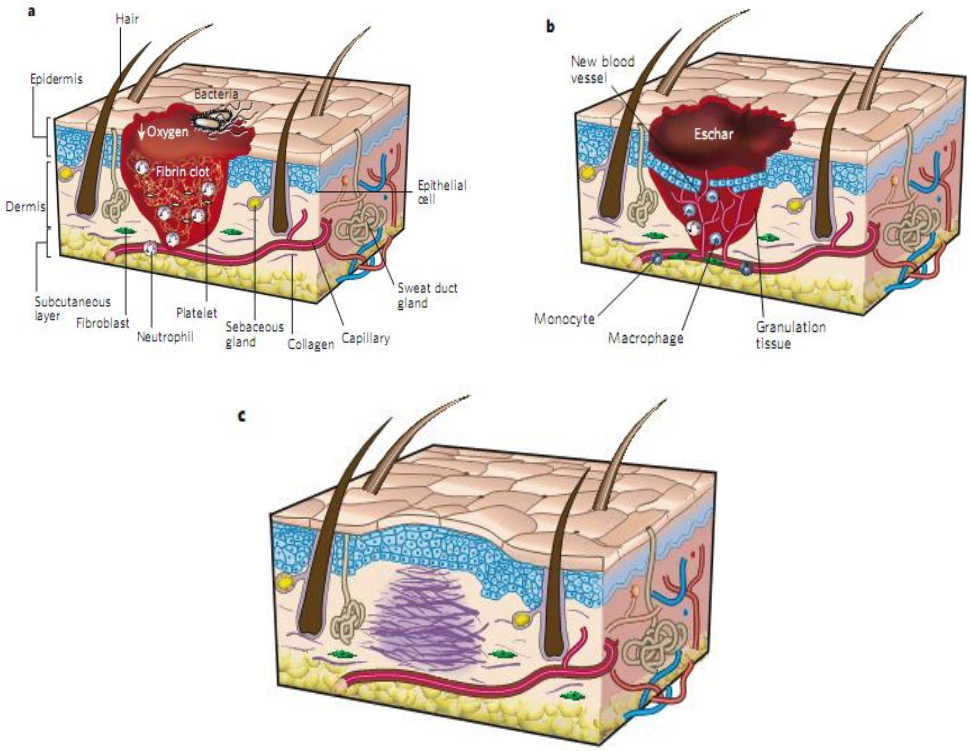

Figure 2.1. Classic stages of wound repair. (a) inflammation (b) new tissue formation (c) remodelling (Source: Gurtner et al., 2008).

Wound healing process depends on type of wounds, extent and depth of lesion, factors like nutritional status, age, systemic disease and medication that individual uses specifically. Cases like deep partial thickness and full thickness burns give rise to scar tissue formation because dermis repairs itself by granulation tissue formation. Scar tissue does not contain elastic fibers and is populated with myofibroblasts which are intermediate between fibroblasts and smooth muscle cells. Basement membrane complex is slowly established therefore complications like blistering and deformation on skin surface and contraction of muscles due to fibrosis. General researches on wound healing process focuses on three principles (Balasubramani et al., 2001)

1. Improvement of wound healing by factors which speed up the process and reduce scarring.

2. Design and development of skin substitutes mimicking functionality and morphology of autograft skin.

3. Identifying cues that induce the skin to heal by regeneration rather than repair to eliminate scarring.

Dermal substitutes constitute key components of contemporary treatment which stimulates wound healing process by delivering a living human dermal matrix to the debrided wound bed (Sibbald et al., 2005).

2.1.3 Wound Dressings

Wound dressings have developed over the years from the crude applications of plant herbs, animal fat and honey to tissue engineered scaffolds. Wound dressings can be produced from synthetic and biological materials. Synthetic dressings are suitable for superficial and small-sized wounds. Composite synthetic dressings, as a subgroup, are composed of outer layer designed for durability and inner layer for maximum adherence and elasticity. Biological dressings include allograft, heterograft from pigs, amniotic membranes and films, sponges and fibers from natural polymers. Allografts from cadavers and heterografts carry the risk of contamination and rejection unless applied with immunosupressents, therefore natural polymeric based materials are candidate to be used as wound dressings. Biocompatilibity, uniformity in composition, and standardized evaluation determine the effiency in utilization of a skin substitute. Modifications applied on cellular biopolymer and biomolecular composition during preparation procedure promote epithelization and vascularization in order to minimize inflammatory responses and rejection. Wound dressings are classified due to their compositions (Balasubramani et al., 2001). Class I consists of cultured epidermal equivalent, class II includes dermal components as collagen and matrix proteins and class III is a combination of dermal and epidermal components, also referred as composite skin (Ramos-Silva and Castro, 2002, Zhong et al., 2010).

Ideal wound dressing should (Purser K, 2010);

1. Provide an optimum environment for moist wound healing. Eschar formation is observed in dried wounds which forces epidermal cells to move deeper, prolonging healing process

2. Allow gaseous exchange of oxygen, carbon dioxide and water vapour to provide epithelial cell division in order to aid healing

3. Provide thermal insulation to maintain optimum temperature for cell regeneration which is 37ºC by preventing wound bed from cooling

4. Impermeable to micro-organisms to prevent delayed healing process

5. Free from particulate contaminants to decrease infection risk

6. Non-adherent as adherent dressing removal causes pain and disrupt the newly organised tissue, also capillaries may be damaged

7. Safe to use which means non toxic, non sensitizing and non-allergenic, to prevent sensitivities due to content of dressings

8. Be acceptable to the patient

9. High absorption properties for highly exuding wounds in initial stage

10. Cost effectiveness including fast healing rate, short wear time and total material cost

11. Allow monitoring of the wound without disturbance

12. Provide mechanical protection against trauma, bacterial invasion, UV radiation

13. Be non-inflammable

14. Be sterile to protect cross contamination

15. Be available

16. Long wear time provides fewer change which results in low infection risk, stability in wound bed temperature and less disturbance of patient.

It should also promote reepithelization by delivering specific, active molecules (Schneider et al., 2009). Challange among various membranes formed by natural and synthetic compounds focuses on question of biocompatibility, mechanical property and biofunctionalization.

Wound dressings are sorted from traditional gauzes to hydrocolloids, alginates, hydrogels, polyurethane, collagen, chitosan, pectin and hyaluronic acid dressings used for wound care and delivery of drugs to acute, chronic and other types of wound (Table 1) (Purser, 2010). Antimicrobial agents such as silver, povidone-iodine and polyhexamethylene biguanide are sometimes incorporated into dressings to control or prevent infection. Herbal extracts of olive leaf, chlorophyll, gum arabic and labdene-type diterpenes have also been characterized as antimicrobial and antioxidant materials that can be loaded on wound dressings.

Table 2.1. Wound dressing materials

Material	**Origin**	**Morphological feature**	**Advantages**	**Pitfalls**
Gauze pads	Cotton	Non-woven fibers	Allows air to circulate around the site, promoting rapid healing	Non-adherent, temporary wound care
Hydrocolloid	Gelatin, pectin	Adhesive, gel forming	Waterproof	Odourous, not suitable for heavily exuding wounds
Hydrogels	Silk fibroin, chitosan	Amorphous, water based	Re-hydrate dry necrotic tissue, create moisture	Requires a secondary dressing
Alginate	Alginic acid	Soft, flexible gel	Provide moist healing environment, also functions as haemostatic agent	Should be changed daliy in case of diabetic wounds, not applicable on dry wounds because of adherence
Hydrofibre	Sodium carboxymethy cellulose	Soft, non-woven, flat dressing	More adsorbent than alginates, needs reduced number of changes	Should be used in heavily exuding wounds to prevent adherence
Foam (sponge)	Silk fibroin, collagen	Porous structure	Allows cell proliferation when used as scaffold, easy diffusion of nutrients and waste materials	Needs organic solvent treatment or crosslinking agents to be stabilized
Nanofiber	PVA, collagen, chitin, silk fibroin	Non-woven structure	High suface area	Organic solvents may be used due to polymer origin

2.2 Nanofiber properties and fabrication techniques

Nanofibers have received much attention, besides materials like hydrogels and films because they are potential candidates for the applications where high specific surface areas are required. As they have ultra-fine pore structure, they provide controlled evaporative water loss, excellent oxygen permeability, promotion of fluid drainage, and inhibition of exogenous microorganism invasion (Schneider et al., 2009). Furthermore, fiber surface can be modified with specific functions such as enhanced aqueous solubility, biocompatibility, and bio-recognition (Zhang et al., 2005). Also polymer nanofibrous structures usually provide superior hydrophobic property because an effective contact angle increases with decrease in fiber diameter. Fiber structure can also be functionalized by incorporation of bioactive molecules that retain signaling to accelerate wound healing process, integration of bone morphogenic protein-2 (BMP-2) for bone formation and epidermal growth factor (EGF) in wound healing process can be given as example (Schneider et al., 2009). Overall, wound dressings should have the ability to release initiator molecules while it provides sterility against infection as covering the wound site (Ramos-Silva and Castro, 2002). Methods of nanofiber functionalization and samples from studies will be mentioned above in detail.

Several fabrication techniques such as electrospinning, melt-blown, phase separation, self-assembly, and template synthesis have been employed to produce suitable polymer nanofibers. Among them electrospinning is the most popular and preferred technique due to its easiness, low-cost, wide application area from polymers to ceramics and it can be developed for large scale production of continuous nanofibers for industrial applications. As the diameter of polymer fibers gets smaller from micrometers to nanometers, surface area gets larger.

2.2.1 Electrospinning

Electrospinning refers to fabrication process that collect continous polymer fibers, diameter ranging from microns to nanometers, by using an electric field (Matthews et al., 2002). System consists of a syringe pump, a high voltage source, and a collector (Figure 2.2). During the process polymer solution is held at a needle tip by surface tension. When electric field is applied using high voltage source, polymer

solution is induced and charge imbalance occurs which overcomes the surface tension at a critical voltage and forms an electrically charged jet. While this electrically charged jet is directed and collected at a target, solvent evaporates and continous fibers are formed (Pham et al., 2006, Chakraborty et al., 2009).

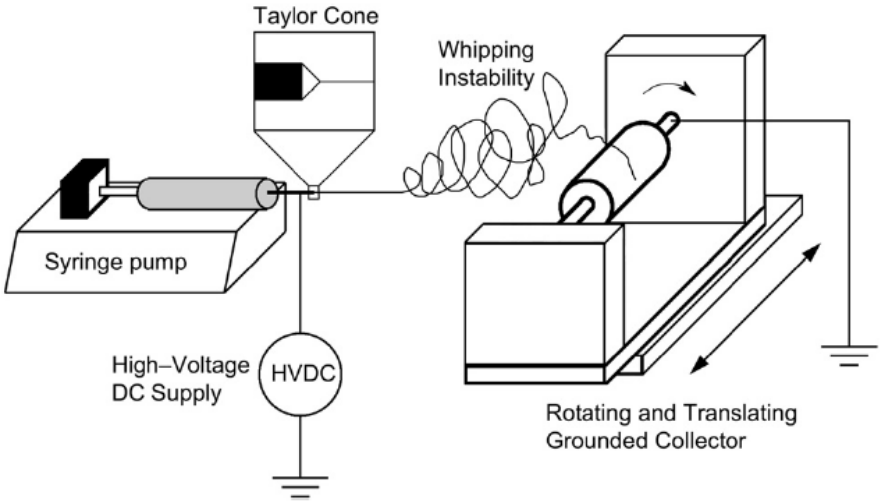

Figure 2.2. Electrospinning process, set up and components
(Source: Sill and von Recum, 2008)

Factors affecting electrospinning process can be divided into three groups

1. Substrate and solution related parameters, such as the chemistry, molecular weight and molecular weight distribution of the polymer, rheological properties of the solution such as concentration, viscosity, elasticity, conductivity, surface tension (Zhang et al., 2009). The types of polymer that can be electrospun is classified by their hydrophilicity. Hydrophilic polymers as polysaccharides or extracellular matrix proteins as collagen and hyaluronic acid are electrospun into fibers by dissolving the polymers in water, strong acids or a mixture of water and polar organic solvents. Viscosity and surface tension of the solution is affected by changes in polymer concentration and molecular weight and these parameters influence the electrospun product. In case of low viscosity, droplet formation occurs. (Chakraborty et al., 2009, Wang et al., 2006).

2. Process related controlled parameters, such as hydrostatic pressure in the capillary tube, applied electrical potential, flow rate of the solution, distance from tip to collector, needle tip design, and collector composition and geometry

3. Environment related parameters, such as temperature, humidity and air velocity in the electrospinning chamber (Zhang et al., 2009).

Electrospun fiber diameter is one of the parameters that affects their end use (Amiraliyan et al., 2009). Fiber diameter is related with the jet size, elongation of the jet, and evaporation rate of the solvent. Elasticity of the fluid determines the nanofiber morphology. Elongation of the jet and evaporation of the fluid together change the shape and the charge per unit area carried by the jet. Polymer skin formed on the liquid jet also affect the morphology. Koombhongse et al.. (2001) explained that after the skin is formed, the solvent inside the jet escapes and the atmospheric pressure tends to collapse the tube like jet. The circular cross section becomes elliptical and then flat, forming a ribbonlike structure. Shape and continuty of the fibers are also related with the amount of molecular chain entanglements in the polymer solution. Sufficient molecular entanglement can prevent the polymer jet breakup, allow the electrostatic stresses to further elongate the jet and draw it into fibers (Wang et al., 2006).

2.2.2 Natural nanofibers

The use of polymer nanofibers for biomedical and biotechnological applications has some intrinsic advantages. Natural biomaterials are deposited in fibrous forms or structures. including silk, keratin, collagen, viral spike proteins, tubulin and actin, polysaccharide cellulose and chitin which are characterized by well-organized hierarchical fibrous structures down to a nanometer scale (Zhang et al., 2005). With this understanding polymer nanofibers can mimic biological structures such as native extracellular matrix and are therefore considered as promising tissue engineering scaffolds. Morphological similarity with native tissue is the key to better engineer an artificial tissue (Zhang et al., 2005). They are used as temporary templates for cell seeding, invasion, proliferation and differentiation prior to the regeneration of biologically functional tissue or natural extracellular matrix (ECM).

Nanofibrous 3D scaffolds have high porosities and surface-area-to-volume ratios that makes it suitable for cellular adhesion and proliferation. 3D scaffold environment is more like in vivo and influences diffusion and adhesion of proteins, growth factors, and enzymes, which ensures cell viability and can influence function (Nisbet et al., 2009). Also engineered scaffold must meet the criteria of biocompatilibility, support the tissue held within, maintaining the normal state of differentiation in the cellular compartment and being resorbable (Pham et al., 2006).

2.2.2.1 Collagen

As collagen type I and type III are the principal structural elements of the extracellular matrix, it has widely been used in tissue engineering applications, providing support to connective tissues such as skin, tendons, bones, cartilage, blood vessels, and ligaments and interacting with connective tissue, having a role as transducer for the regulation of cell anchorage, migration, proliferation, differentiation, and survival (Malafaya et al., 2007). The collagen nanofibers were characterized by a wide range of pore size distribution, high porosity, excellent mechanical strength, and high surface area-to-volume ratios, which are favorable parameters for cell attachment, growth, and proliferation. These properties make collagen ideal for biomedical applications, such as wound dressing and scaffolds for tissue engineering. On the other hand collagen has limitations as high swelling degree which decreases its porosity and structural integrity in an aqueous environment such as in the human body. Its rate of degredation is also hard to control and nearly all sterilization methods alter properties of collagen at some degree (Yeo et al., 2008). Collagen-based scaffold or dressing often has poor biostability and low mechanical properties and wound contraction easily occurs (Zhong et al., 2010). However, the combination of collagen with biocompatible polymers such as ECM, GAGs, chitosan, polycaprolactone (PCL), and *poly(lactic-co-glycolic acid)* (PLGA) are used to increase mechanical properties by forming intra- and interchain bridges within collagen molecules with or without external crosslinking agents. Therefore the more mechanical properties increase, the longer the clinical durability of the graft. Besides, integration of ECM components has an important role in cell guidance through wound healing and enhancement of biological interactions with cells speeds up tissue regeneration.

2.2.2.2 Silk fibroin

Silk fibroin (SF) is one candidate for this combination with its biocompatibility, biodegradability, and minimal inflammatory reactions. SF matrices are useful for culturing fibroblasts, osteoblasts, and stem cells as they enhance the adhesion, growth, and differentiation of cells in a manner similar to collagen matrices. What the silkworm Bombyx mori produces to weave the cocoon is silk, which has the fibroin and sericin as

the components. Fibroin is a fibrous protein constituting the core of silk, while sericin is a glue-like protein surrounding fibroin.

The physiological properties of silk fibroin matrices strongly depend on molecular conformation and surface texture. SF consists of heavy (H) and light (L) chain polypeptides of ~390 kDa and ~26 kDa, respectively, linked by a disulfide bond at the C-terminus of the two subunits, and associates with the H-L complex primarily by hydrophobic interactions. Silk fibroin has three crystalline forms: silk I, silk II, and alpha-helix which can interchange to each other under certain conditions (Min et al., 2004). Silk I refers to random coil structure and silk II is the more stable, crystalline β-sheet conformation. β-sheets are formed through hydrogen bonding and hydrophobic interactions, forming the basis for the tensile strength of SF (Zhang et al., 2009). Convertion from random coil to β -sheet is accomplished by simple physical (thermal), mechanical or chemical treatments among which methanol aqueous solution treatment is the most common method. Temperature increase has two effects. Firstly water structure decreases and results in decreasing the solvation of hydrophobic regions of protein. Second, protein is unfolded and hydrophobic regions are more exposed to water, encouraging aggregation. Organic solvents affect the solubility of proteins in water because charged and ionic residues tend to be less solved by solvents with lower dielectric solvents (Hardy et al., 2008). Ethanol and methanol treatment promote β – sheet formation due to dehydration of α helices. Treated SF matrices are often brittle due to their high content of crystalline regions (Yeo et al., 2008).

2.2.2.3 Chitin

Chitin is another biopolymer that is blended with silk fibroin and used as wound dressing. The chitin/silk fibroin blends at varied ratios were electrospun into nanofibrous matrices and evaluated for initial cell attachment and spreading. Optimal ratio for spreading of keratinocytes and fibroblasts was determined as 75% chitin and 25% silk fibroin (Zhang et al., 2009).

Chitin is the principal structural polysaccharide of arthropods and is the second most abundant polysaccharide after cellulose. Due to its poor solubility, attention is paid to chitosan, deacetylated form of chitin. Chitin and chitosan are candidates for biomedical applications due to their good biocompatibility, biodegradability and wound

healing effects (Kweon et al., 2003). As chitin has structural characteristics similar to glycosaminoglycans, such as chondroitin sulfates and hyaluronic acid, in the ECM, it could be have potential itself or coated with collagen type I, for cell attachment and spreading of normal human keratinocytes and fibroblasts that is especially useful for wound healing and regeneration of the oral mucosa and skin. Chitosan also can stimulate collagen synthesis but as a disadvantage, it has rapid biodegradability especially in acid environment that is often formed in wound healing. Severe shrinkage and deformation after drying can be listed as other pitfalls. Crosslinking treatments can be applied to increase structural stability (Zhong et al., 2010).

2.2.2.4 Hyaluronic acid

Hyaluronic acid (HA), also known as hyaluronan is a natural non-sulfated glycosaminoglycan and a component of the intercellular matrix of most connective tissues such as cartilage, vitreous of the human eye, umbilical cord and synovial fluid (Malafaya et al., 2007). It can also be produced in large scales through microbial fermentation, from strains of bacteria such as *Streptococci*. Hyaluronan forms the backbone for the organization of proteoglycans as an integral part of ECM. It consists of repeating disaccharide units of D-glucuronic acid and N-acetyl-D-glucosamine with a molecular weight range from 103 to 107.

Hyaluronan has many physiological roles such as tissue and matrix water regulation, structural and space-filling properties and especially lubrication due to its enhanced viscoelastic properties. It works as molecular filter, shock absorber, and support structure for collagen fibrils. As an early response to tissue injury, hyaluronan-rich matrix is formed to support influx of fibroblasts and endothelial cells into the wound site and subsequent formation of granulation tissue (Chen et al., 1999).

Hyaluronan has been widely studied for drug delivery, for dermal, nasal, pulmonary, parenteral, liposome-modified, implantable delivery devices and for gene delivery (Um et al., 2004, Bölgen et al., 2006). Hyaluronan also serves as a scavenger of free radicals and as an antioxidant. These functions of hyaluronan may be particularly important in skin physiology, as a protectant against solar radiation (Chen et al., 1999).

Hydrophilic and polyanionic characteristic of hyaluronan gives rise to a major problem by not favoring cell attachment and tissue formation (Ji et al., 2006). One way

to improve cell attachment has been found as coating extracelluar matrix (ECM) proteins such as type I collagen and fibronectin (FN) onto HA biomaterials or covalently linking fibronectin functional domains (FNfds) to the HA backbone. Fabrication of an HA microporous scaffold which serves to direct the growth of cells within the scaffold by solvent casting and lyophilization has been developed as another method.

HA also attracts great interest in electrospinning but high viscosity even at very low concentrations and high surface tension is a major drawback in this process. One solution may be crosslinking treatment (Ji et al., 2006, Um et al., 2004).

2.2.2.5 Zein

Zein is the prolamine, comprimising 60% of protein content in corn and consisting of one-third hydrophilic and two-thirds hydrophobic amino acid residues in its primary structure (Figure 2.3) (Zhang et al., 2010). Glutamic acid, leucine, proline and alanine comprise amino acid composition of zein and absence of basic and acidic amino acids results in solubility behaviour of zein in aqueous alcohol solutions (Shukla and Cheryan, 2001).

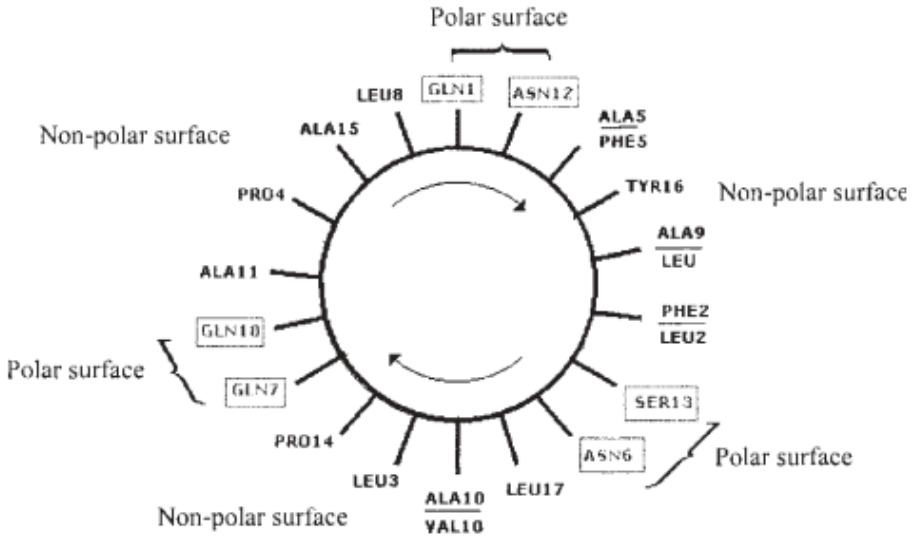

Figure 2.3. Polar and non-polar regions of zein
(Source: Corradini et al., 2004)

Zein utilization is dominant in food packaging and coating as well as pharmaceutical industry due to its biodegradability and hydrophobicity (Miyoshi et al., 2005). Liu et al (2005) performed a study that used zein microspheres for drug targeting and overcome the disadvantage of hydrophilicity by using a hydrophobic protein. The model drug they chose was ivermectin which is an effective parasiticide. Gong et al (2006) presented a study developing porous zein scaffold for bone substitution. Final product had displayed good mechanical properties and degradation behaviour. Also mesenchymal stem cells were seeded on the scaffold and they demonstrated succesful adhesion, growth and proliferation.

Edible films made of carbohydrates, lipids and proteins are commonly used in packaging industry. Protein films have better tensile properties and perform as oxygen barriers (Ghanbarzadeh et al., 2008). Zein has great potential in film casting due to its hydrophobicity and thermoplastic behaviour. Film is usually formed through hydrophobic, hydrogen and disulfide bonds between zein chains (Bourtoom, 2008). As zein is dissolved in ethanol, films have brittle characteristics and tendency to break. Their mechanical properties and water vapour barrier feature can be improved by crosslinking agents. Parris et al (1997) performed a study using a series of agents as crosslinker in zein films, they used formaldehyde, glutaraldehyde, epichlorohydrin, citric acid and 1,2,3,4- butanetetracarboxylic acid based on zein content. All films performed higher tensile strength than control, formaldehyde as the highest. They had

also used polymeric dialdehyde starch as an alternative to formaldehyde due to toxicity and had moderate tensile strength. Glutaraldehyde is another alternative to formaldehyde. Sessa et al. (2007) conducted a study using glutaraldehyde as crosslinker agent. Tensile strength and Young's modulus were increased due to glutaraldehyde amount in zein solution, meaning increase in mechanical properties.

2.3 Functionalization of Nanofibers

Polymer nanofibrous membranes can be made bioactive by incorporating therapeutical compounds into via the electrospinning process and their efficiency can be enhanced in this way. Antibiotics, proteins, small molecules, and DNA can be released by functionalized nanofibrous matrices which can be termed as "drug" overall (Chakraborty et al., 2009). When these matrices are employed for cell culture or tissue regeneration, release properties offer improved biocompatibility and can induce specific biological responses, as decreased inflammation, increased cellular proliferation, migration, and differentiation (Zhang et al., 2009). When growth factors are embedded in the matrice, cell attachment, proliferation and differentiation are facilitated. The use of growth factors has been considered as a way to manipulate not only the host healing response at the site of injury to facilitate the tissue repair, but also to manipulate and improve the in vitro tissue growth in order to produce more biofunctional engineered tissues. Hence, the strategy is to mimic matrix and provide the necessary information or signaling for cell attachment, proliferation and differentiation to meet the requirement of dynamic reciprocity for tissue engineering. This justifies the importance of drug delivery in tissue engineering applications.

Interaction modes of drugs and fiber structure can be as following upon mixture of drugs and carriers (Zhang et al., 2005).

1. Pre-spinning embedding bioactive agents in nanofibrous matrices by mixing with polymer solutions.

2. Post-electrospinning covalently conjugating or coating nanofibrous matrices with bioactive agents.

3. Encapsulating bioactive agents in the core of fibers with core–shell structure through coaxial electrospinning (Zhang et al., 2009). Modes 1 and 2 tend to give rise to

a problem of burst release in the initial stage, and therefore mode 3 is preferred (Zhang et al., 2005).

Controlled release function integrated into a tissue engineering scaffold can offer temporal–spatial gradient of biochemical signals to mimic the complex tissue microenvironment for tissue development or regeneration (Chakraborty et al., 2009). Since many interesting biochemical factors for tissue development are protein or nucleic acid in nature, they do not dissolve in organic solvent and may suffer loss of bioactivity when dispersed in the polymer solution.

The strength of the polymer–drug interaction is another variable that greatly influences the extent of drug release. Hydrophilicity, charge density, and degradability are characteristics of a polymer carrier that can play roles in its interaction with the drug of interest. Flow rate ratio and scaffold porosity are other parameters that can be changed to fine-tune drug release kinetics.

Depending on the stage of treatment and the intended functionality of the drugs, active components including pharmaceutical compounds such as antiseptics, antifungals, vasodilators, growth factors as fibroblast growth factor (FGF), epithelia growth factor (EGF), and transforming growth factor (TGF), and even cells such as keratinocytes can be integrated into the same nanofibrous substrate (Zhang et al., 2009). Functionalization of silk mats was performed to enhance wound healing by using epidermal growth factor (EGF) as EGF motivates wound healing process by stimulation of proliferation and migration of keratinocytes. EGF has high affinity receptors expressed in both fibroblasts and keratinocytes and has been shown to accelerate wound healing in vivo (Schneider et al., 2009).

Katti et al.. (2003) incorporated cefazolin into electrospun poly (lactide-*co*-glycolide) (PLGA) nanofibers as an antibiotic delivery system for wound treatment, by mixing both the polymer and the drug in a same solvent. PLGA based nanofibrous scaffolds were also selected as a carrier for the release of a hydrophilic antibiotic drug (Mefoxin, cefoxitin sodium). In another study performed by Verreck et al. (2003), two kinds of poor water-soluble drugs (Itraconazole and ketanserin), having potential use in wound healing and topical drug delivery were loaded in water-soluble (hydroxylpropyl-methylcellulose, HPMC) and water-insoluble (polyurethane, PU) nanofibrous polymer carriers. Polyurethane (PU) is frequently used in wound dressings because of its good barrier properties and oxygen permeability (Ashammakhi et al., 2008).

Zhong et al.. (2005) have added chondroitin-6-sulfate (CS) sodium salt (from bovine trachea) to type I collagen (calf skin) and the blend was electrospun to to have biomimetic scaffolds that may also enhance biological interactions with cells and speed up tissue regeneration by introducing cell-specific ligands or extracellular signaling molecules and by CS interaction with serum growth factors and cytokines.

Zhang et al.. (2005) encapsulated two kinds of medically pure drugs into cores of bioabsorbable PCL (polycaprolactone) polymer nanofibers through co-axial electrospinning. One of them was Gentamycin Sulfate, a water-soluble antibiotic that inhibits or kills bacteria, and the other one is a alcohol-soluble natural antioxidant Resveratrol, used as vasodilator. No other carrying agent, such as a high molecular weight polymer, except for the proper solvents was mixed with the drugs in making the cores. It is noted that the pure drug solutions alone cannot be formed into a fiber.

Control of release of multiple agents as antibiotics, growth factors, antimicrobials is especially important for the success and multifunctionality of tissue engineering. Therefore a delivery system working for appropriate duration and to target location is essential. While designing delivery system, drug properties such as stability, solubility or toxicity should be considered. Polymeric nanofiber-based scaffolds have great potential in designing multifunctional scaffolds upon drug release feature besides mimicking native ECM in tissue repair and regeneration. As nanotechnology and drug release technologies are combined, they can be find application area in tissue engineering.

2.3.1 Olive Leaf Extract

The olive (*Olea europaea*) is a species of small tree native to coastal areas of the eastern Mediterranean region. The olive tree is one of oldest cultivated trees and the olive leaf has been used medicinally throughout history. The leaves of this plant are used for centuries as a therapeutic in malaria and fever cases, decreasing the blood pressure and preventing atherosclerosis. Many researchers emphasize that there are a great deal of useful phenolic compounds such as oleuropeosides (oleuropein and verbascoside); flavones (luteolin-7-glucoside, apigenin-7-glucoside, diosmetin-7-glucoside, luteolin and diosmetin); flavonols (rutin); flavan-3-ols (catechin) and substituted phenols (tyrosol, hydroxytyrosol, vanillin, vanillic acid and caffeic acid)

and antioxidative activity in olive leaf (Garcia et al., 2000, Altıok et al., 2008). The content of crude protein (CP) also varies between 9.5 and 12.9%; they are rich in amino acids such as arginine, leucine, proline, glycine, valine and alanine and poor in cysteine, methionine and lisine. The greatest proportion of hemicellulose fibers are arabionosa type, whereas the branches have predominantly mannose (Vogel et al., 2014).

Phenolic compounds which are secondary products to the metabolism of vegetables, result in reactivity to pathogen attack and the response to insect injuries to protect the olive tree itself. Due to high antioxidant capacity and amount of phenolic compounds, extract obtained from olive leaf is one of the most effective natural compound in order to destroy microorganism and free radicals that cause diseases such as cancer, coronary diseases, romatoid arthritis and neurodegenerative diseases (Sudjanaa et al., 2009, Lee et al., 2010). Olive leaf extract was also shown to have antimicrobial activity against bacteria and fungi, especially resistant species such as *Klebsiella* and *Pseudomonas*, besides *E.coli* and *C.albicans* (Markin et al., 2004, Bayçın et al., 2007). Oleuropein also guards the plant against infections and herbivorous animals, resembling antimicrobial effect of olive leaf extract. Such a combination of antifungal and antibacterial effect may overcome opportunistic infections due to long-term antibiotic usage in wound healing. Antioxidant and antimicrobial properties of polyphenolic compounds will be mentioned in next section.

2.3.1.1 Antioxidant Activity and Role of Polyphenols

Antioxidants contribute to protect against oxidative damage of biologically important cellular components such as, proteins, membrane lipids and also DNA, from reactive oxygen species attacks. Free radicals and reactive oxygen species (ROS) are released continuously during the essential aerobic metabolism as unwanted metabolic by-products. The role of antioxidants may directly react with and inactive free oxygen radical. Antioxidants show functions as terminators of free radicals chain, or chelators of redox active transition metal ions that are capable of catalyzing lipid peroxidation (Al-Mustafa & Al-Thunibat, 2008; Wellwood & Cole, 2004). There are many pathways of antioxidant to intercept free radical oxygen species in the biological systems, such as, act as reducing agents, induce the preparation of anti-oxidative enzymes, or suppress the production of oxidative enzymes, i.e. cyclooxygenase, telomerase, lipoxygenase

(Naasani et al., 2003; Su et al., 2007). The activity of these enzymes are responsible for inhibiting free radical oxygen species under normal circumstance, but the enzymes can deform or the gene of the enzymes cannot make transcription during stress conditions. The antioxidant activity can prevent stress response.

Natural antioxidants are recently in high demand because of their potential in health improvement and disease prevention, and their developed safety and consumer acceptability (Bellik et al., 2012). The properties of antioxidant in medicinal plants depend on the plant which phytochemical contains secondary metabolites. In addition, concentration and composition of a phytochemical are related to antioxidant activity. Plants, the main sources of antioxidants, comprise a great diversity of compounds. These compounds which are phytochemicals, vary in structure, the number of phenolic hydroxyl groups and their position, leading to variation in their anti-oxidative capacity (Buchanan et al., 2000). Phytochemicals are classified as carotenoids, alkaloids, nitrogen-containing compounds, organ sulfur and phenolic compounds, based on their biosynthetic origins. The most studied of the phytochemicals are the phenolics and carotenoids. The basic classification of phytochemicals has been given in Figure 2.4 with the subgroups.

Phenolic compounds (POH) are bioactive substances widely distributed in plants. Phenolic compounds prevent oxidative damage with a number of different mechanisms. Basically, the action of phenolic compounds as antioxidants respectively acts as free radical acceptors. Thus, they inhibit or delay the oxidation of lipids and other molecules by rapid donation of a hydrogen atom to radicals (R) and suppressing the formation of reactive oxygen species (ROS) (Dai et al., 2010).

$$R^{\cdot} + POH \rightarrow RH + PO^{\cdot} \qquad (2.1)$$

The phenoxy radical intermediates ($PO^{\cdot}$) are less stable due to forming of resonance structure. Thus, the phenoxy radical intermediates also continue to interfere with chain-propagation reactions by reacting with other free radicals.

$$PO^{\cdot} + R^{\cdot} \rightarrow POR \qquad (2.2)$$

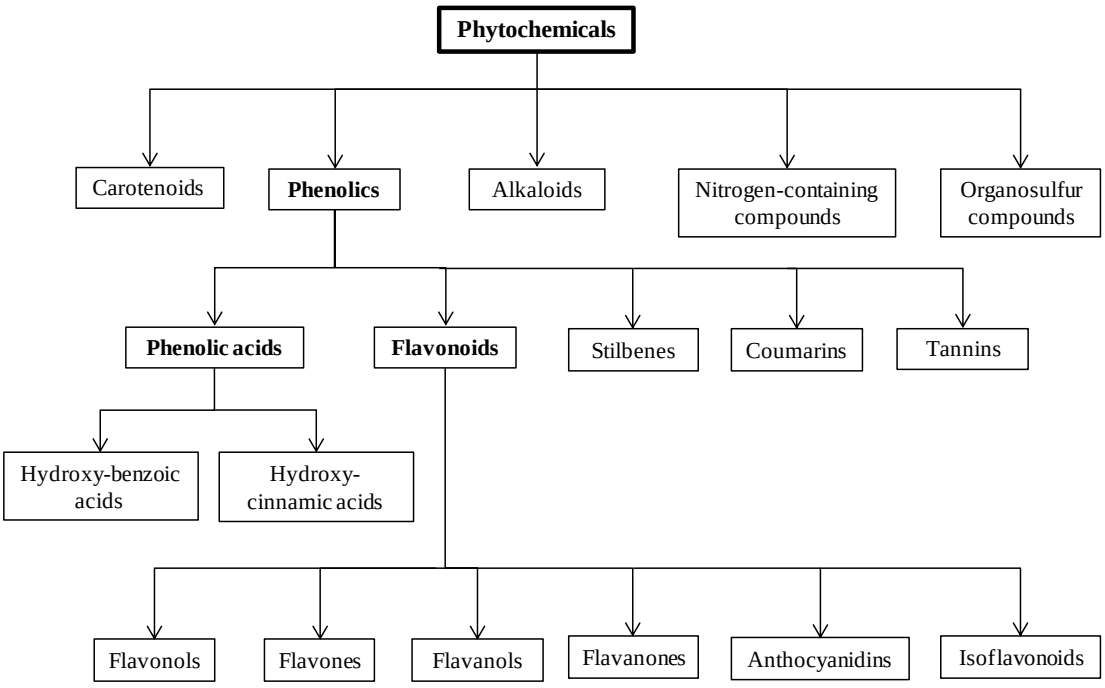

Figure 2.4. Classification of phytochemicals
(Source: Liu, 2004)

Phenolic compounds have dominant and ideal structure chemistry for free radical scavenging activities. Due to their phenolic hydroxyl groups that are prone to donate a hydrogen atom or an electron to a free radical, phenolic compounds exhibit strong antioxidant capacity. The mechanism of phenolic compounds as antioxidant activity is defined with major chemical expression in equation 2.1 and 2.2. According to classification depicted by Liu (2004), plant phenolics consist of flavonoids, phenolic acids, tannins and less common lignans and stilbenes. Flavonoids are the most plentiful polyphenols in human diets. The basic structure of flavonoid is flavan nucleus, including fifteen carbon atoms arranged in three rings as depicted in Figure 2.4 and as A, B and C (Dai et al., 2010). Flavonoids are divided into subgroups in terms of the oxidation state of the central C ring (Bellik et al., 2012; Dai & Mumper, 2010).

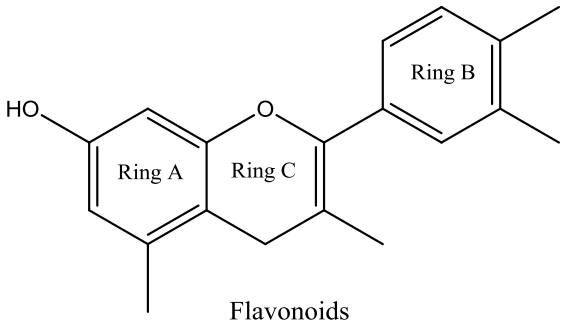

Figure 2.5. Structure of flavonoids

Flavonols have a double bond between second carbon and third carbon in C rings, with a hydroxyl group in third carbon of the C ring. Colorimetric methods and HPLC combined with UV detector or mass spectrometry have been used to determine the total content of phenolics.

2.3.1.2. Application of Polyphenols

Polyphenols present a wide range of pharmacological attribution. Phenolic compounds are known for their antioxidant activity that is useful for diabetes mellitus or preservation against cancer. Interestingly, several studies revealed that some polyphenols, such as tannins or flavonoids, cause oxidative strand breakage in DNA in the presence or absence of metal ion (Nobili et al., 2009; Ziech et al., 2012). The reason of this is that cancer cells are known to include high amount of copper ion. When exposed to redox reactions with polyphenols, cancer cells generate reactive oxygen species and phenoxyl radicals lead to breakdown of the structure of DNA, lipid or protein (Sawadogo et al. 2012)., referring to polyphenols' act as pro-oxidants.

2.3.1.3. Antimicrobial Activity of Phytochemicals

Phytochemicals with antioxidant activity may show pro-oxidant behavior under pathogenic microorganisms' circumstances. It is thought that the toxicity of bioactive polyphenols to microorganisms is associated with the sites and number of hydroxyl groups they have (Das et al., 2010). In addition, some researchers have observed that more highly oxidized phenols are more inhibitory against pathogenic microorganisms (

Paiva et al., 2010). According to the researches, there are many mechanisms of antimicrobial action of phytochemicals, yet they are also not fully understood. It is thought that flavonoids act as inhibiting cytoplasmic membrane function while they are able to change cell morphology with damage formation of filamentous cells (Cushnie et al., 2005). It is important that not only a single compound is responsible for observed microbiological activity but also the combination of compounds may show bioactivity when they interact in synergistic manner. In addition to molecular antimicrobial activity of antioxidants, antimicrobial compounds can be classified as bacteriocidal, bacteriostatic and bacteriolytic in terms of observing their effects of bacterial culture (Madigan et al., 2008). Bacteriostatic compounds are inhibitors of protein synthesis and affect by binding to ribosomes. Bacteriocidal compounds attach to their cellular targets and are not removed by dilution and kill the cells. Bacteriolytic compounds include antibiotics that prevent the cell wall synthesis. One of the methods to determine antimicrobial activity is determination of minimum inhibitory concentration (MIC) (Madigan et al., 2008). The lowest concentration of the extract which inhibited the growth of the test organism was taken as MIC value as a result of turbidity assay.

CHAPTER 3

OBJECTIVES

Main objective of this study can be divided into two sections as olive leaf extract characterization and preparation of wound dressing contact layer by incorporating olive leaf extract into biopolymer. Objectives can be summarized as follows:

- ✓ Determination of olive leaf extract components
- ✓ Determining the effects of the components on cell migration under exogenous stress
- ✓ Establishing a relationship between antioxidant properties and wound closure
- ✓ Fabrication of fibers that can be used as wound dressing contact layer
- ✓ Functionalization of fibers by incorporating olive leaf extract
- ✓ Determination of release properties
- ✓ Determination of sustainability of extract efficiency
- ✓ Determination of cellular responses to wound dressing contact layer

CHAPTER 4

MATERIALS & METHODS

4.1. Materials

4.1.1. Plant Materials and Chemicals

Olive leaves were collected from Aquaculture Central Research Institute in İzmir. Analytical grade ethanol, acetic acid and zein were purchased from Merck (Germany). HPLC grade acetonitrile was obtained from Sigma (Germany). Sodium carbonate, Folin-ciocalteu reagent and gallic acid standard, used in total phenol content determination, were purchased from Merck (Germany). ABTS (2,2'-azinobis(3-ethylbenzothiazoline-6-sulphonic acid), potassium peroxodisulfate (K2S2O8) and Trolox standard (6-hydroxy-2,5,7,8-tetramethylchroman-2-carboxylic acid), used in antioxidant analysis, were purchased from Fluka (Germany). HPLC standards of oleuropein, luteolin, hydroxytyrosol, verbascoside and rutin were obtained from Sigma (Germany).

Nutrient broth and potato broth were purchased from Merck (Germany) and BD (UK) respectively. Bacteriological agar and bacteriologic peptone was obtained from Oxoid (UK). Penicillin, Gentamycin and Ampicillin antibiotics purchased from pharmacy were used for comparison to evaluate the antimicrobial activities of extracts and fractions of extracts in microdilution assays.

Dulbecco's Modified Eagle Medium (DMEM), fetal bovine serum (FBS), phosphate-buffered saline (PBS), Penicillin–streptomycin antibiotic solution were purchased from Gibco (USA). MTT (3-(4,5-dimethylthiazol-2-yl)-2,5-diphenyl) tetrazolium bromide) was obtained from Sigma Aldrich (Germany).

4.1.2. Instruments and Equipments

Olive leaves were grinded by a small coffee grinder. After grinding, extractions were performed in Thermo MaxQ-4000 orbital shaker. Ethanol was evaporated by Heidolph Laborata 4001 and aqueous extracts were frozen in -20°C freezer. In order to obtain lyophilized extracts, Telstar Cryodos freeze drier was used. MIC, total phenol and antioxidant capacity determination and cytotoxicity assays were performed by Varioskan (Thermo) and Multiskan Spectrophotometers (Thermo) were used. In situ measurement of phenolic compounds from olive leaf crude extract incorporated zein fibers was conducted by UV spectrophotometer from Perkin Elmer. Phenolic compounds of olive leaf extract was analysed with HPLC Agilent Technologies 1100 series equipped with UV-Diode Array Detector (DAD). Experiments were carried out by Zorbax C18 semi-preparative column. Crude extract was fractionated by fraction collection unit.

Electrospinning setup consisted of syringe pump (Programmable Single Syringe Pump Model NE-1000, U.S.A) and GAMMA High Voltage Supplier. Zein solutions were prepared by magnetic stirrers (IKA). Characterization of the fibers were carried out by Philips XL 30S FEG scanning electron microscope, Perkin Elmer Diamond TG/DTA Instrument and Shimadzu FT-IR spectroscopy.

Microbiological and cell culture studies were performed in Laminair Flow Cabinet Class II and Thermo Jouan MSC12 biosafety cabinets, respectively. Microbial population was determined in terms of McFarland unit by Biosan DEN 1B spectrophotometer. Microorganisms and animal cell lines were cultivated in Nuve EN055 series and Thermo Stericycle Incubators, respectively. Cells were observed under light microscope (Olympus CKX31) and inverted phase contrast microscope (Olympus CKX41). Cell migration studies were performed by microscopic digital camera system (Olympus DP25). Sterilization of broths and equipment were carried out by Hirayama HVE-50 Autoclave. All microbial strains were stored at -80°C in Revco Ulti1786 series refrigerator. Cell lines were kept in liquid nitrogen tank (Thermo).

4.2. Methods

4.2.1. Preparation of Olive Leaf Extract

Olive leaves used in this study were collected from Aquaculture Central Research Institute in İzmir. They were collected during pruning season before flowering period. Collected plant material was dried at room temperature. The dried olive leaves were grinded in a coffee blender to obtain the powder form. Extraction was performed in 70% aqueous ethanol with solid-liquid ratio of 1:20, at 180 rpm at room temperature for 2 hours. Extract was vacuum-filtered and evaporated at 40°C to remove ethanol. Aqueous phase of extract was centrifuged at 4000 rpm for 5 minutes to remove solid residues. The liquid extracts were lyophilized in freeze drier for three days. The percent (w/w) extraction mass yields of plant materials were calculated.

4.2.1.1. Fractionation of Olive Leaf Extract

Olive leaf extract (50 mg/ml) was fractioned according to relative polarity by using semi-preparative C-18 column and fraction collector. Flow rate was kept constant at 4.5 ml/min. Mobile phase consisted of 5% acetonitrile and 95% acetic acid (2.5%) and a linear gradient elution system was used as given in Table 4.1 Samples were filtered through 0.45 μm membrane before injection to HPLC. Fractions were collected at 2 minute intervals. Residue of the mobile phase in the fractions was removed by rotary evaporator and concentrated 20 times by dissolving in distilled water for HPLC analysis to determine the amount of active compounds.

Table 4.1. HPLC elution program

Time (min.)	Mobile Phase A (%) (2.5 % acetic acid)	Mobile Phase B (%) (100% acetonitrile)
0	95	5
20	75	25
40	50	50
50	20	80
60	5	95

4.2.2. Characterization of Crude Olive Leaf Extract and Fractions

4.2.2.1. High Performance Liquid Chromatography (HPLC) Analysis

Oleuropein, hydroxytyrosol, verbascoside and luteolin were chosen as each standard was a component in separate fractions due to retention time difference as a result of HPLC analysis. Prior to fraction analysis, active compounds in fractions were confirmed by standard addition method. Calibration curve of each standard was also established in order to determine the amount of components in fractions.

4.2.2.2. Determination of Total Phenol Contents (TPC)

Total phenol contents of extracts and fractions obtained from olive leaves were determined by using Folin-ciocalteu method. Olive leaf extracts were dissolved in deionized water (dH2O). Prepared plant extracts and gallic acid solutions were mixed with Folin- ciocalteu reagent. While taking 20 µl from each sample, 100 µl Folin-ciocalteu reagent (1:10 diluted with deionized water) was added to each sample. After 2.5 min, 80 µl sodium carbonate solution (prepared as 7% in deionized water) was added to this mixture. After incubation for 1 hour at room temperature in dark, absorbance was measured at 725 nm with a UV spectrophotometer. Results were expressed as miligrams of gallic acid equivalents (GAE) per gram dried weight.

Calibration curve of gallic acid can be seen in Appendix B. Assay was repeated in triplicate.

4.2.2.3. Determination of Trolox Equivalent Antioxidant Capacity (TEAC)

Trolox equivalent antioxidant capacity (TEAC) assay was performed by ABTS method. The ABTS+ radical was generated by a reaction between 14 mM ABTS and activated with 4.9 mM K2S2O8. The ABTS+ solution was diluted with absolute ethanol and subjected to spectrophotometric measurement at 734 nm until to an absorbance of 0.70 (±0.03) was achieved. 10µl of each sample in triplicates were prepared in 96 well-plates. Then, 200µl ABTS+ solution was added into each sample and kinetic absorbance data were obtained during 1h. First absorbance value was used as initial time reading and the absorbance value recorded at the end of analysis was termed as final reading. Inhibition percentage was calculated by the formula given below.

% inhibition = 1- (Absorbance final /Absorbance initial) x 100

Calibration curve was obtained against Trolox concentration versus inhibition percentage as given in Appendix C. In this assay, the antioxidant activity was expressed as milimole TEAC per gram dried extract.

4.2.2.4. Minimum Inhibition Concentration Assay

The strains were purchased as lyophilized powders from suppliers, America Type Culture Collections (ATCC). Inoculation medium was potato broth for *Candida albicans* and nutrient broth for *Escherichia coli* and *Staphylococcus epidermidis*, which were incubated overnight at 37°C. In order to prolong usage time, stock cultures and their reserves were prepared in 40% glycerol broth by inoculating the fresh culture (1:1). Stock cultures were kept at -80°C for further studies after they were labeled.

In order to determine the Minimum Inhibition Concentration (MIC) of the plant extracts and fractions; *Escherichia coli* and *Staphylococcus epidermidis* were used as gram negative and positive bacteria, respectively. *Candida albicans* was used as fungus. Crude extracts were dissolved in sterile deionized water for a concentration of 3000 µg/ml. Serial dilutions of each extract were carried out with a final concentration of 1

µg/ml. 100 µl of each extract concentration and 95 µl nutrient broth were added in each well of 96 well microplate. Each well inoculated with 5µl of overnight culture. Negative control was only microbial suspension with broth. Antibiotic containing samples were used as positive controls. Plates were incubated at 37°C for 24 hours and growth kinetic assays for each strain were performed by growth curves. MIC values of each extract and antibiotics were determined by a microplate reader at 640 nm.

4.2.2.5. Cell Viability Assay

NIH 3T3 mouse fibroblast cell line was grown in DMEM medium supplemented with 2 mM L-glutamine, 10% fetal bovine serum (FBS), 1% Penicillin–Streptomycin. The cells were maintained fibroblast morphology between 80-90% of cells for 7 days after initiation of differentiation in a dark cell incubator having 5% carbondioxide (CO_2) and 95% humidity at 37ºC. Cell viability tests were carried out for the fractions of the extract and extract in crude form using 3- (4,5dimethylthiazol-2-yl) -2,5-diphenyl tetrazolium bromide (MTT) Cell Viability assay. Test principle was based on reduction of tetrazolium salt (MTT) into its insoluble formazan giving a purple color by mitochondrial reductase in living cells (Yanez et al., 2004). Briefly, fibroblast cells were seeded a day prior to sample exposure at 10000 cells per well in 96 well-plate filled with culture medium containing DMEM with 10% FBS. Fractions obtained were dissolved in DMEM containing 10% FBS after removal of mobile phase along with crude extract, both prepared in serial dilutions. Pre-seeded cells were treated with dilutions of crude extract and the fractions for 24, 48 and 72 hours. At the end of each time point, samples were removed, cells were washed with PBS and replaced with 100 µl MTT (0.5 mg/ml). After incubation for 4 h at 37 °C in dark, samples were centrifuged (1800 rpm, 10 min) to carefully remove non-metabolized MTT. Formazan crystals formed were dissolved by adding 100 µl of DMSO. Absorbance values in each plate were measured by using microplate reader at 545 nm.

Cell viability (%) = (Absorbance value of sample / Absorbance value of control) x100

4.2.2.6. Wound Scratch Assay

NIH-3T3 mouse fibroblast cells were seeded on 24-well plates at a concentration of $2*10^5$ cells/well and incubated in an atmosphere of 37°C and 5% CO_2 to adhere on surface. Afterwards cells were scratched by a polyoxymethylene originated, pre-sterilized circular cell scratcher of 5 mm diameter (Figure 4.1). Suspended cells were removed and adhered cells were exposed to crude olive leaf extract and its fractions which were concentrated in DMEM supplemented with 10% FBS. Assay was also performed under exogenous stress created by hydrogen peroxide. Cells were exposed to hydrogen peroxide at concentrations of 1, 10, 50 and 100 µM for 1 hour. After incubation, medium was replaced with the medium containing crude olive leaf extract and fractions. Selected concentrations were 1, 10 and 50 µg/ml. Measurement of wound diameters and observation of cell migration were performed by camera mounted on a phase contrast inverted microscope. Medium of the cells were renewed every 48 hours without changing the composition of extract and fractions to prevent cell death caused by nutritional deficiency.

Figure 4.1. Cell scraper used for wound scratch

Mouse fibroblast cells were also subjected to confocal microscopy after wound scratch assay. Cells were seeded on 35 mm dishes (Ibidi, Germany) at 400.000 cells/ml and incubated for 24 hours for adherence. Cells were scratched by a sterile pipette tip. After removal of suspended cells, adhered cells were exposed to 100 µM hydrogen peroxide for 1 hour. At the end of incubation period, cells were treated with OLE at the concentrations of 1 and 50 µg/ml. Cells were subjected to confocal microscopy (Andor Revolution) after treatment with red flourescent mitochondrial dye, MitoRed (Excitation/Emission: 622/648 nm) (Sigma Aldrich, Germany).

4.2.3 Fabrication of Zein Fibers

4.2.3.1 Preparation of Zein Solutions

Zein from maize was dissolved in 70%, 80% and 90% aqueous ethanol solutions (v/v) between a concentration range of 20% and 40% (w/v). Electrospinning solutions containing 30% (w/v) zein in 70% aqueous ethanol were mixed with lyophilized OLE at concentrations of 5, 7.5 and 10% (w/v). Aqueous ethanol phase (70%) (v/v) of OLE containing 5, 7.5 and 10% dry matter was also used to dissolve 30% zein (w/v) to observe the effect of the single preparation step of the polymer solution.

Fractions were also incorporated into zein polymer solutions as aqueous phase in order to compare the crosslinking effect with the crude extract. Concentration of the fractions were calculated as to contain 10% crude olive leaf extract.

4.2.3.2 Electrospinning of Zein

The prepared zein solutions were fed into a 5 ml plastic syringe with a needle having a tip diameter of 0.6 mm. The flow rate of the pump was adjusted to 6 ml/h. The fibers were deposited on a constant target of aluminum foil under 15, 20 and 25 kV. The distance between the needle tip and the target was 10 cm.

Fraction-incorporated fibers were fabricated under 25 kV, with all other parameters kept equal with the previous trial.

4.2.4 Characterization of Zein Fibers

4.2.4.1 Scanning Electron Microscopy

Morphology of zein fibers, either with fractions and crude olive leaf extract and without extract, were observed by SEM (FEI Quanta 250 FEG) after gold sputtering. Images were taken by applying an electron voltage of 5 kV. The size distribution was generated by measuring and processing the diameter of fibers with Image J software.

4.2.4.2 Fourier Transform Infrared Spectroscopy (FT-IR)

Alterations in bond structures of fibers were observed by FT-IR spectroscopy (Shimadzu-8400S). Zein fibers were mixed with potassium bromide and IR spectra were collected by operating in the region from 4000 to 400 cm-1, averaging 40 scans at 2 cm-1 resolution.

4.2.4.3 Thermogravimetric Analysis (TGA)

The degradation behavior of zein fibers were analyzed by TGA (Shimadzu TA 50) by scanning from 25 to 600°C at a heating rate of 10°C/min under nitrogen atmosphere.

4.2.4.4 In vitro Release Studies

OLE loaded zein fibers of 25 mg were immersed in 4 ml of deionized water in 12-well plate for batch release and incubated at 37°C for 1, 2, 3 and 6 days. The entire release medium was collected for each time interval and subjected to total phenol content determination by Folin–Ciocalteu method. In-situ release experimental set-up consisted of a peristaltic pump, a diffusion cell and a UV-spectrophotometer (Figure 4.2). 10 mg of OLE loaded zein fiber was placed in the diffusion cell and 50 ml of deionized water was pumped through the system. Zein fibers without OLE were used as

control. Effluent was returned to the source after spectrophotometric measurement. Absorbance data were collected at 280 nm for 210 min., and the amount of the soluble phenolic compounds was determined by OLE calibration curve.

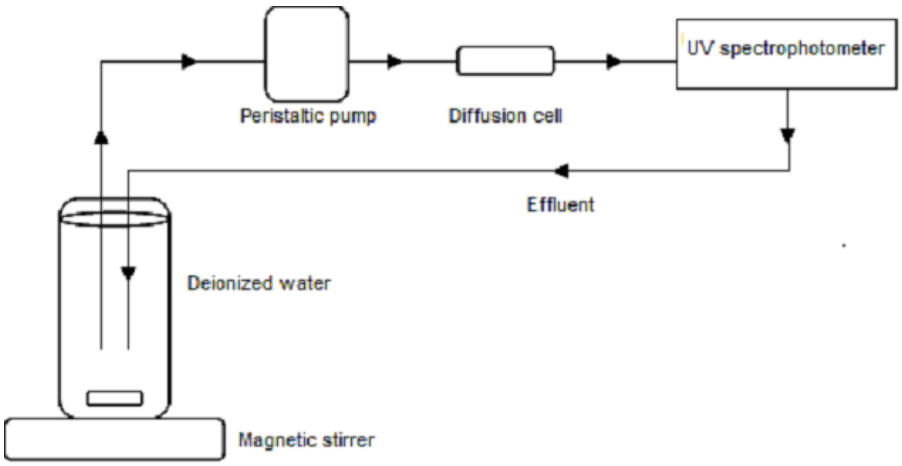

Figure 4.2. In situ measurement set-up for continuous release.

4.2.4.5 Cell Attachment on Zein Fibers

NIH/3T3 mouse fibroblast cell line was maintained in DMEM supplemented with L-glutamine, 10% fetal bovine serum, 100 µg/ml streptomycin and 100 U/ml penicillin in an atmosphere of 5% CO_2 at 37°C. Cells were subcultured every 48 hours.

For *in vitro* attachment, fiber-coated coverslips were prepared (Ifkovits et al, 2007). Zein and OLE loaded zein solutions were electrospun onto autoclaved glass coverslips (18 mm x 18 mm) for 20 min. until a thin layer was formed. Fiber-coated coverslips were then subjected to UV sterilization for 1 hour and after washing with copious amounts of PBS, they were placed in 6-well tissue culture plates. Cells were seeded onto coverslips at a density of 10^5cells/well and allowed to attach for 1 week. Polarized light microscope with Differential Interference Contrast (DIC) module (Olympus) was used to visualize cell attachment on coverslips of electrospun zein fibers.

CHAPTER 5

RESULTS AND DISCUSSION

5.1 Characterization of Olive Leaf Extract Fractions

5.1.1 Fraction Collection of Olive Leaf Components

Crude extract of olive leaf was subjected to fractionation by automatic fraction collection unit. After removal of mobile phase and concentration of fractions in deionized water, fractions were analyzed by HPLC to confirm the separation. They could be distinguished from each other by means of retention times. Purity of fractions is depicted in chromatograms in Figure 5.1. Ensuring that fractionation was successfully achieved, further analysis was composed of determination of possible active compounds in related fractions. Four active compounds with different polarities, hydroxytyrosol, verbascoside, oleuropein and luteolin, were selected to be specified in each fraction. Serial dilutions of standards dissolved in deionized water were subjected to HPLC analysis to determine their retention time and obtain calibration curves, which were used in amount calculation. Retention times of the standards referred to their localization in individual fractions, as seen in Table 5.1. Calibration curves of each standard are in Appendix A.

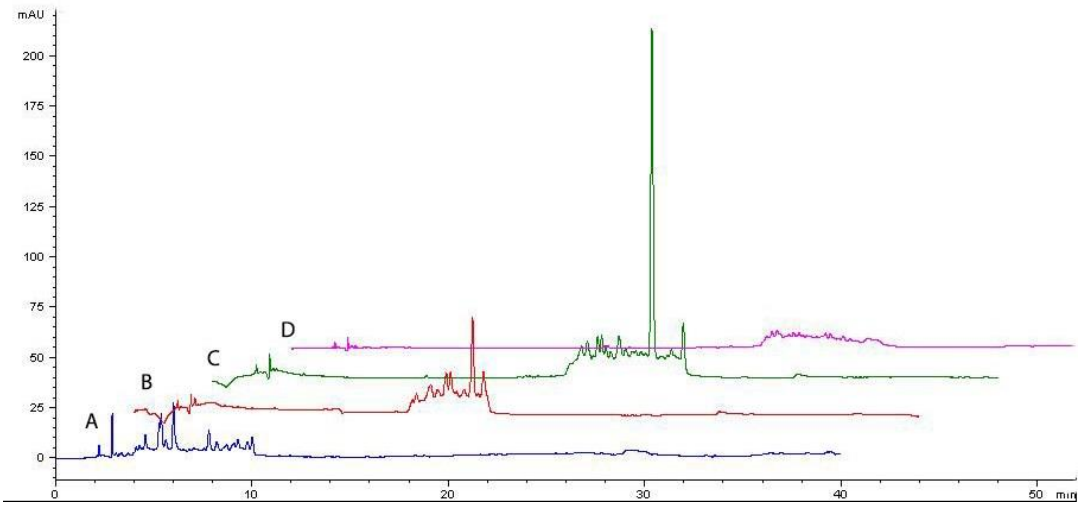

Figure 5.1. Fractionation of olive leaf extract (OLE) A. Hydroxytyrosol-containing fraction 2 (fr2), B. Verbascoside- containing fraction 4 (fr4), C. Oleuropein-containing fraction 5 (fr5), D. Luteolin- containing fraction 6 (fr6).

Table 5.1. Retention time of standards and estimated fraction numbers

Compound	**Retention time (min.)**	**Estimated fraction number**
Hydroxytyrosol	5.9	2
Verbascoside	17.2	4
Oleuropein	21.7	5
Luteolin	26.2	6

After determination, presence of each component in fractions was confirmed by standard addition method. Fractions were mixed with relevant standards at a concentration of 1 mg/ml at 1:1 ratio. When HPLC analysis of fractions and standard-added fractions were compared, there was a prominent change between the absorbances at the same retention periods, referring to presence of relevant standard. Matching chromatograms were indicated in Figure 5.2.

Concentration of active compounds in crude extract and fractions were calculated based on calibration curves, prior to further analysis of antioxidant capacity, total phenol content and cytotoxicity. Crude olive leaf extract was analyzed by HPLC, obtained chromatogram can be seen in Figure 5.3. Concentration of each selected active compound in crude extract and fractions are depicted in Table 5.2, in addition to abundance percentage of active compounds in crude extract. Oleuropein was found as

the most abundant active compound by 22% in crude extract as figured out by Altıok et al. (2008). Percentages of hydroxytyrosol, verbascoside and luteolin were found as 0.6%, 1.4% and 0.6%, respectively (Benavente-Garcia et al., 2000). The chemical composition of olive leaves varies according to origin, proportion of branches present in the extract, storage conditions, weather conditions, moisture content and degree of soil contamination (Vogel et al., 2014). The most abundant compound in olive leaves is oleuropein, followed by verbascoside and hydroxytyrosol in our study. Hydroxytyrosol is also precursor of oleuropein and verbascoside is a conjugated glucoside of hydroxytyrosol and caffeic acid (Benavente-Garcia et al., 2000). The results determined with HPLC analyses are in accordance with the findings reported in the literature earlier.

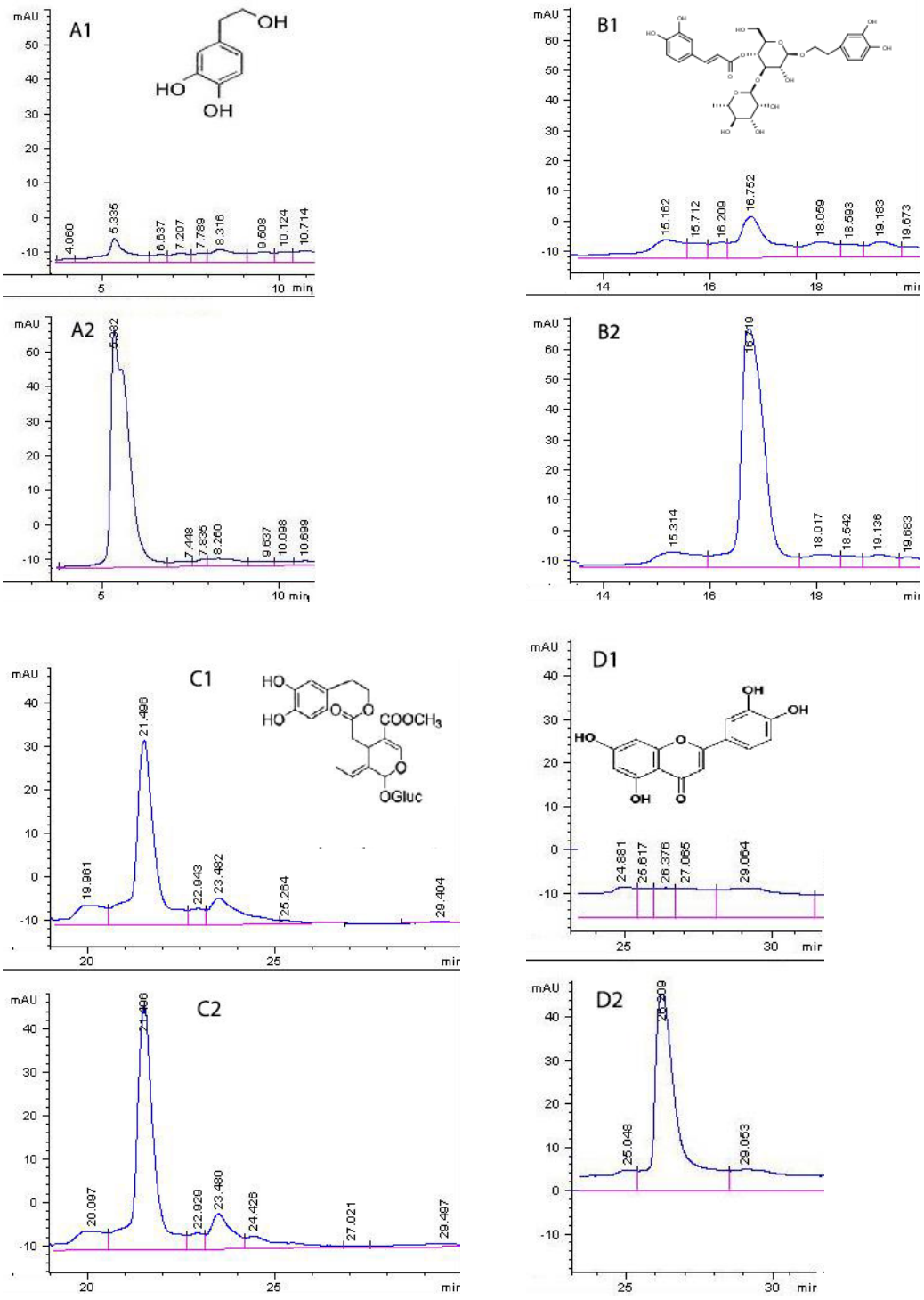

Figure 5.2. Resulting chromatograms of standard addition. Each letter refers to fraction and its extract-added form one under the other. A1-2: Fr2-Hydroxytyrosol-added fr2, B1-2: Fr4-Verbascoside-added fr4, C1-2: Fr5-Oleuropein-added fr5, D1-2: Fr6-Luteolin-added fr6.

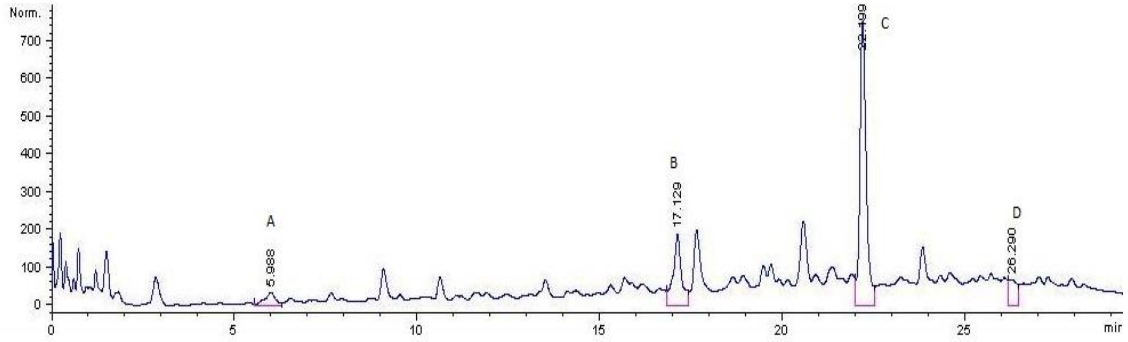

Figure 5.3. Chromatogram of crude olive leaf extract. Letters represent peaks of selected active compounds. A. Hydroxytyrosol, B. Verbascoside, C. Oleuropein, D. Luteolin

Table 5.2. Concentration and abundance percentage of active compounds in crude extract and fractions

Active compound	Concentration in crude extract (mg/ml)	Abundance in crude extract (%)	Concentration of the active compound (no. of related fraction) (mg/ml)
Hydroxytyrosol	0.3	0.6	0.03 (Fr2)
Verbascoside	1.75	3.5	0.23 (Fr4)
Luteolin	0.33	0.65	0.02 (Fr5)
Oleuropein	2.262	22.62	0.34 (Fr6)

5.1.2 Determination of Total Phenol Content and Antioxidant Capacity of Crude Olive Leaf Extract and Fractions

Four fractions of olive leaf extract were subjected to total phenol content and antioxidant activity determination analysis (Figure 5.4). Results were evaluated by calibration curves of Gallic acid and Trolox, given in Appendix B and C respectively. Total phenol content and total antioxidant activity of crude extract were found 184±25 mg Gallic Acid Equivalent (GAE)/g dry weight (DW) and 1.34±0.18 mmole. TEAC/g dry weight (DW), respectively. Kontogianni et al. (2011) determined total phenol

content range of olive leaf extract between 70-483 mg GAE/g DW in their studies on different fractions using a variety of solvents. Hayes et al. (2011) also found polyphenol content for olive leaf extract as 160.8 mg GAE/g DW, complying with our findings.

Total antioxidant capacity range was also between 1.5-7.52 mmole TEAC/g DW (Garcia et al., 2000, Baycin et al., 2011). Total phenol content and total antioxidant capacity of crude olive leaf extract were found in accordance with the range in the literature. Total phenol content of the fractions ranged between 0.038 and 0.1 mg GAE/ml fraction, among which oleuropein-containing fraction 5 had the highest amount of phenolics. High amount of phenolics resulted in higher antioxidant capacity as depicted in Figure 5.4, as oleuropein exhibited the highest value with 0.36±0.06 mmole TEAC/ml fraction. It has been reported that amount of phenolic compounds in olive leaf extract referred to its radical scavenging activity against free radical formation. The antioxidant activity of the olive leaf was attributed to its major phenolic compounds such as oleuropein, hydroxytyrosol, and luteolin-7-O-glucoside acid and the presence of a functional group in their structure, catechol (Lee et al., 2009, Hayes et al., 2011). The antioxidant activity of oleuropein is related to the hydroxytyrosol moiety in its structure. Compared with the hydroxytyrosol, the ability of scavenging the radical cation ABTS•+ is lower because of the molecular weight of the oleuropein. (Vogel et al., 2014). Oleuropein and hydroxytyrosol exhibit their antioxidant capacity in three ways: 1. free radical scavenging and radical chain breaking; 2. anti-oxygen radicals; 3. metal chelating. Catechol structure produces stable resonance structures by scavenging peroxyl radicals and breaking peroxidative chain reactions (Tripoli et al., 2005, Bulotta et al., 2013).

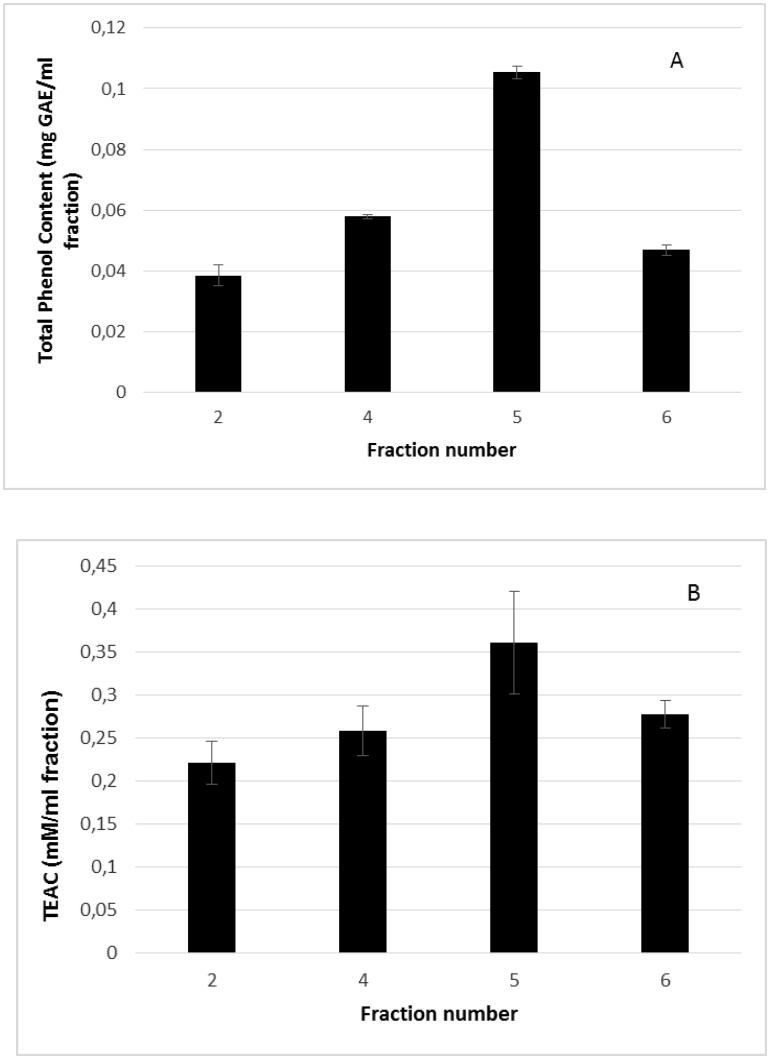

Figure 5.4. A. Total phenol content and B. Antioxidant capacity of olive leaf extract fractions.

5.1.3 Minimum Inhibition Concentration

Antimicrobial acitivity of olive leaf extract was determined by minimum inhibition concentration method (MIC) in 96-well plate. Bacterial culture of *Escherichia coli*, *Staphylococcus epidermidis*, fungal culture of *Candida albicans* was subcultured from stock cultures until they reached logarithmic phase confirmed by measuring OD values. Olive leaf extract serial dilutions was prepared in nutrient and potato broth and filter-sterilized. Bacterial and fungal cultures were incubated with extract dilutions. Negative control was consisted of bacterial suspension in nutrient broth without extract. Plates were subjected to spectrophotometric analysis at 37°C for 24 hours and growth kinetic assays for each strain were determined by growth curves at 600 nm. Sample

dilutions were determined based on cytotoxic activity of olive leaf extract. Figure 5.5 indicates that 3000 µg/ml OLE inhibited growth of both *E. coli* and *S. epidermidis*. This concentration also led the organisms into bacteriostatic phase. *C. albicans* was the only species that was not affected by OLE. Crude extract exhibited antibacterial properties better than antifungal property.

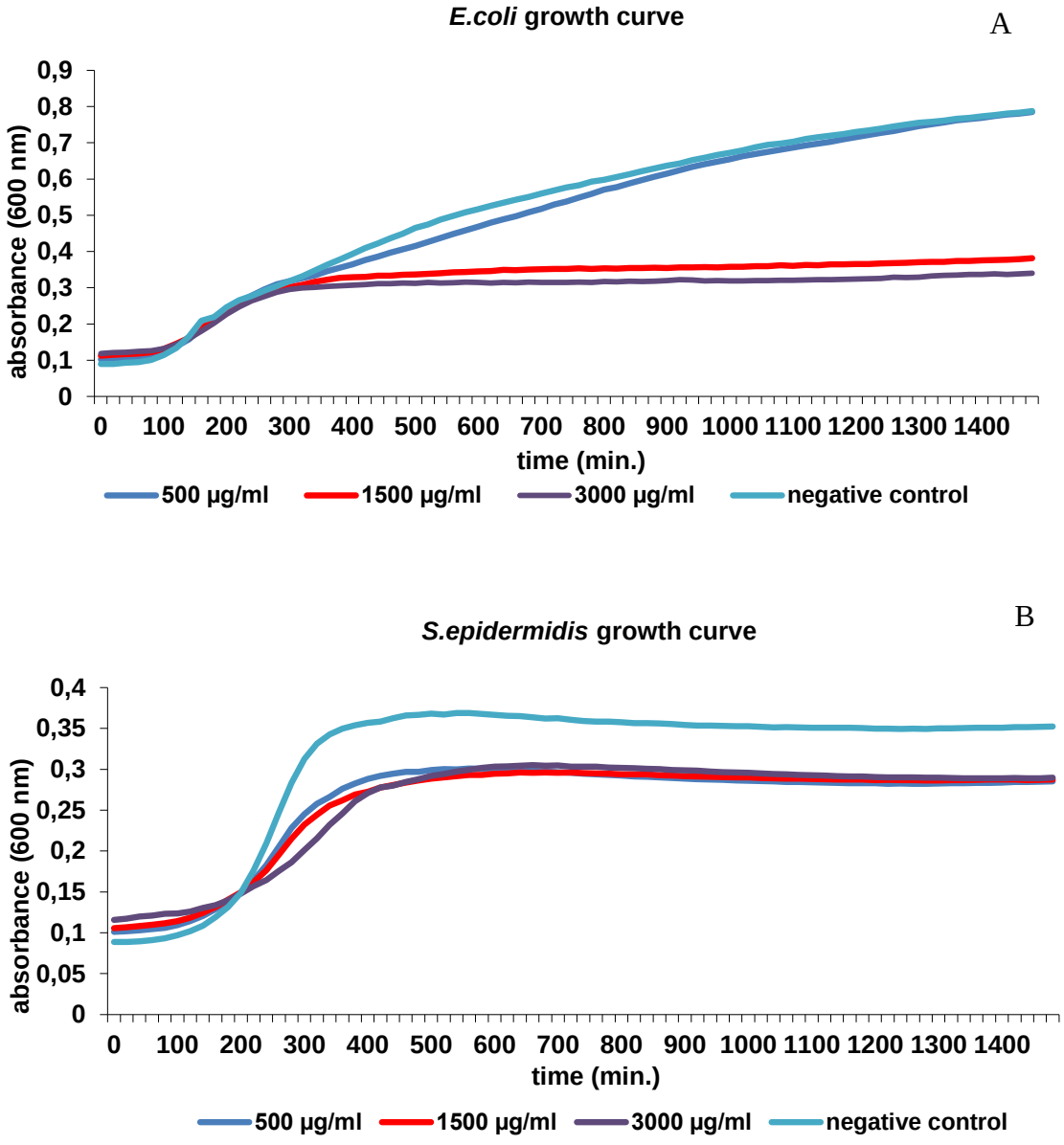

Figure 5.5. Growth curves for A. *E. coli*, B. *S. epidermidis*, C. *C. albicans* in the presence and absence of crude OLE (cont. on next page)

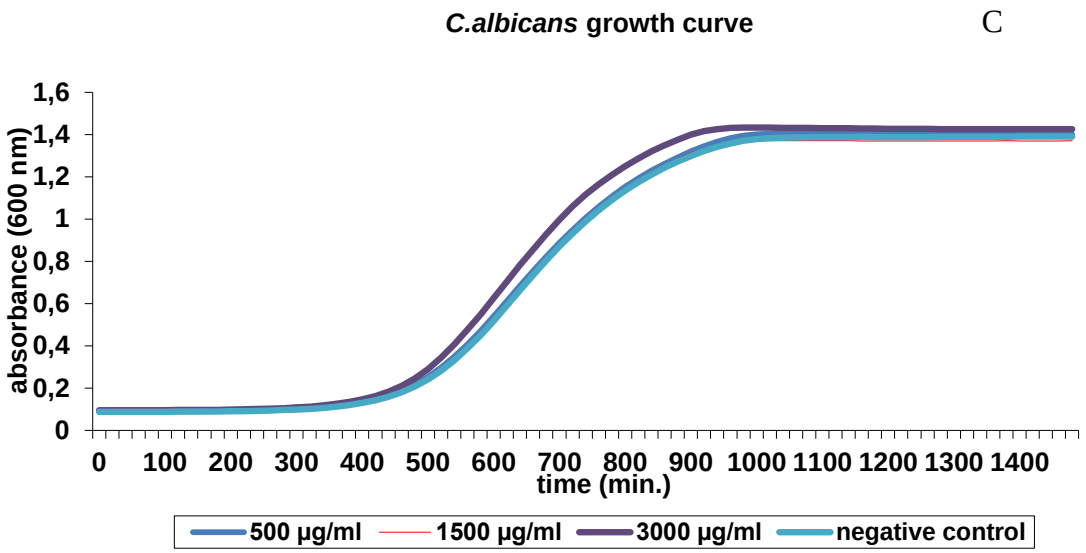

Figure 5.5. cont.

Olive leaf extract fractions were also subjected to MIC assay. *S. epidermidis* and *E. coli* were incubated with Fr2, Fr4, Fr5 and Fr6 at the concentrations of 500, 1500 and 3000 µg/ml. Since crude extract did not exhibit antifungal activity, *C. albicans* was not treated with olive leaf extract fractions. As indicated in Figure 5.6, 3000 µg/ml of Fr6 exhibited better antimicrobial property in both strains, whereas 3000 µg/ml of Fr5 also inhibited the growth of *S. epidermidis*. But neither of the fractions did inhibit the growth of the microorganisms completely. Results also indicate that crude olive leaf extract exhibited better bacteriostatic properties on strains which may be attributed to polyphenolic nature.

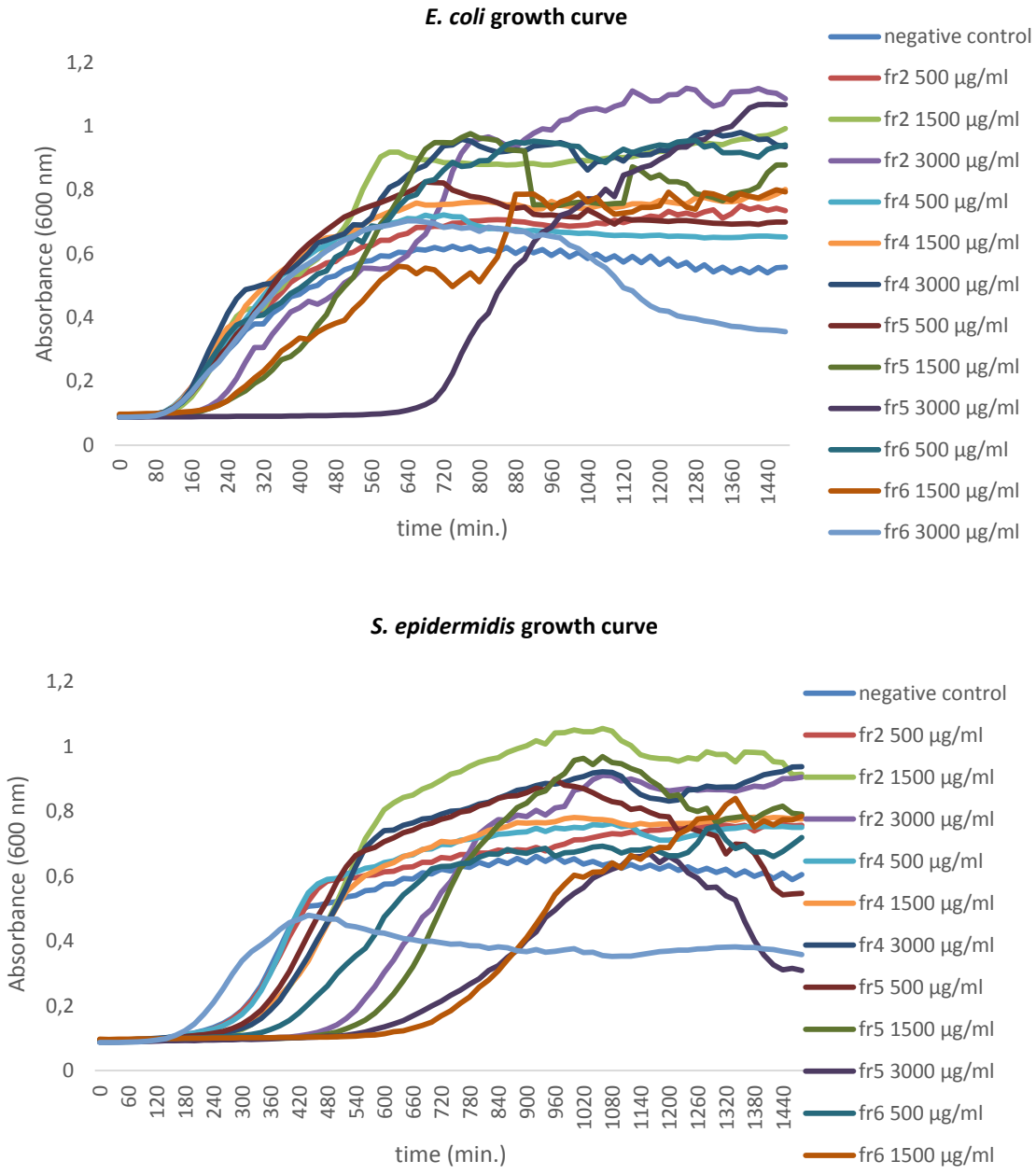

Figure 5.6. Growth curves for *E. coli*, and *S. Epidermidis* in the presence and absence of OLE fractions.

5.1.4 Cytotoxic activity of fractions and crude extract

Crude olive leaf extract and its fractions were subjected to cytotoxicity assay in order to determine cell viability upon exposure. NIH 3T3 mouse fibroblast cell line was used as a model to study the effect of olive leaf extract and its fractions on cell viability. MTT was used to measure cytotoxic activity at 24, 48 and 72 hour time points. Fibroblast cells were treated with extract at concentration range between 1-3000 µg/ml.

Same concentration range was applied for standard oleuropein, the most abundant compound found in olive leaf extract. As seen in Figure 5.7A, concentrations higher than 100 µg/ml exhibited toxicity on fibroblast cells. Cytotoxic profile of oleuropein, as in Figure 5.7B, was also found similar with olive leaf extract.

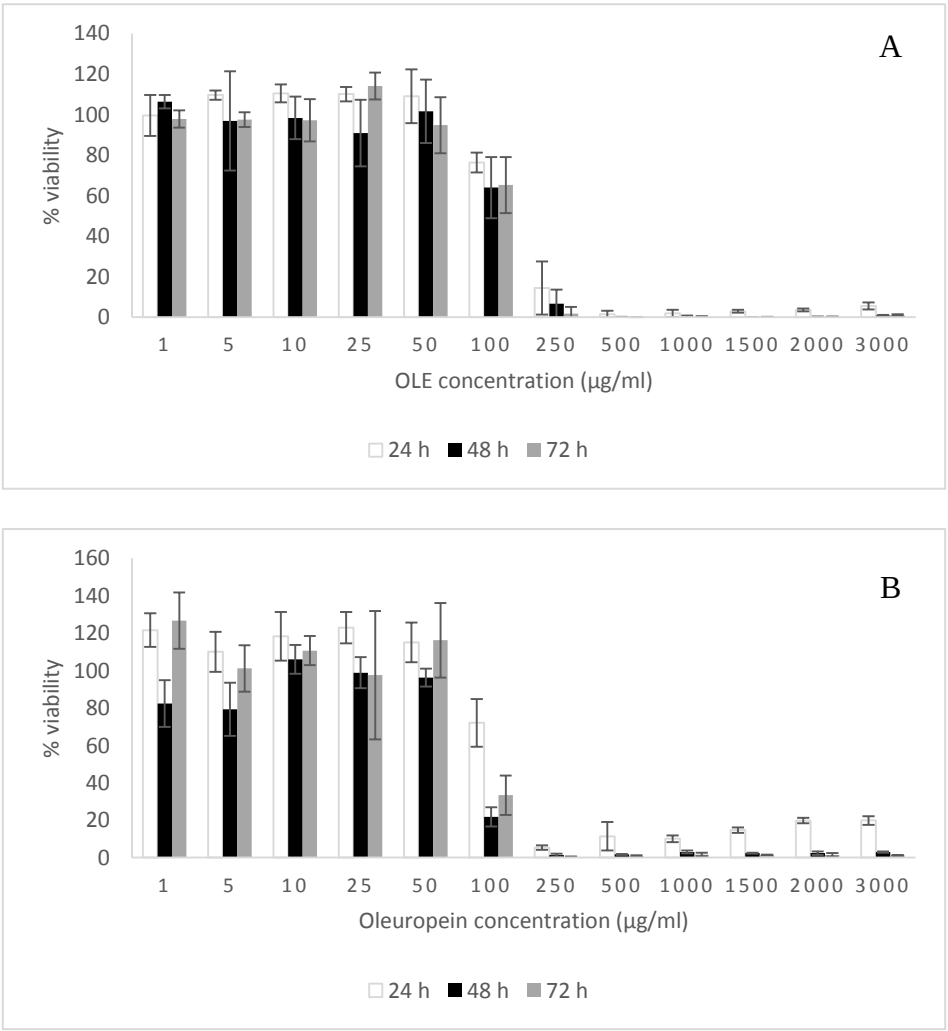

Figure 5.7. Cytotoxic profile of A. Crude olive leaf extract, B. Oleuropein standard

Concentrations of fractions were based on active compounds present in each fraction. Concentration range of fractions for cytotocixity assay was determined based on percent abundance of each active compound in related fraction. For example; hydroxytyrosol consisted 0.6% of crude extract, meaning there was 0.6 mg hydroxytyrosol in 100 mg crude extract. Range of fraction concentrations was calculated by proportioning original crude extract with percentages of active compounds in fractions. Results of cytotoxicity assay were shown in Figure 5.8. Fractions did not

exhibit cytotoxic activity up to 1500 µg/ml equivalent, contrary to crude extract which exhibited cytotoxic activity at lower concentrations as 250 µg/ml. This condition may be attributed to synergistic effect of active compounds in crude extract.

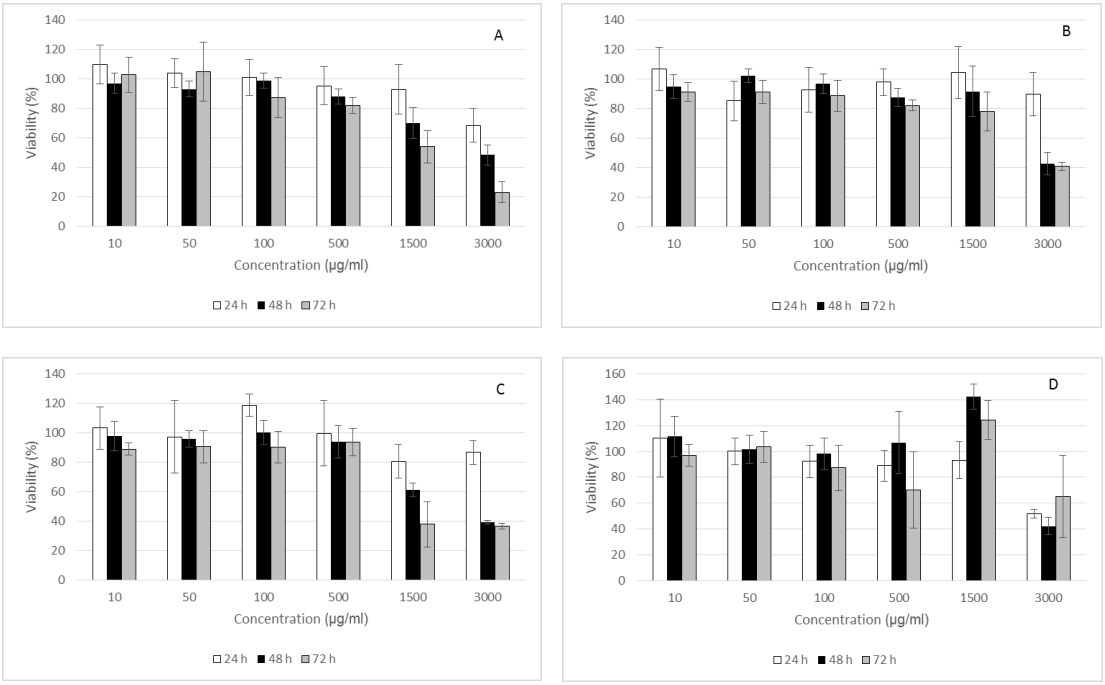

Figure 5.8. Cytotoxic profiles of fractions. A. Hydroxytyrosol- containing Fr2, B. Verbascoside- containing Fr4, C. Oleuropein- containing Fr5, D. Luteolin-containing Fr6

Free radicals are generated due to oxygen consumption in cell growth. The interaction of generated oxygen free radicals with lipid molecules results in formation of superoxide, hydroxyl and lipoid peroxides which may exhibit cytotoxic effect on biological systems (Lee et al., 2009). Scavenging ability of olive leaf extract prevents the cytotoxic activity of free radicals up to a critical concentration where redox balance could not be maintained beyond. Because cells require a redox-balanced environment to maintain a healthy status, the treatment of the cells with a high level of extract which possesses strong antioxidation capacity and high total phenol content, can remove the basal level of reactive oxygen species (ROS) in cells needed for maintaining general health. Thus a redox imbalance occurs resulting in a state hypo-oxidative condition (Pan et al., 2011). An imbalance between generation and removal of ROS can cause an oxidative stress in which excess ROS attacks and damages virtually all biomolecules in the cells, leading to cell death and serious chronic diseases (Scandalios, 2005).

5.1.5 Effect of Olive Leaf Extract and Its Fractions on Cell Migration and Wound Healing

Fibroblast cells were subjected to wound scratch assay in order to determine the effect of crude OLE and its fractions on cell migration and wound closure. Assay was considered to be applied in two parts, under stress-free conditions and under stress conditions via addition of exogenous H_2O_2. Among reactive oxygen species (ROS), H_2O_2 is the most stable oxidant, and it can diffuse across cellular membranes through water channels and causes oxidative protein modifications (Henzler et al., 2000). Therefore, H_2O_2 is often selected as a model agent for oxidation studies.

To determine the concentrations of H_2O_2 to be used for migration assays which are not harmful to the cells, we used MTT assay to examine the effect of 1–1000 μM H_2O_2 on the viability of cells. The range of applied H_2O_2 concentrations and cytotoxic activity on fibroblast cells were indicated in Figure 5.9. H_2O_2 doses up to 50 μM had no adverse effect on cell viability as Alexandrova et al. (2006) reported in a study performed on rat fibroblast cells. It was reported that 50 μM H_2O_2 could increase Ras activity and enhance cell adhesion and cell motility. Haendeler et al. (2004) also indicated that H_2O_2 concentrations between the range of 10–50 μM H_2O_2 was protective for endothelial cells, whereas 100 μM H_2O_2 exerted cytotoxicity.

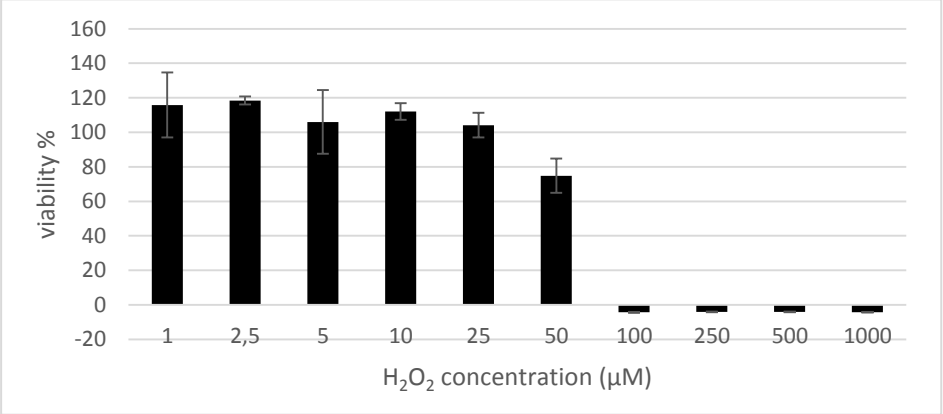

Figure 5.9. Cytotoxic profile of varying H_2O_2 concentrations.

After determination of cytotoxic profile of H_2O_2, a range of H_2O_2 concentrations was applied on fibroblast cells for wound scratch assay. Assay was performed for 5 days, changing the medium every 48 hours to prevent starvation. Wound closure percentage was calculated as follows;

Wound closure percentage (%) = $((D_0-D_x)/D_0)*100$

where D_0 denoted diameter of wound on the first day of assay and D_x denoted diameter of wound on determined time points. X denotes 1st, 3rd and 5th day of the assay in the calculations. Same equation was applied when crude OLE was applied on fibroblast cells in wound scratch assay. Figure 5.10 and 5.11 indicates the percentage of wound closure upon exposure to a range of H_2O_2 and OLE concentrations, respectively. H_2O_2 concentration of 100 µM did not provide wound closure during 5 days and wound diameter on 3rd and 5th days could not be measured due to loss of adherence in cells. Hence diameters of those wounds were noted as zero. Quantified data of wound closure percentage after H_2O_2 and OLE exposure on fibroblast cells are also depicted in Appendix D.

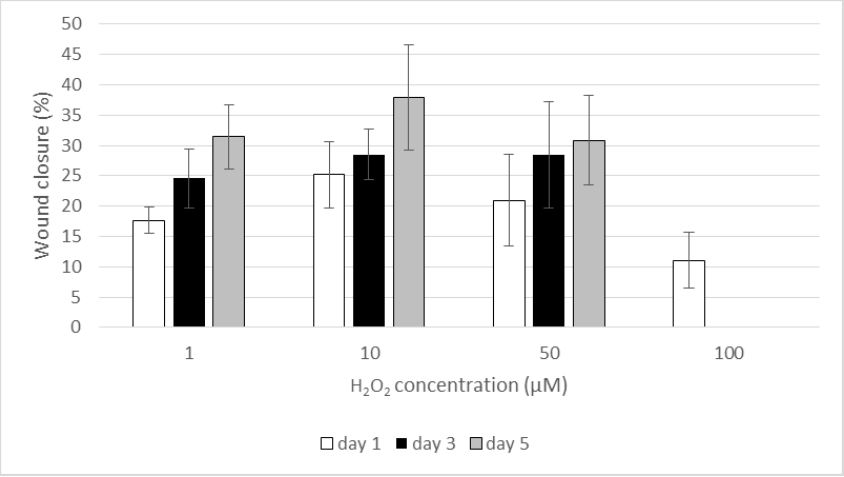

Figure 5.10. Wound closure percentage of fibroblast cells upon exposure to H_2O_2

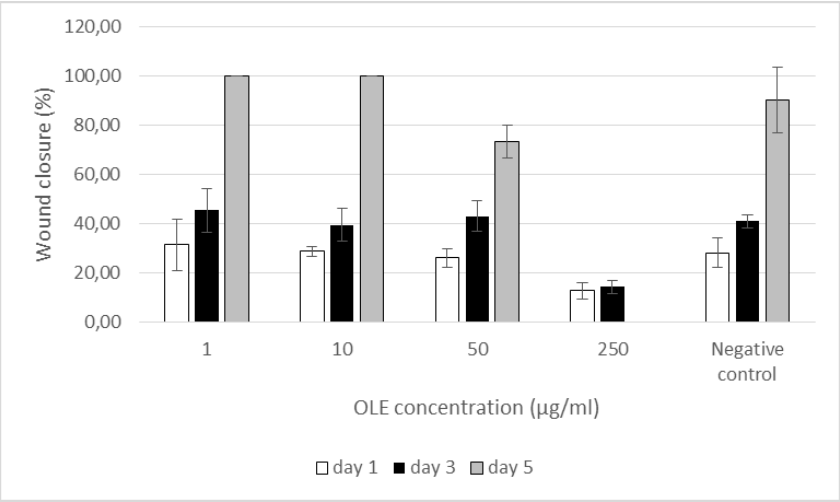

Figure 5.11. Wound closure percentage of fibroblast cells upon exposure to OLE

Pan et al (2011) investigated role of exogenous reactive oxygen species (ROS), generated by H_2O_2, at low concentrations on cultured primary rabbit corneal epithelial (RCE) cells, ex vivo model of pig eye cornea, and the in vivo model of mouse eye cornea. They found that cells treated with H_2O_2 at 20 µM showed no adverse effect on cell viability but actually stimulated adhesion and migration in cultured cells and enhanced pig eye cornea wound healing ex vivo as well as mouse cornea wound healing in vivo. These data show correlation with our findings in the aspect of tendency of cells to migrate under lower concentrations (between 1-50 µM) of H_2O_2. ROS can directly activate tyrosine kinase Src by oxidizing its two conserved Cys moieties during cell spreading in fibroblasts (Chiarugi et al., 2003, Giannoni et al., 2008). ROS also regulates integrin-extracellular matrix engagement by activating epidermal growth factor receptor, EGFR (Pan et al., 2011) to enhance cell adhesion and spreading (Giannoni et al., 2008)

Prior to determination of the effect of crude OLE and OLE fractions on wound healing under stress conditions, exogenous stress-free cells were exposed to crude OLE. Non-cytotoxic concentrations of OLE also exhibited wound healing by promoting cell migration, indicated as accelerated wound closure. Concentrations of 1 and 10 µg/ml OLE provided wound closure completely while 250 µg/ml OLE was not sufficient to perform wound healing effect due to its cytotoxic activity. Lower concentrations of OLE exhibited wound healing equivalent to negative control which was not exposed to OLE.

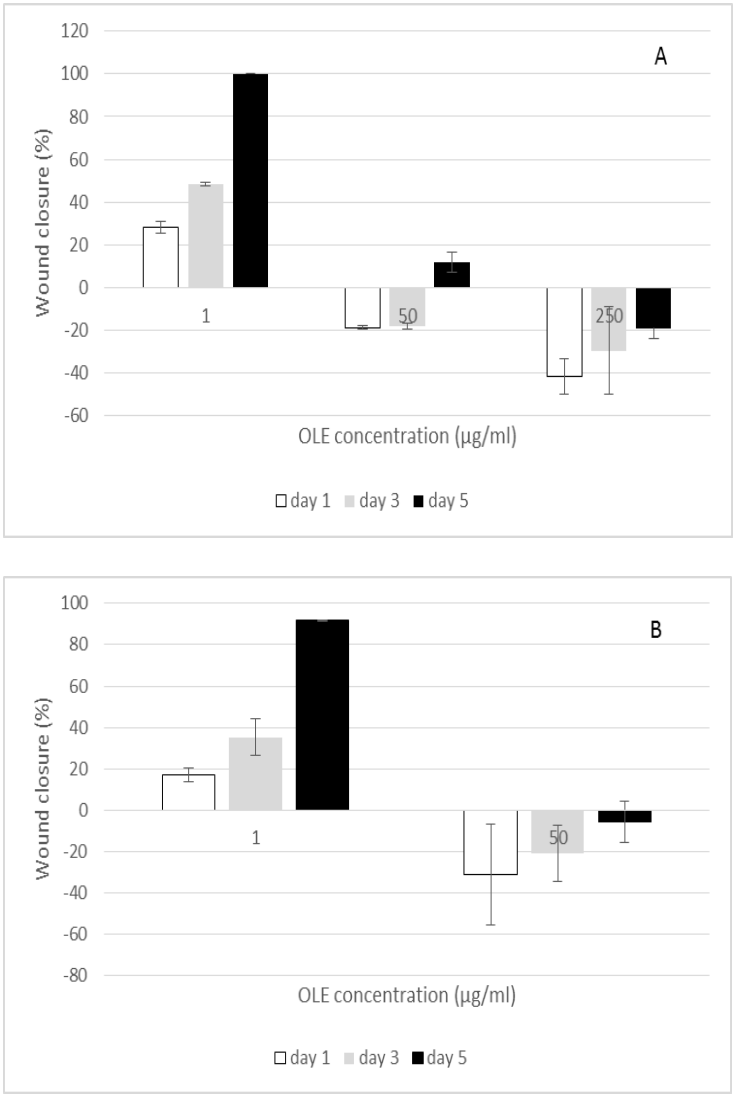

Figure 5.12. Wound closure percentage of fibroblast cells upon exposure to crude OLE under exogenous H_2O_2 of A. 1 µM and B. 50 µM.

Wound scratch assay performed under exogenous H_2O_2, combined with crude OLE on fibroblast cells showed that lower concentrations of H_2O_2 may promote cell migration and wound closure, in combination with low concentrations of crude extract (1 µg/ml) (Figure 5.12). When compared with results depicted in Figure 5.10, addition of OLE after H_2O_2 exposure performed a significant acceleration towards cell migration in a positive manner, perhaps scavenging with the generated oxidative stress. Tsuraya et al., (2014) performed a study on fibroblast cells pretreated with proanthocyanidin. As they induced the cells with hydrogen peroxide, generated oxidative stress was suppressed due to proanthocyanidin treatment. This study suggested antioxidant effect of polyphenols could directly scavenge oxidative stress. Pan et al. (2011) also performed a study with N-acetylcysteine (NAC), which had been considered as toxic to

cornea in previous studies (Huo et al., 2009) due to its over-antioxidation effect. They revealed that when NAC was administered alone, wound healing process was retarded due to toxic nature but administration with H_2O_2 promoted cell adhesion and migration, which in turn facilitated wound healing. Tsai et al. (2015) evaluated wound healing effect of citrus polyphenols on fibroblast cells. They treated the cells with a range of concentrations extending from 0.01% to 1% citrus polyphenol and recorded the motility of fibroblasts to the scratched area. As a result, cells treated with 0.01% polyphenol accelerated wound healing and reached to a confluent state after 2 days, in contrast to 1% polyphenol treatment due to increased cytotoxic activity.

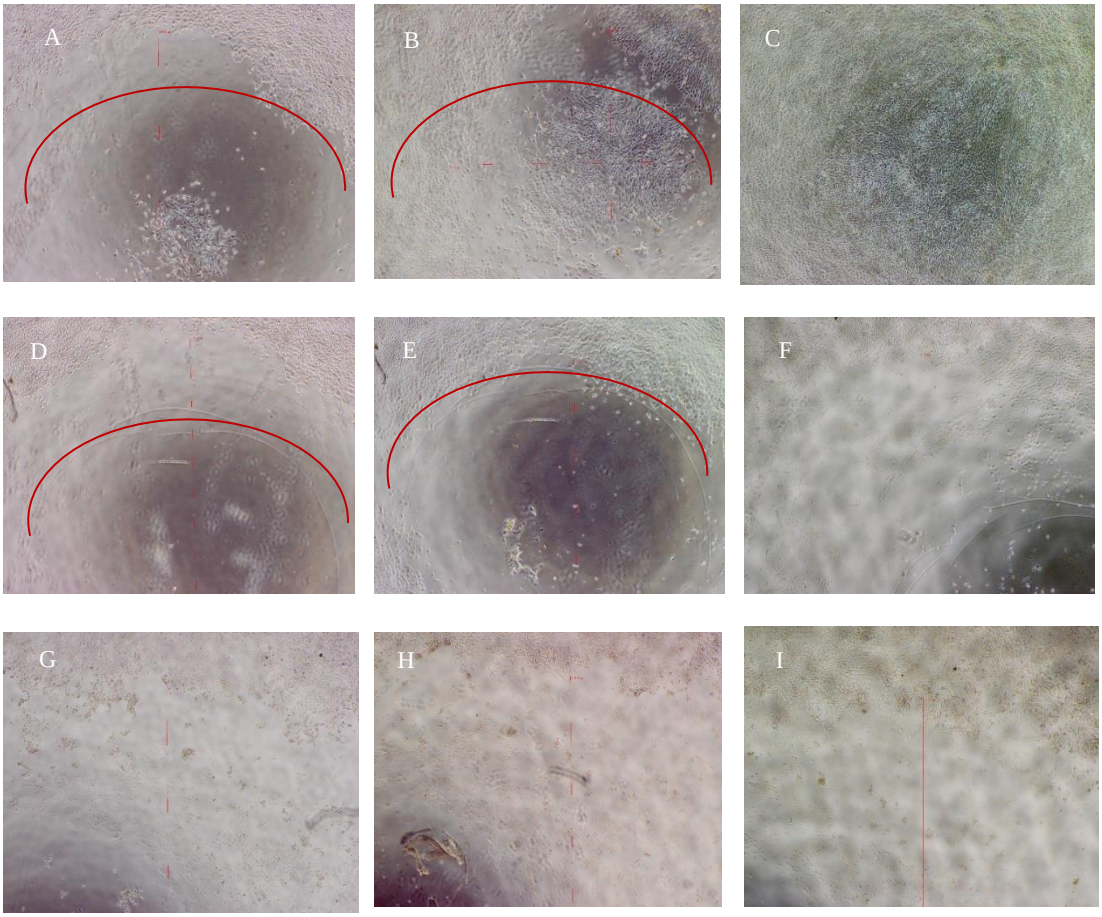

Figure 5.13. Micrographs of wound scratch assay. Cells were exposed to 1 µM H_2O_2 Micrographs were taken on 1st, 3rd and 5th days, denoted as A-C, D-F and G-I, respectively. Cells were treated with 1 µg/ml OLE: A-C, 50 µg/ml OLE: D-F and 250 µg/ml OLE: G-I. Red line indicates the border of wound area.

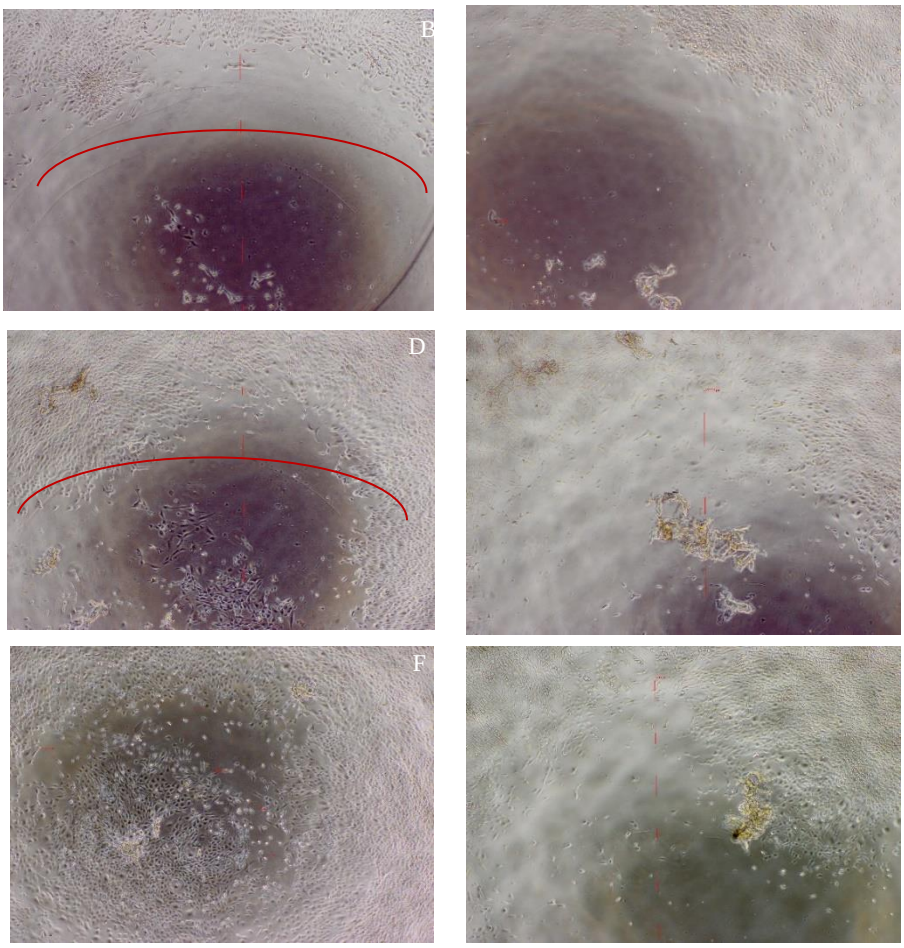

Figure 5.14. Micrographs of wound scratch assay. Cells were exposed to 50 µM H_2O_2 A and B denote the micrographs taken on 1st day, C and D denote 3rd day and E and F denote 5th day. Cells were treated with 1 µg/ml OLE: A-C, 50 µg/ml OLE: D-F and 250 µg/ml OLE: G-I. Red line indicates the wound area.

Table 5.3. Wound closure percentages of fibroblast cells on the 5th day after exposure to olive leaf extract fractions of various concentrations. Cells were pretreated with a range of H_2O_2 concentrations.

H_2O_2 concentration (μM)	1	10	50	100
fr2 concentration (μg/ml)				
1	47.26±5.53	44.95±4.92	49.91±13.07	47.29±6.65
10	100.00	74.04±8.73	24.23±4.47	35.61±6.12
50	28.52±1.07	53.15±3.81	100.00	15.77±2.47
fr4 concentration (μg/ml)				
1	65.45±9.3	31.85±3.56	66.69±5.85	35.50±8.86
10	100.00	100.00	31.60±7.81	60.39±1.08
50	78.30±6.23	20.54±4.55	26.71±6.76	23.39±5.4
fr5 concentration (μg/ml)				
1	89.87±9.56	100.00	25.12±5.22	N/A*
10	51.72±0.71	81.75±4.13	58.14±0.74	N/A*
50	35.55±1.34	30.82±6.18	20.15±1.21	N/A*
fr6 concentration (μg/ml)				
1	41.07±9.97	88.90±6.71	100.00	51.46±3.33
10	56.21±4.51	34.72±3.54	49.19±1.51	N/A*
50	38.78±5.51	11.65±5.36	N/A*	N/A*

* Denotes that diameter measurement could not be achieved due to loss of cell adherence

As the last part of wound scratch assays, fibroblast cells were treated with olive leaf extract fractions. Cells were pretreated with H_2O_2 concentrations between 1-100 μM for 1 hour. Table 5.3 denotes the wound closure percentages of the experimental setup. As an overview it can be concluded that combination of higher H_2O_2 concentrations (50 and 100 μM) with higher fraction concentrations (50 μg/ml) led to failure in wound closure, due to combination of high antioxidant level of fractions and high level of oxidative stress caused by H_2O_2. Scavenging ability of fractions were not sufficient to promote cell proliferation and migration for wound healing. Wound scratch assay performed with crude extract under exogenous H_2O_2 stress also indicated that combination of low extract concentrations and lower H_2O_2 concentration led to induced cell migration and wound closure, as depicted in Figure 5.13 and 5.14. In this case, cell migration promotion by H_2O_2 and proliferative effect of olive leaf extract and its

fractions may result in acceleration in wound closure. With respect to effect of fractions on wound healing, oleuropein-containing fraction 5 can be considered as having the highest potential to close the wound area by promoting cell migration. This fraction also exhibits the highest cytotoxicity at 50 µg/ml when applied after 100 µM H_2O_2 exogenous stress. The cells in this condition were not able to cover the wound area and diameter measurement could not be achieved as denoted by N/A wound closure percentage data obtained during 5 days' time period is given in Appendix D. Cell migration and wound closure period can be observed in photographs in the Appendix E.

Confocal micrographs, depicted in Figure 5.15, also indicated that lower concentrations of fractions did not affect mitochondrial membrane potential in a negative manner in the presence of exogenous stress. Membrane depolarization effect became obvious as fraction concentrations got higher. MitoRed, a membrane permeable rhodamine based dye, was used to stain mitochondrial membranes. Since this dye became brightly fluorescent upon accumulation in the mitochondrial membrane, it indicated live cells that exhibited mitochondrial membrane integrity. Lower concentrations of olive leaf extract fractions exhibited scavenging activity sufficient to maintain membrane integrity and they also promoted cell proliferation to enhance migration. Higher concentrations of fractions contributed to membrane depolarization effect of exogenous stress by altering redox potential, which in turn affected cell viability negatively.

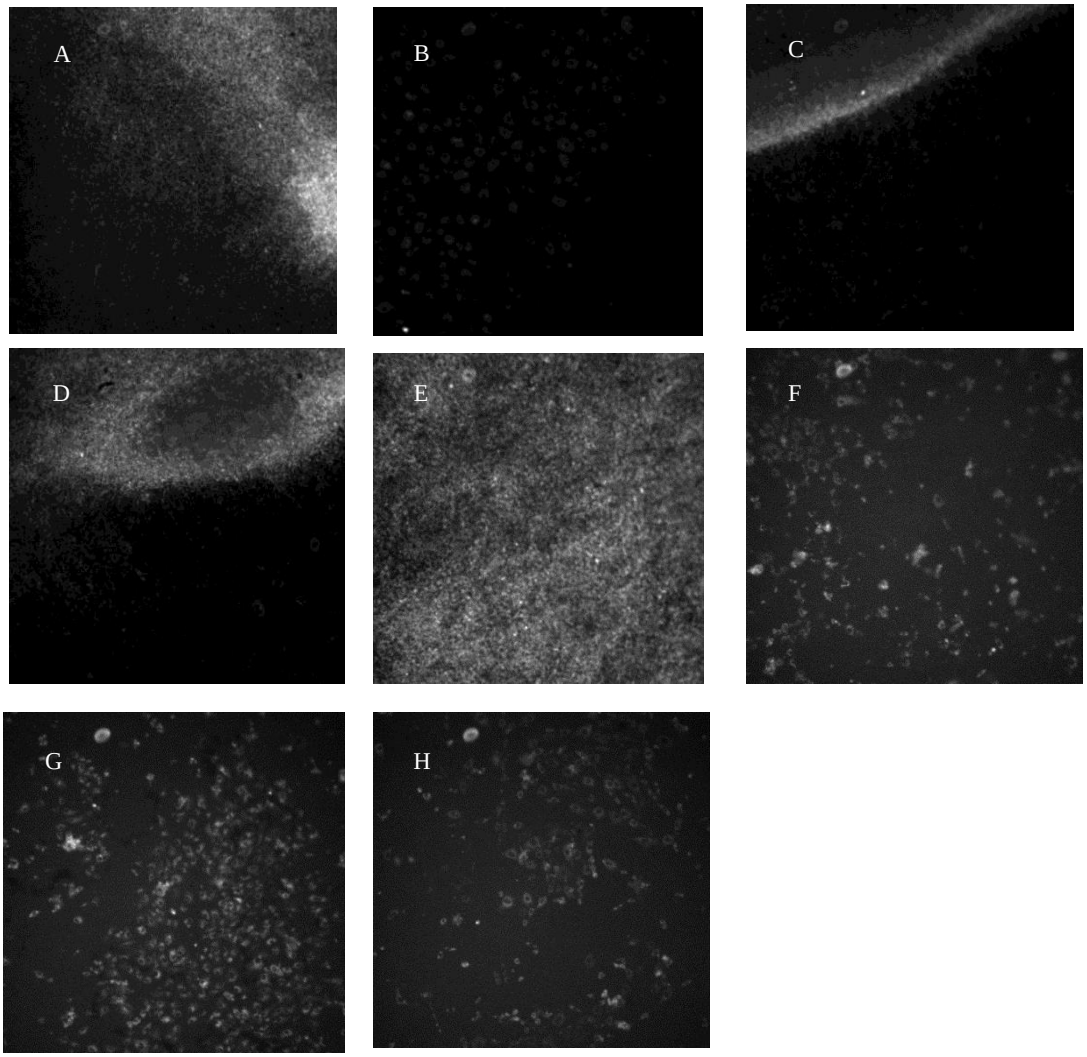

Figure 5.15. Confocal microscopy micrographs of wound scratch assay. Cells were exposed to 100 μM H_2O_2. Micrographs were taken on 3rd day of the assay. Cells were treated with 1 μg/ml OLE: A, C, E and G, and 50 μg/ml OLE: B, D, F and H.

5.2. Fabrication of Zein Fibers

5.2.1 Fiber morphology

Zein fibers had diverse appearance ranging from bead formation to ribbon-shaped morphology due to the increased zein content as observed in SEM micrographs (Figure 5.16). Bead formations were dominant in fibers having 20% zein content dissolved in 70% aqueous ethanol solution. Beads were converted into fibers as zein content of the solution increased. Ribbon shaped fibers were observed with an increase in zein content, most abundantly in fibers having 40% zein. Koombhongse et al. (2001) defined the beads as "toroids" and the ribbon shapes as collapsed tubular skins. They explained the fact as evaporation of the solvent while atmospheric pressure collapsed the tube, the tube became flat and formed a ribbon shape afterwards. Arinstein and Zussman (2007) also explained this phenomenon as "fiber buckling" which resulted from rapid evaporation of the solvent. They stated that when solvent evaporated rapidly, polymer formed a "shell" around the fiber that resisted solvent evaporation. This resistance resulted inhomogeneous pressure distribution. Residual solvent in the fiber prevented deformation in the fiber at initial stage. As evaporation proceeded, pressure drop across fiber shell was developed due to increase in external pressure. With the removal of solvent, fiber showed tendency to deform by means of buckling.

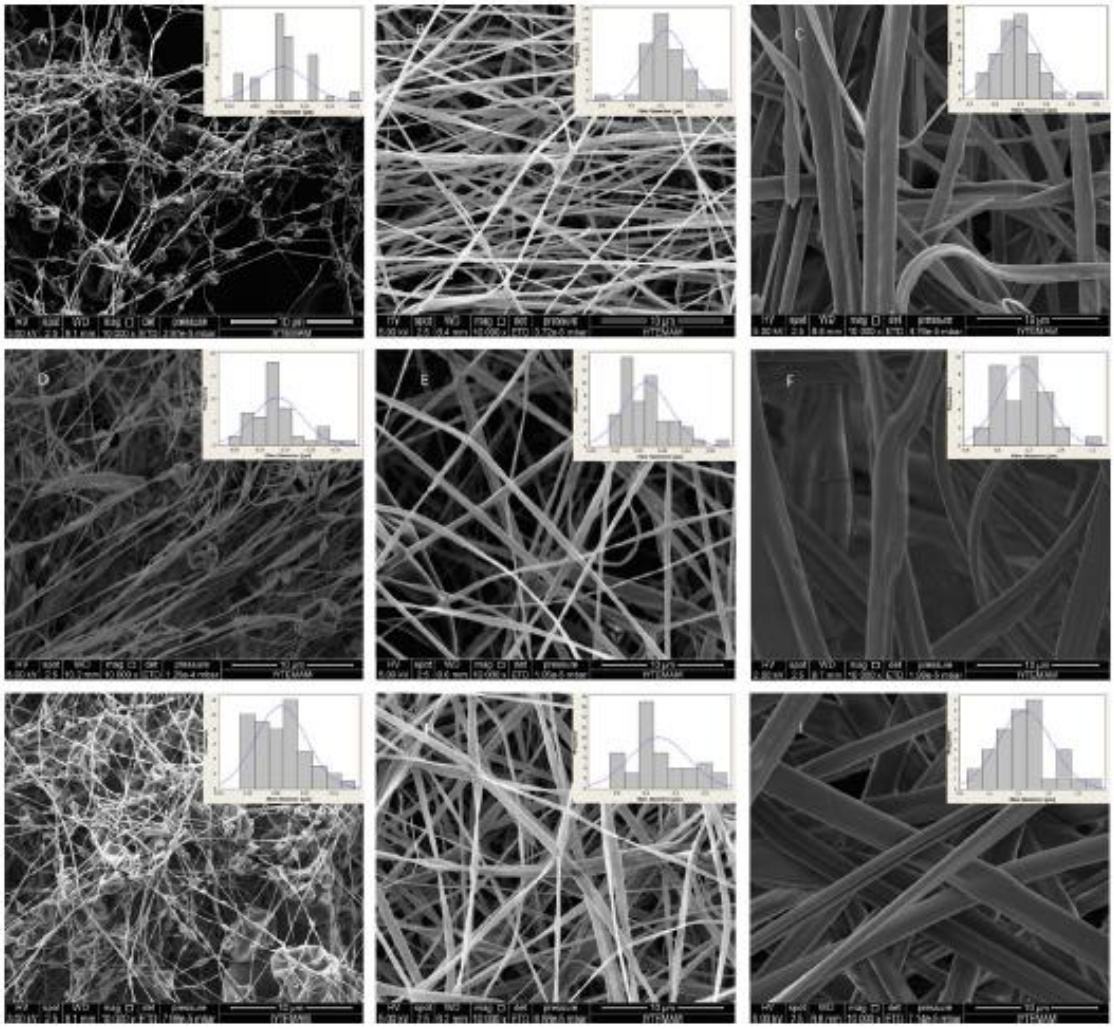

Figure 5.16. The morphology of fibers prepared at varying zein concentrations and applied voltage in 70% aqueous ethanol solution. Applied voltage is A-C: 15 kV, D-F: 20 kV and G-I: 25 kV. Zein concentrations are 20% for A, D and G, 30% for B, E and H, 40% for C, F and I. Scale bar is 10 μm.

The average diameters of zein fibers also showed that fiber diameter was mostly affected by zein content of the electrospinning solution. The average diameters of zein fibers prepared at varying conditions are tabulated in Table 5.4. When the average diameters of 50 zein fibers were evaluated, it can be seen that average fiber diameter increased ten times as zein content was increased from 20 to 40% (w/v). Increase of standard deviations in direct proportion to zein content of the solution, as seen in Table 5.4, also indicated that the uniformity of the fiber diameter distribution was decreased. This observation indicates that homogeneous fiber morphology can be obtained under process conditions of 30% zein content (w/v). Increase in fiber diameter under increasing voltage can be explained by decreased distribution of bead formation. It can

be seen that bead formation is mostly dominant under working voltage of 15 kV when zein concentration was 20% and fiber formation began to emerge as voltage was increased to 25 kV. Solvent content also affected fiber diameter due to influence on net volume charge density of electrospun jet. Torres-Giner et al.(2008) stated that increasing ethanol content caused increase in fiber diameter because of increase in evaporation rate and facilitation in solidification and formation of fibers. They also noted that this increasing effect was significant as ethanol content was superior to 80%, which align with our findings depicted in Table 5.4.

Table 5.4. The average diameter of fibers prepared at different process parameters.

Parameter	Values	Average diameter (μm) (± standard deviation)
Zein [a] (%) (w/v)	20	0.13±0.05
	30	0.37±0.16
	40	1.44±0.62
Ethanol [b] (%) (v/v)	70	0.48±0.20
	80	0.65±0.24
	90	0.81±0.36
Voltage[c] (kV)	15	0.22±0.07
	20	0.37±0.16
	25	0.48±0.20

Constant values for the parameters were [a] 70% aqueous ethanol solution and 20 kV voltage, [b] 30% zein content and 25 kV voltage, [c] 70% aqueous ethanol solution and 30% zein content.

In this study, zein content was found to be the most influencing factor for the diameter of electrospun zein fibers in accordance with the findings in the related literature. Fiber diameter decreased with a decrease in zein content, with the lowest for the fibers prepared from 70% aqueous ethanol solutions having 20% zein content. Bead formation did not allow regular fiber formation.

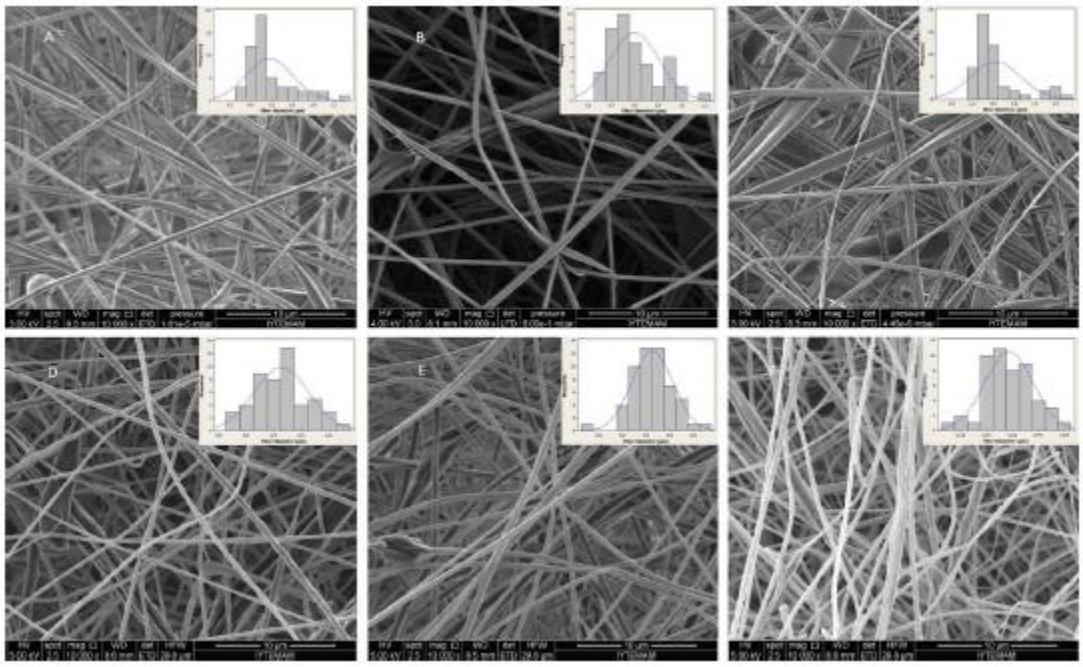

Figure 5.17. The morphology of OLE loaded fibers prepared at varying conditions. A-C: fibers prepared with lyophilized extract; D-F: fibers prepared with extract in aqueous ethanol solution. Solutions consist of 30% zein in 70% aqueous ethanol. OLE concentrations are 5% for A and D, 7.5% for B and E, 10% for C and F. Fibers were prepared under 20 kV. Scale bar is 10 μm.

Effect of olive leaf extract was also reflected on fiber morphology. Ribbon-shaped zein fibers without extract were replaced with curved form in OLE-loaded zein fibers due to possible crosslinking effect of oleuropein (Figure 5.17). Yao et al. (2007) also revealed that zein fibers were curved when crosslinked with tetrahydrofuran containing 1% hexamethylene diisocyanate (HDI). When the effect of lyophilized and aqueous ethanol phase of OLE were compared, a decrease in fiber diameter could be observed in fibers prepared with OLE in aqueous ethanol solution (Table 5.5). The increasing amount of OLE caused significant decrease in fiber diameter as well. When zein fibers with and without OLE that were produced under the same process parameters were compared, it was observed that fiber diameter was decreased between the range of 17% and 27%. The difference of standard deviations between the diameters of the fibers prepared from solutions containing dry powder and aqueous ethanolic extract also indicated that fiber morphology was more homogeneous when aqueous ethanolic extract was used in fiber preparation. Difference in fiber morphology and diameter distribution in OLE-loaded zein solutions was based on extract form used in

polymer mixture. Aqueous ethanolic extract caused decrease in fiber diameter in proportion with extract concentration, while dry powder extract did not cause decrease in fiber diameter.

Fibers in ribbon shape were dominant in case of dry powder extract utilization, but zein fibers were transformed to more curved like morphology in aqueous ethanolic extract usage. These differences emerged from integration of extract with the polymer solution. Aqueous ethanolic extract showed a better integration with zein than dry powder extract, which led to more homogeneous mixture of polymer and crosslinker.

Table 5.5. Diameter of fibers prepared with different concentrations and phases of OLE. Zein concentration was kept constant at 30% (w/v) and fibers were formed under voltage of 20 kV.

Extract phase used in preparation	Extract concentration (%) (w/w)	Average diameter (μm) (± standart deviation)
Dry powder extract	5	0.58±0.22
	7.5	0.60±0.21
	10	0.62±0.24
Aqueous ethanolic extract	5	0.43±0.10
	7.5	0.43±0.09
	10	0.31±0.07

Fractions of olive leaf extract were also incorporated into zein polymer solutions as aqueous phase at a concentration equivalent to active component content in 10% olive leaf extract. Electrospun fibers were analyzed by SEM, and it was indicated that fiber formation was achieved by OLE incorporation (Figure 5.18). Individual fractions did not transform the fibers from ribbon-shape to thinner fiber formation as crude extract did, indicating synergistic effect of compounds as a whole on fiber morphology. Fiber diameters in Table 5.6 also indicates synergistic extract effect.

Table 5.6. Diameter of fibers prepared with zein, OLE and fractions of OLE. Zein concentration was kept constant at 30% (w/v) and OLE concentration was 10%. Active compound amount in each fraction was equivalent to the amount in 10% OLE. Fibers were formed under voltage of 20 kV.

Sample	Average diameter (μm) (± standard deviation)
Fraction 2	0,68±0,15
Fraction 4	0,98±0,24
Fraction 5	0,81±0,19
Fraction 6	0,93±0,22
OLE	0,46±0,09
Zein only	0,71±0,15

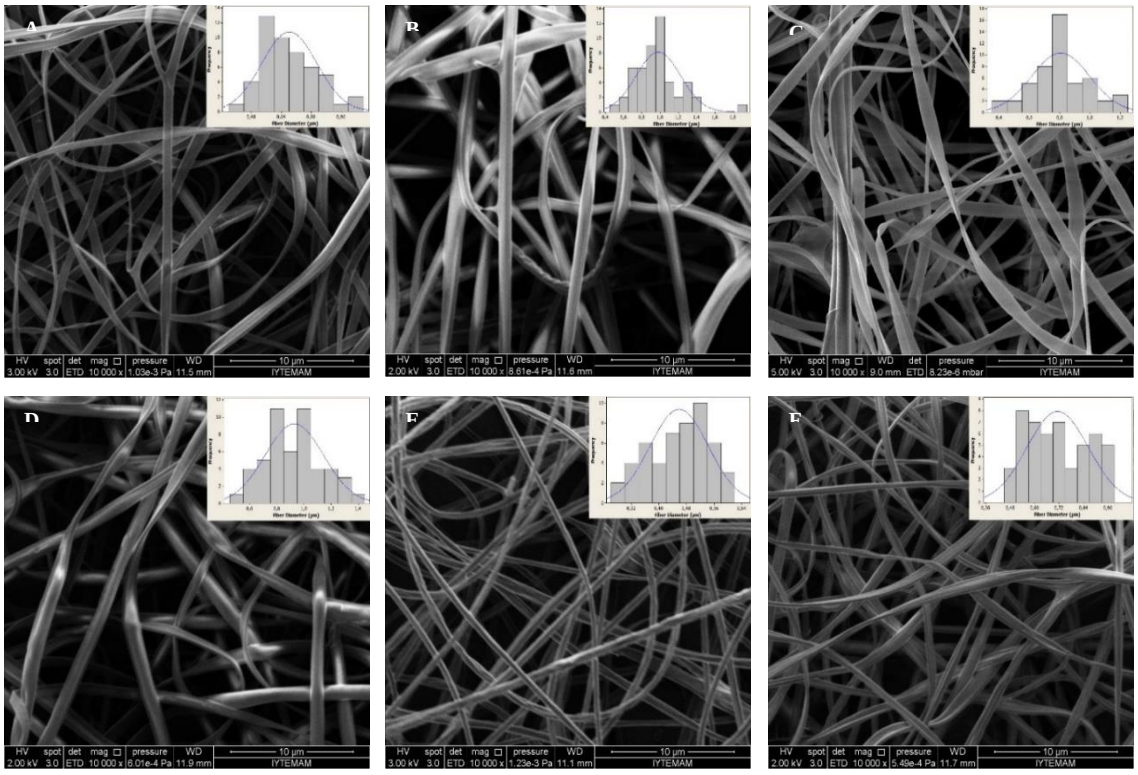

Figure 5.18. The morphology of fibers with A: Fraction 2, B: Fraction 4, C: Fraction 5, D: Fraction 6, E: OLE, F: Zein. Solutions consist of 30% zein in 70% aqueous ethanol. OLE concentration was 10% and active compound amount in fractions was equivalent to crude extract. Fibers were prepared under 20 kV. Scale bar is 10 μm.

5.2.2 Fourier Transform Infrared Spectroscopy (FT-IR)

OLE-incorporated zein fibers were subjected to FT-IR spectroscopy to observe the differences in bond structure as an indicator of crosslinking effect. Zein proteins show a typical absorption referring amide I band between 1600-1690 cm^{-1}, amide II between 1480-1575 cm^{-1} and amide III between 1229-1301 cm^{-1} (Georget et al, 2006, Sessa et al, 2008, Adochitei et al, 2011). These characteristic bands of peptide backbone were observed in zein fibers at 1665, 1545 and 1269 cm^{-1} for amide I, II and III respectively and can be seen in Figure 5.19. Each band was marked with a vertical line. Intensity difference of amide bands between zein fibers containing OLE and pure zein fibers used as control is an indicator of change in bond structure. Intensity increase of the band in the region of 3200-3500 cm^{-1} and peak at 1643 cm^{-1} also indicated OLE incorporation into fibers when FT-IR spectra of OLE loaded and pure zein fibers were compared. Specifically, fibers prepared with aqueous phase of OLE exhibited higher intensities in comparison with fibers prepared with lyophilized OLE, which might indicate better incorporation and bond formation. The region between 3200-3500 cm^{-1} and peak at 1643 cm^{-1} represent NH bending of amide groups (Haroun et al, 2010) of protein which interacts with hydroxyl (-OH) groups of polyphenols as a possible crosslinking interaction. Band intensity differences between fibers prepared with lyophilized and aqueous form of OLE might result from homogeneity of extract in preparation of electrospinning solutions. Aqueous form of OLE was more integrated into zein structure. More homogenous electrospinning solutions were formed since aqueous ethanol phase of extract was used as solvent which provided better integration of the extract and polymer. Olive leaf extract incorporation was also reflected in comparison of oleuropein and zein fibers' FT-IR spectra. Typical oleuropein band at 1090 cm^{-1} (Bayçın et al, 2007), indicated by Line 4 was present in zein fibers prepared with both lyophilized and aqueous ethanol phase of OLE. As expected, oleuropein band was not observed in the FT-IR spectrum of pure zein fibers. The results overall indicated that zein fibers prepared with aqueous form of OLE was incorporated into zein structure successfully at a higher degree with a potential of crosslinking reaction.

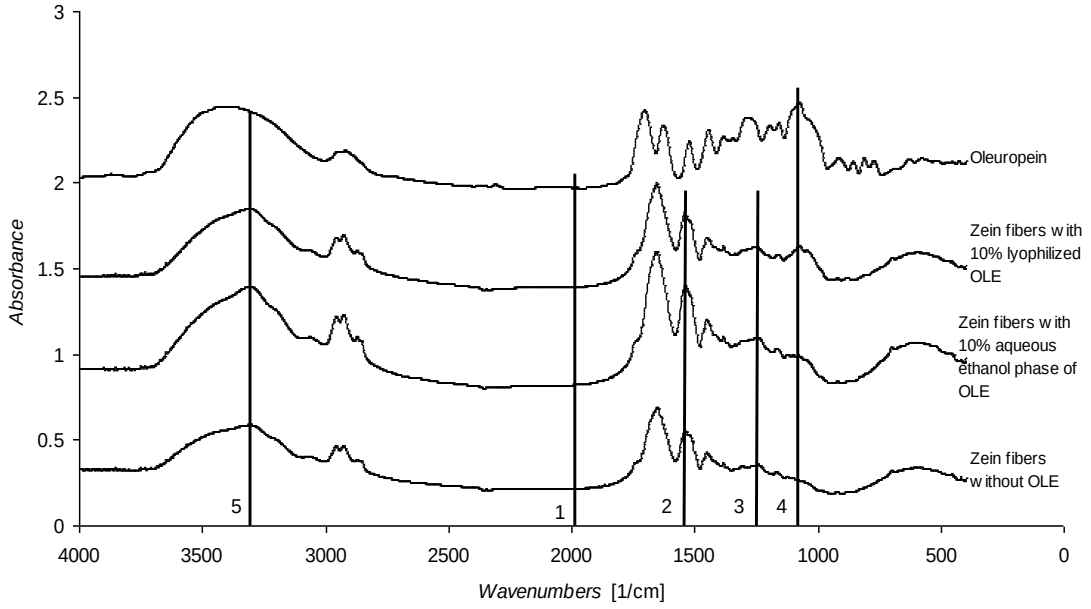

Figure 5.19. FT-IR spectra of zein fibers with and without OLE and oleuropein standard. Electrospinning solutions were prepared in 70% aqueous ethanol containing 30% zein. The applied voltage was 20 kV. Vertical lines 1, 2 and 3 represents characteristic zein bands; amide I, II and III respectively. Vertical line 4 refers to oleuropein and vertical line 5 represents the interactions between polyphenols in olive leaf extract and zein protein.

5.2.3 Thermogravimetric Analysis (TGA)

Thermogravimetric analysis (TGA) was used to evaluate and compare thermal stabilities and decomposition behavior of zein fibers, aqueous ethanol phase of OLE incorporated zein fibers and OLE as seen in Figure 5.20.

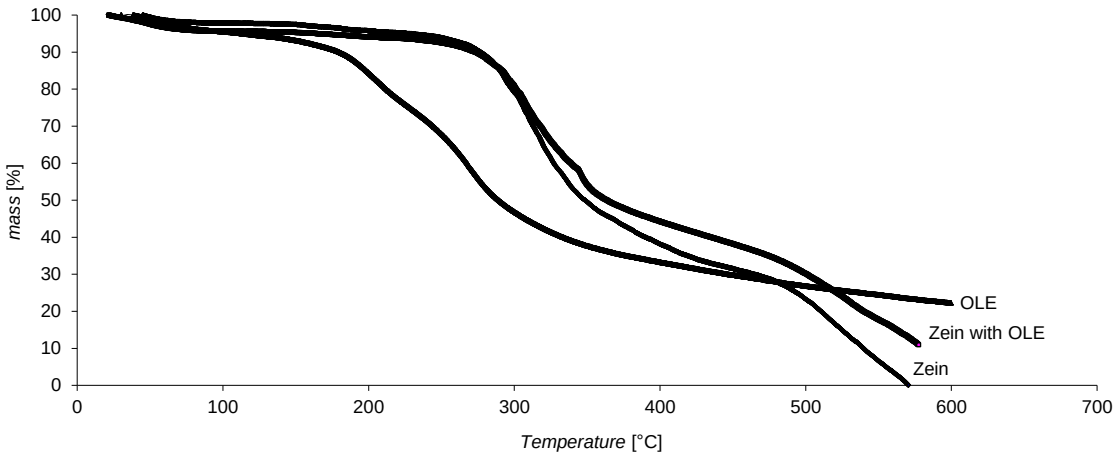

Figure 5.20. TGA thermogram of zein fibers, aqueous ethanol phase of OLE incorporated zein fibers and OLE. OLE in aqueous ethanolic phase contained 10% dry matter.

Initial weight loss of 10% was observed between 50 and 150°C, which was attributed to vaporization of water from the samples. The second weight loss occurred at 300°C as 50% for zein and OLE loaded zein fibers, related to thermal degradation of polymer structure, in agreement with other studies (Torres-Giner et al., 2008). OLE showed different degradation profile within the same temperature range, initial mass loss due to water evaporation, an additional mass loss of 55% occurred at 180°C and degradation rate decreased after 300°C. OLE had 22% of mass undegraded at 600°C at the end of analysis and it was estimated that degradation would be complete at temperatures higher than 800°C. The degradation profile of zein and OLE-incorporated zein fibers also differed after 300°C, as degradation rate of zein was higher than OLE-incorporated zein fibers. Zein was fully degraded at 600°C while OLE-incorporated zein fibers still had 10% of its mass undegraded. Mixing aqueous ethanol phase of OLE with zein may have caused irreversible changes in the structure that increase the mechanical properties and establishing resistance to thermal degradation as well.

5.2.4 *In vitro* release studies and fluid uptake properties of the fiber

The release study was performed by two methods as *in situ* continuous measurement and batch release. *In situ* continuous measurement was performed in order to observe saturation in the system. Zein fibers prepared with OLE in aqueous ethanol phase, containing 10% dry matter, were used for both continuous and batch release

measurements. Zein fibers prepared without OLE were used as blank and the blank subtracted values were used in calculations. Figure 5.21 shows cumulative OLE release in terms of concentration, which was calculated using OLE calibration curve. The profile indicated that there was a continuous release from OLE-incorporated zein fibers, offering sustained release of incorporated compounds. The released amount of extract in elapsed time was not sufficient for the system to reach saturation.

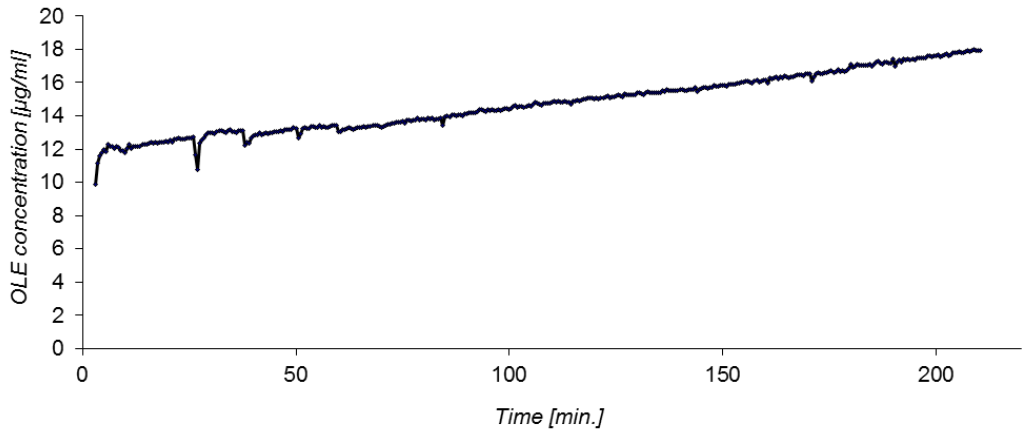

Figure 5.21. *In-situ* cumulative release of OLE from zein fibers.

Fiber samples were also immersed in deionized water to perform batch release during 6 days. Release media were subjected to total phenol analysis to determine the phenolic properties of the extract after release. Figure 5.22 shows the amount of the soluble phenolic compounds in Gallic Acid Equivalent (GAE). It was observed that amount of phenolic compounds in release media of OLE-incorporated zein fibers increased in a time-dependent manner. Soluble phenolic content reached to highest level in 8 days. Zein fibers released approximately 50% of initial phenolic content at the end of 8 day period. The results of *in situ* measurement of OLE and soluble phenolic content determination might indicate that the excess amount of OLE deposited on the surface of the fibers was released in sustained manner. The high amount of soluble phenolics on the 8^{th} day of the batch release period might result from degradation of zein fibers in release media due to the burst release of OLE incorporated into fiber structure.

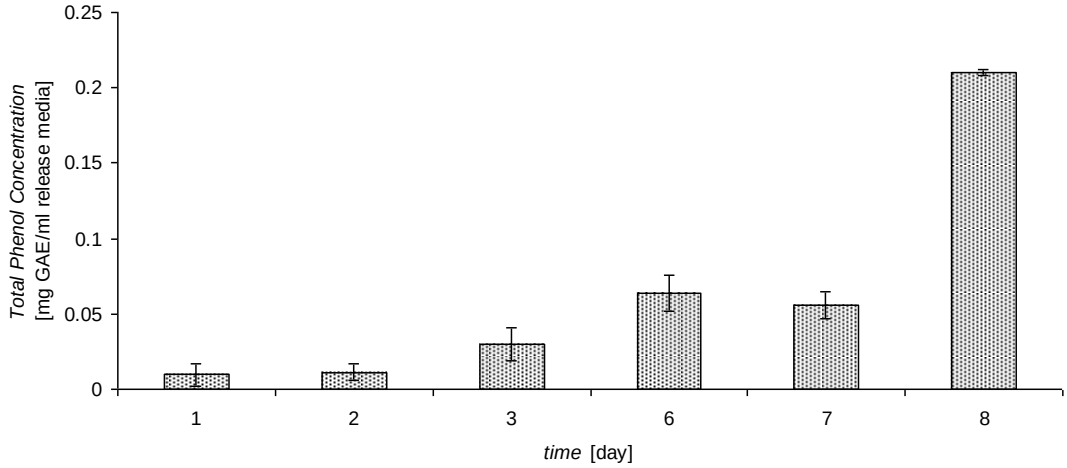

Figure 5.22. Batch release of OLE released from zein fibers in terms of GAE. Fibers contained aqueous ethanol phase of OLE with 10% dry matter.

Zein fibers after subjected to 6 days batch release were also investigated by SEM. Collapse of fiber formation and fused morphology were clearly observed in pure zein fibers (Figure 5.23a) while pore structures were present in OLE-incorporated fibers (Figure 5.23b). OLE incorporation caused decrease in fiber diameter since it integrated within zein structure, therefore swelling properties of the fibers also changed. Fiber structure was maintained in zein fibers containing OLE more than pure zein fibers, which may indicate crosslinking effect.

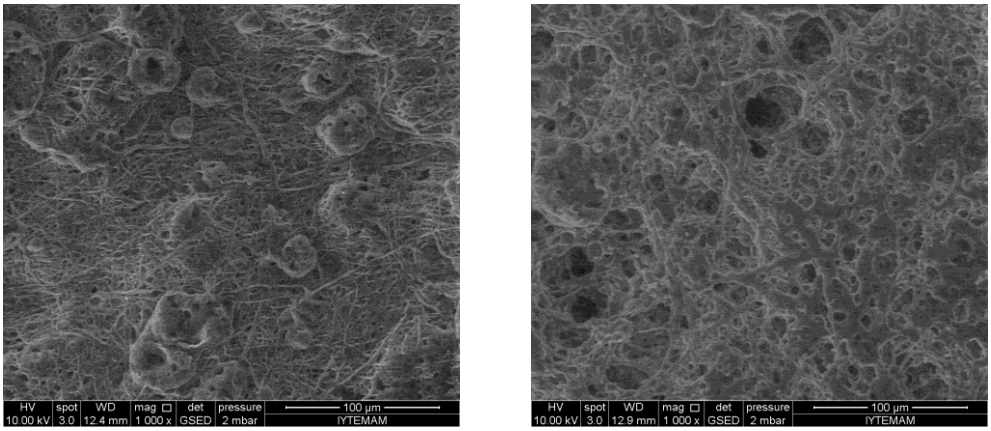

Figure 5.23. SEM micrographs of A. Zein fibers without OLE and B. OLE-loaded (10%) zein fibers after subjected to 6 days of batch release at 37°C. Scale bar is 100 μm.

5.2.5 Cell Attachment on Zein Fibers

Biocompatibility of OLE-loaded zein fibers was investigated by seeding NIH3T3 mouse fibroblast cells on fibers. Zein fibers without OLE was used as control. Figure 5.24A and 5.24B show cells on pure and OLE-loaded zein fibers, respectively. Cells were allowed to attach for 1 week. Attachment of the cells on pure zein fibers can be observed in Figure 5.24A by red arrows. Cells on pure zein fibers did not spread over fiber surface when compared to cells on OLE-loaded zein fibers. Morphology of cells on OLE-loaded zein fibers were also changed due to spreading which may indicate better proliferation of these cells (Figure 5.24B). It can be concluded that OLE addition enhanced fibroblast spreading and proliferation with regard to better fiber formation and providing higher surface area than pure zein.

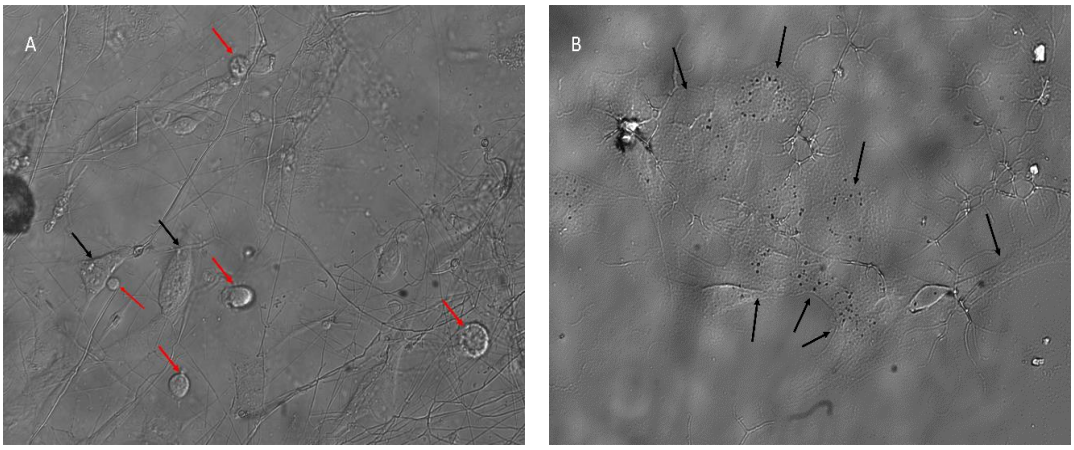

Figure 5.24. Phase contrast microscope images of cells seeded on A. Zein fibers without OLE and B. OLE-including zein fibers after 1 week of incubation. Red arrows indicate fibroblast cells that did not spread as black arrows show cells spread and proliferated better. Images were taken at a magnification of 20x.

CHAPTER 6

CONCLUSION

This study focused on characterization of olive leaf extract in terms of active compound content, antioxidant capacity and total phenolic content and correlation of these properties with cytotoxic activity and cell migration, within wound healing concept. Fractionation was also employed to obtain active compound-enriched parts of crude extract in order to understand whether the effect exerted by the extract was based on an individual compound or synergistic effect of all compounds.

Oleuropein, as the major component of the crude olive leaf extract, exhibited its dominancy in total phenolic content, antioxidant activity and cytotoxicity. Among four fractions, oleuropein-containing fraction 5 had the highest total phenolic content and antioxidant activity. This result may be attributed to its high abundance as well as presence of a functional group in its catechol structure. Cytotoxicity profile of standard oleuropein also showed similarities with cytotoxic activity of crude olive leaf extract, exhibiting approximate IC50 values. However, when wound healing was taken into consideration, crude olive leaf extract promoted cell migration better than its fractions. Results of wound scratch assay indicated that rate of cell migration and wound closure is higher when crude olive leaf extract was used, even under stress conditions generated by exogenous H_2O_2. Wound area was populated by fibroblast cells on the 3rd day of the assay when exposed to crude extract, while equivalent wound area could not be closed on the 5th day when same concentration of active compound-enriched fraction was used. Crude olive leaf extract also exhibited higher antioxidant activity and total phenolic content. When all these results are taken together, total amount of phenolic compounds analyzed may be more important for antioxidant activities of the olive leaf extracts and fractions than the amount of individual components. Further, possibility of unidentified phenolic compounds may also play roles in the antioxidative property and wound healing effect in relation with scavenging activity.

Olive leaf extract was also incorporated into zein, a biopolymer that has potential to be used as a wound dressing contact layer due to its hydrophobic nature and biocompability. The incorporation of olive leaf extract affected morphology, water

stability, bond structure and thermal properties of the electrospun zein fibers. The decrease in fiber diameters and homogeneous fiber morphology could be attributed to the effects of OLE, which are based on alterations in bond structure as depicted in FT-IR analysis and resistance to thermal degradation indicated by TGA analysis. As well as reinforcing water stability of zein fibers in aqueous media, which referred to crosslinker effect, OLE addition also functionalized zein fibers, due to sustained release of phenolic contents. OLE-loaded zein fibers were also found biocompatible with fibroblast cells which proliferated and spread on fiber surface better than pure zein. Our results are align with the findings of the related studies in the field. To the best of our knowledge, this is the first study to present olive leaf extract as a crosslinking agent in zein fibers which are commonly used in tissue engineering applications. In the light of these findings it can be proposed that olive leaf extract has a potential to be used as a crosslinker in zein fibers as well as providing functionality attributed to its high antioxidant capacity and antimicrobial property.

REFERENCES

Adochitei, A., & Drochioiu, G. (2011). Rapid characterization of peptide secondary structure by FT-IR spectroscopy. *Rev. Roum. Chim., 56*(9), 783-791.

Alexandrova, A.Y., Kopnin, P.B., Vasiliev, J.M., Kopnin, B.P. (2006). ROS upregulation mediates Ras-induced changes of cell morphology and motility. Exp Cell Res., 312(11), 2066–2073.

Al-Mustafa, A.H., & Al-Thunibat, O.Y. (2008). Antioxidant activity of some Jordanian medicinal plants used traditionally for treatment of diabetes. Pak J Biol Sci., 11(3), 351-358.

Altıok, E., Bayçın, D., Bayraktar, O., Ülkü, S. (2008). Isolation of Polyphenols from the Extracts of Olive Leaves (Olea europaea L.) by Adsorption on Silk Fibroin. *Separation and Purification Technology, 62*(2), 342-348.

Amiraliyan, N., Nouri, M., Kish, M.H. (2009). Effects of Some Electrospinning Parameters on Morphology of Natural Silk-Based Nanofibers. *Journal of Applied Polymer Science, 113*(1), 226–234.

Arinstein, A., Zussman, E. (2007). Post processes in tubular electrospun fibers. *Phys Rev E Stat Nonlin Soft Matter Phys., 76*(5).

Ashammakhi, N., Yang, Y., Ylikauppila, H., Nikkola, L. (2008). Nanofiber-based scaffolds for tissue engineering *Eur J Plast Surg*., *35*(2), 135-149.

Balasubramani, M., Kumar, T.R., Babu, M. (2001). Skin substitutes: a review. *Burns, 27*(5), 534–544.

Bayçın, D., Altıok, E., Ülkü, S., Bayraktar, O. (2007). Adsorption of Olive Leaf (Olea europaea L.) Antioxidants on Silk Fibroin. *J. Agric. Food Chem., 55*(4), 1227−1236.

Bellik, Y., Boukraâ, L., Alzahrani, H.A., Bakhotmah, B.A., Abdellah, F., Hammoudi, S.M. Iguer-Ouada, M. (2012). Molecular Mechanism Underlying Anti-Inflammatory and Anti-Allergic Activities of Phytochemicals: An Update. *Molecules, 18*(1), 322-353.

Benavente-Garcia, O.B., Castillo, J., Lorente, J., Ortuno, A., Del-Rio, J.A. (2000). Antioxidant Activity of Phenolics Extracted from Olea Europaea Leaves. *Food Chemistry, 68*(4), 457-462.

Boateng, J.S., Matthews, K.H, Stevens, H.N.E., Eccleston, G.M. (2008). Wound Healing Dressings and Drug Delivery Systems: A Review. *Journal of Pharmaceutical Sciences, 97*(8), 2892-2923.

Bourtoom, T. (2008). Edible flms and coatings: characteristics and properties. *International Food Research Journal*, 15(3).

Bölgen, N., Vargel, I., Korkusuz, P., Menceloğlu, Y.Z., Pişkin, E. (2006). In Vivo Performance of Antibiotic Embedded Electrospun PCL Membranes for Prevention of Abdominal Adhesions. *Journal of Biomedical Materials Research Part B: Applied Biomaterials, 81*(2), 530-543.

Buchanan, B.B., Gruissem, W., Jones, R.L. (2000). *Biochemistry & molecular biology of plants*: American Society of Plant Physiologists Rockville.

Bulotta, S., Oliverio, M., Russo, D., Procopio, A. (2013). *Natural Products*. Berlin, Heidelberg Springer-Verlag.

Chakraborty, S., Liao, I-C., Adler, A., Leong, K.W. (2009). Electrohydrodynamics: A facile technique to fabricate drug delivery systems. *Advanced Drug Delivery Reviews, 61*(12), 1043–1054.

Chen, W.Y.J., Abatangelo, G. (1999). Functions of hyaluronan in wound repair. *Wound Rep Reg., 7*(2), 79–89.

Chiarugi, P., Cirri, P. (2003). Redox regulation of protein tyrosine phosphatases during receptor tyrosine kinase signal transduction. *Trends Biochem Sci., 28*(9), 509–514.

Corradini, E., Mattoso, L.H.C., Guedes, C.G.F., Rosa, D.S. (2004). Mechanical, thermal and morphological properties of poly(e-caprolactone)/zein blends. *Polym. Adv. Technol., 15*(6), 340–345.

Cushnie, T.P., Lamb, A.J. (2005). Antimicrobial activity of flavonoids. *International journal of antimicrobial agents, 26*(5), 343-356.

Dai, J., Mumper, R.J. (2010). Plant phenolics: extraction, analysis and their antioxidant and anticancer properties. *Molecules, 15*(10), 7313-7352.

Das, K., Tiwari, R.K.S., Shrivastava, D.K. (2010). Techniques for evaluation of medicinal plant products as antimicrobial agent: Current methods and future trends. *Journal of Medicinal Plants Research, 4*(2), 104-111.

Dong, J., Sun, Q., Wang, J.Y. (2004). Basic study of corn protein, zein, as a biomaterial in tissue engineering, surface morphology and biocompatibility. *Biomaterials, 25*(19): 4691-4697.

Falanga V. (2004). The chronic wound: impaired healing and solutions in the context of wound bed preparation. *Blood Cells, Molecules, and Diseases, 32*(1), 88– 94.

Georget, D.M.R., Belton, P.S. (2006). Effects of temperature and water content on the secondary structure of wheat gluten studied by FTIR spectroscopy. *Biomacromolecules, 7*(2), 469-475.

Ghanbarzadeh, B., Oromiehi, A., Razmi-Rad, E. (2008). Surface Evaluation of Resin Zein Films Containing Sugar Plasticizers by Permeability and Atomic Force Microscopy Analysis. *Iranian Journal of Pharmaceutical Sciences, 4*(1): 23-30.

Giannoni, E., Buricchi, F., Raugei, G., Ramponi, G., Chiarugi, P. (2008). Intracellular Reactive Oxygen Species Activate Src Tyrosine Kinase during Cell Adhesion and Anchorage-Dependent Cell Growth *Mol. Cell. Biol., 25*(15), 6391-6403.

Gong, S., Wang, H., Sun, Q., Xu, S-T., Wang, J-Y. (2006). Mechanical properties and in vitro biocompatibility of porous zein scaffolds. *Biomaterials, 27*(20), 3793–3799.

Gurtner, G.C., Werner, S., Barrandon, Y., Michael Longaker T. 2008. Wound repair and regeneration. *Nature, 453*, 314-321.

Haendeler, J., Tischler, V., Hoffmann, J., Zeiher, A.M., Dimmeler, S. (2004). Low doses of reactive oxygen species protect endothelial cells from apoptosis by increasing thioredoxin-1 expression. *FEBS Lett., 577*(3), 427–433.

Hardy, J.G., Römer, L.M., Scheibel, T.R. (2008). Polymeric materials based on silk proteins. *Polymer, 49*(20), 4309‑4327.

Haroun, A. A., El Toumy, S.A. (2010). Effect of natural polyphenols on physicochemical properties of crosslinked gelatin-based polymeric biocomposite. *Journal of Applied Polymer Science, 116*(5), 2825-2832.

Hayes, J.E., Allen, P., Brunton, N., O'Grady, M.N., Kerry, J.P. (2011). Phenolic composition and in vitro antioxidant capacity of four commercial phytochemical products: Olive leaf extract (Olea europaea L.), lutein, sesamol and ellagic acid. *Food Chemistry, 126*(3), 948–955.

Henzler, T., Steudle, E. (2000). Transport and metabolic degradation of hydrogen peroxide in Chara corallina: model calculations and measurements with the pressure probe suggest transport of H_2O_2 across water channels. *J Exp Bot., 51*(353), 2053–2066.

Huo, Y., Qiu, W.Y., Pan, Q., Yao, Y.F., Xing, K., Lou, M.F. (2009). Reactive oxygen species (ROS) are essential mediators in epidermal growth factor (EGF)-stimulated corneal epithelial cell proliferation, adhesion, migration, and wound healing. *Exp Eye Res., 89*(6), 876–886.

Ifkovits, J.L., Burdick, J.A. (2007). Review: Photopolymerizable and Degradable Biomaterials for Tissue Engineering Applications. *Tissue Engineering, 13*(10): 2369-2385.

Ji, Y., Ghosh, K., Shu, X.Z., Li, B., Sokolova, J.C., Prestwich, G.D., Clark, R.A.F., Rafailovich, M.H. (2006). Electrospun three-dimensional hyaluronic acid nanofibrous scaffolds. *Biomaterials, 27*(20), 3782–3792.

Katti, D.S., Robinson, K.W., Ko, F.K., Laurencin, C.T. (2004). Bioresorbable nano-based systems for wound healing and drug delivery: Optimization of fabrication parameters. *J Biomed Mater Res B Appl Biomater, 70*(2), 286 –296.

Koombhongse, S., Liu, W., Reneker, D.H. (2001). Flat polymer ribbons and other shapes by electrospinning. *Journal of Polymer Science Part B: Polymer Physics, 39*(21), 2598 – 2606.

Kontogianni, V.G. Gerothanassis, I.P. (2011). Phenolic compounds and antioxidant activity of olive leaf extracts. *Nat. Prod. Res., 26*(2), 186–189.

Kweon, D-K., Song, S-B., Park, Y-Y. (2003). Preparation of water-soluble chitosan/heparin complex and its application as wound healing accelerator. *Biomaterials 24*(9), 1595–1601.

Lee, O-H., Lee, B-Y. (2010). Antioxidant and antimicrobial activities of individual and combined phenolics in Olea europaea leaf extract. *Bioresource Technology, 101*(10), 3751–3754.

Lee, O-H., Lee, B-Y., Lee, J., Lee, H-B., Son, J-Y., Park, C-S., Shetty, K., Kim, Y-C. (2009). Assessment of phenolics-enriched extract and fractions of olive leaves and their antioxidant activities. *Bioresource Technology, 100*(23)6107–6113.

Liu, X., Sun, Q., Wang, H., Zhang, L., Wang, J-Y. (2005). Microspheres of corn protein, zein, for an ivermectin drug delivery system. *Biomaterials, 26*(1), 109–115.

Liu, R.H. (2004). Potential synergy of phytochemicals in cancer prevention: mechanism of action. *The Journal of Nutrition, 134*(12), 3479S-3485S.

Madigan, M.T., Martinko, J.M., Dunlap, P.V., Clark, D.P. (2008). *Brock Biology of microorganisms* (12th ed.). San Francisco, Benjamin Cummings.

Malafaya, P.B., Silva, G.A., Reis, R.L. (2007). Natural–origin polymers as carriers and scaffolds for biomolecules and cell delivery in tissue engineering applications. *Advanced Drug Delivery Reviews, 59*(4-5), 207–233.

Markin, D., Duek, L., Berdicevsky, I. (2003). *In vitro* antimicrobial activity of olive leaves. *Mycoses, 46*(3-4), 132–136.

Matthews, J.A., Wnek, G.E., Simpson, D.G., Bowlin, G.L. (2002). Electrospinning of Collagen Nanofibers. *Biomacromolecules, 3*(2) 232-238.

Mathiowitz, E., Bernstein, H., Morrel, E., Schwaller, K. (1993). Method for producing protein microspheres. Patent US ed., vol. 5, 271, 961.

Min, B-M., Jeong, L., Nam, Y.S., Kim, J-M., Kim, J.Y., Park, W.H. (2004). Formation of silk fibroin matrices with different texture and its cellular response to normal human keratinocytes. *International Journal of Biological Macromolecules, 34*(5), 223–230.

Miyoshi, T., Toyohara, K., Minematsu, H. (2005). Preparation of ultrafine fibrous zein membranes via electrospinning. *Polym Int, 54*(8), 1187–1190.

Mustoe T. (2004). Understanding chronic wounds: a unifying hypothesis on their pathogenesis and implications for therapy. *The American Journal of Surgery, 187*(5A), 65–70.

Naasani, I., Oh-hashi, F., Oh-hara, T., Feng, W.Y., Johnston, J., Chan, K., Tsuruo, T. (2003). Blocking telomerase by dietary polyphenols is a major mechanism for limiting the growth of human cancer cells in vitro and in vivo. *Cancer research, 63*(4), 824-830.

Nisbet, D.R., Forsythe, J.S., Shen, W., Finkelstein, D.I., Horne, M.K. (2009). Review Paper: A Review of the Cellular Response on Electrospun Nanofibers for Tissue Engineering. *Journal Of Biomaterials Applications, 24*(1), 7-29.

Nobili, S., Lippi, D., Witort, E., Donnini, M., Bausi, L., Mini, E., & Capaccioli, S. (2009). Natural compounds for cancer treatment and prevention. *Pharmacological Research, 59*(6), 365-378.

O'Meara, S., Cullum, N., Majid, M., Sheldon, T. (2000). Systematic reviews of wound care management: (3) antimicrobial agents for chronic wounds; (4) diabetic foot ulceration. *Health Technology Assessment, 4*(21), 1-237.

Paiva, P.M.G., Gomes, F.S., Napoleão, T.H., Sá, R.A., Correia, M.T.S., Coelho, L. (2010). Antimicrobial activity of secondary metabolites and lectins from plants. *Current Research, Technology and Education Topics in Applied Microbiology and Microbial Biotechnology, Badajoz: Formatex*, 396-406.

Parris, N., Coffin, D.R. (1997). Composition Factors Affecting the Water Vapor Permeability and Tensile Properties of Hydrophilic Zein Films. *J. Agric. Food Chem., 45*(5), 1596−1599.

Pan, Q., Qiu, W-Y., Huo, Y-N., Yao, Y-F., Lou, M.F.(2011). Low Levels of Hydrogen Peroxide Stimulate Corneal Epithelial Cell Adhesion, Migration, and Wound Healing. *Investigative Ophthalmology & Visual Science, 52*(3), 1723-1734.

Pham, Q.P., Sharma, U., Mikos, A.G. (2006). Electrospinning of Polymeric Nanofibers for Tissue Engineering Applications: A Review. *Tissue Engineering, 12*(5), 1197-1211.

Purser K. 2010. Wound Dressing Guidelines. *Royal United Hospital Bath NHS Trust*.

Ramos-E-Silva, M., De Castro, M.C.R. (2002). New Dressings, Including Tissue-Engineered Living Skin. *Clinics in Dermatology, 20*(6), 715–723.

Sawadago, W.R., Schumacher, M., Teiten, M.H., Dicato, M., Diedreich, M. (2012). Traditional West African pharmacopeia, plants and derived compounds for cancer therapy. *Biochem Pharmacol. 84*(10), 1225-40.

Scandalios, J.G., (2005). Oxidative stress: molecular perception and transduction of signals triggering antioxidant gene defense. *Braz. J. Med. Biol. Res., 38*(7), 995–1014.

Schneider, A., Wang, X.Y., Kaplan, D.L., Garlick, J.A., Egles, C. (2009). Biofunctionalized electrospun silk mats as a topical bioactive dressing for accelerated wound healing. *Acta Biomaterialia, 5*(7), 2570-2578.

Sessa, D.J., Mohamed, A., Byars, J.A., Hamaker, S.A.H., Selling, G.W. (2007). Properties of Films from Corn Zein Reacted with Glutaraldehyde. *Journal of Applied Polymer Science, 105*(5), 2877–2883.

Shukla, R., Cheryan, M. (2001). Zein: the industrial protein from corn. *Industrial Crops and Products, 13*(3), 171–192.

Sibbald, R.G., Zuker, R., Coutts, P., Coelho, S., Williamson, D., Queen, D. (2005). Using a Dermal Skin Substitute in the Treatment of Chronic Wounds Secondary to Recessive Dystrophic Epidermolysis Bullosa: A Case Series. *Ostomy Wound Management, 51*(11), 22-46.

Sill, T.J., von Recum, H.A., Electrospinning: Applications in drug delivery and tissue engineering. *Biomaterials, 29*(13), 1989-2006.

Su, L., Yin, J.J., Charles, D., Zhou, K., Moore, J., & Yu, L.L. (2007). Total phenolic contents, chelating capacities, and radical-scavenging properties of black peppercorn, nutmeg, rosehip, cinnamon and oregano leaf. *Food Chemistry, 100*(3), 990-997.

Sudjanaa, A.N., D'Orazio, C., Ryan, V., Rasool, N., Ng, J., Islam, N., Riley, T.V., Hammer, K.A. (2009). Antimicrobial activity of commercial Olea europaea (olive) leaf extract. *International Journal of Antimicrobial Agents 33*(5), 461–463.

Tsuruya, M., Niwano, Y., Nakamura, K., Kanno, T., Nakashima, T., Egusa, H., Sasaki, K. (2014). Acceleration of Proliferative Response of Mouse Fibroblasts by Short-Time Pretreatment with Polyphenols. *Appl Biochem Biotechnol, 174*(6), 2223–2235.

Tsai, H-C., Li, Y-C., Young, T-H., Chen, M-H. (2015). Citrus polyphenol for oral wound healing in oral ulcers and periodontal diseases. *Journal of the Formosan Medical Association, S0929-6646*(15).

Torres-Giner, S., Gimenez, E., Lagaron, J. M. (2008). Characterization of the morphology and thermal properties of Zein Prolamine nanostructures obtained by electrospinning. *Food Hydrocolloids 22*(4), 601-614.

Tripoli, E., Giammanco, M., Tabacchi, G., Di Majo, D., Giammanco, S., La Guardia, M. (2005). The phenolic compounds of olive oil: structure, biological activity and beneficial effects on human health. *Nutr Res Rev, 18*(1), 98–112.

Um, I.C., Fang, D., Hsiao, B.S., Okamoto, A., Chu, B. (2004). Electro-Spinning and Electro-Blowing of Hyaluronic Acid. *Biomacromolecules, 5*(4), 1428-1436.

Wang, H., Shao, H., Hu, X. (2006). Structure of Silk Fibroin Fibers Made by an Electrospinning Process from a Silk Fibroin Aqueous Solution. *Journal of Applied Polymer Science, 101*(2), 961–968.

Verreck, G., Chun, I., Rosenblatt, J., Peeters, J., Dijck, A.V., Mensch, J., Noppe, M., Brewster, M.E. (2003). Incorporation of drugs in an amorphous state into electrospun nanofibers composed of a water-insoluble, nonbiodegradable polymer. *J Controlled Release, 92*(3), 349 –360.

Visioli, F., Bellosta, S., Galli, C. (1998). Oleuropein, the bitter principles of olives, enhances nitric oxide production by mouse macrophages. *Life Sci. 62*(6), 541-546.

Vogel, P., Machado, I., Garavaglia, J., Zani, V., Souza, D., Dal Bosco, S. (2014). Polyphenols benefits of olive leaf (Olea europaea L) to human health. *Nutr Hosp. 31*(3), 1427-1433.

Wellwood, C.R.L, Cole, R.A. (2004). Relevance of carnosic acid concentrations to the selection of rosemary, Rosmarinus officinalis (L.), accessions for optimization of antioxidant yield. *Journal of agricultural and food chemistry, 52*(20), 6101-6107.

Yao, C., Li, X., Song, T. (2007). Electrospinning and crosslinking of zein nanofiber mats. *Journal of Applied Polymer Science, 103*(1), 380-385.

Yeo, I-S., Oh, J-E., Jeong, L., Lee, T.S., Lee, S.J., Park, W.H., Min, B-Y. (2008). Collagen-Based Biomimetic Nanofibrous Scaffolds: Preparation and Characterization of Collagen/Silk Fibroin Bicomponent Nanofibrous Structures. *Biomacromolecules, 9*(4), 1106–1116.

Zhang, B., Luo, Y., Wang, Q. (2010). Development of Silver-Zein Composites as a Promising Antimicrobial Agent. *Biomacromolecules, 11*(9), 2366–2375.

Zhang, Q., Yan, S., Li, M. (2009). Silk Fibroin Based Porous Materials. *Materials, 2*(4), 2276-2295.

Zhang, Y, Lim, C.T., Ramakrishna, S., Huang, Z-M. (2005). Recent development of polymer nanofibers for biomedical and biotechnological applications. *Journal Of Materials Science: Materials in Medicine, 16*(10), 933– 946.

Zhong, S., Teo, W.E., Zhu, X., Beuerman, R., Ramakrishna, S., Yung, L.Y. (2005) Formation of collagen-glycosaminoglycan blended nanofibrous scaffolds and their biological properties. *Biomacromolecules, 6*(6), 2998-3004.

Zhong, S.P., Zhang, Y.Z., Lim, C.T. (2010). Tissue scaffolds for skin wound healing and dermal reconstruction. *WIREs Nanomed Nanobiotechnol, 2*(5), 510–525.

Ziech, D., Anestopoulos, I., Hanafi, R., Voulgaridou, G.P., Franco, R., Georgakilas, A.G., Pappa, A., Panayiotidis, M.I. (2012). Pleiotrophic effects of natural products in ROS-induced carcinogenesis: The role of plant-derived natural products in oral cancer chemoprevention. *Cancer Letters*, *327*(1-2), 16-25.

APPENDIX A

CALIBRATION CURVES OF SELECTED ACTIVE COMPOUNDS IN OLIVE LEAF EXTRACT

All standards were dissolved in deionized water and subjected to serial dilution to obtain a range of concentrations. Afterwards they were analyzed in HPLC elution program aforementioned in Materials and Methods section.

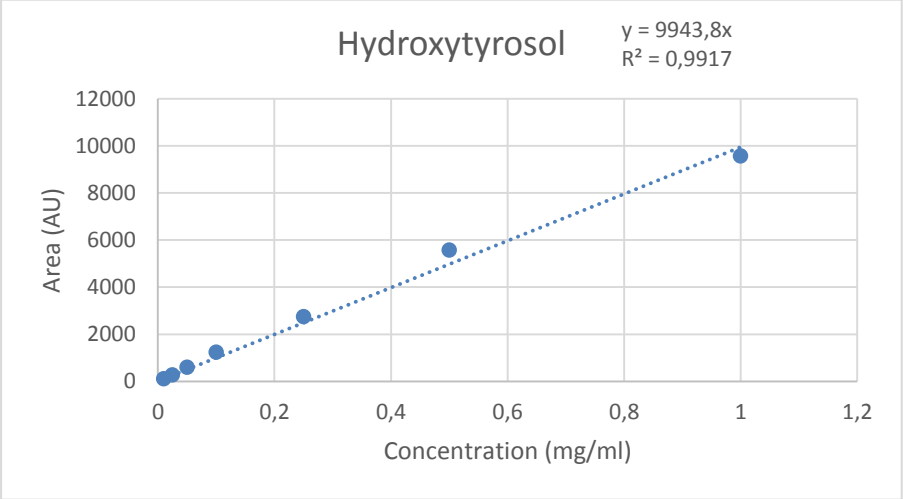

Figure A1. Hydroxytyrosol calibration curve

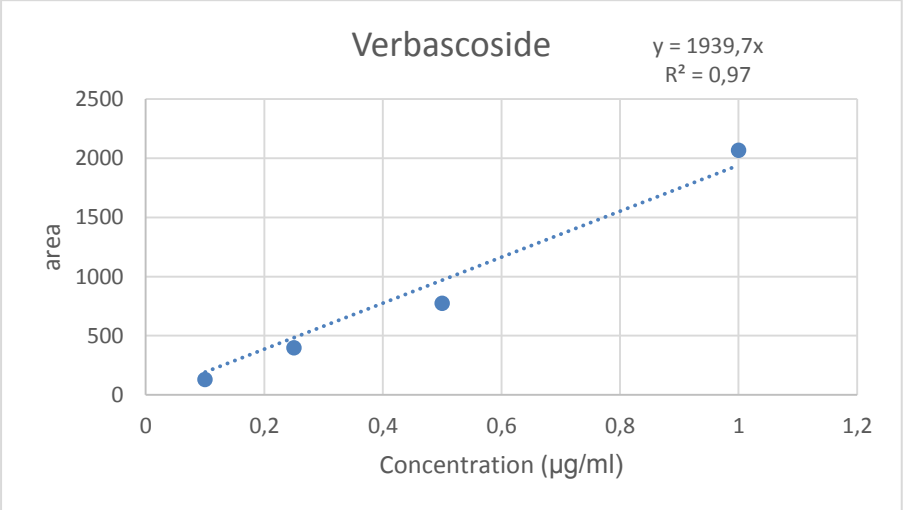

Figure A2. Verbascoside calibration curve

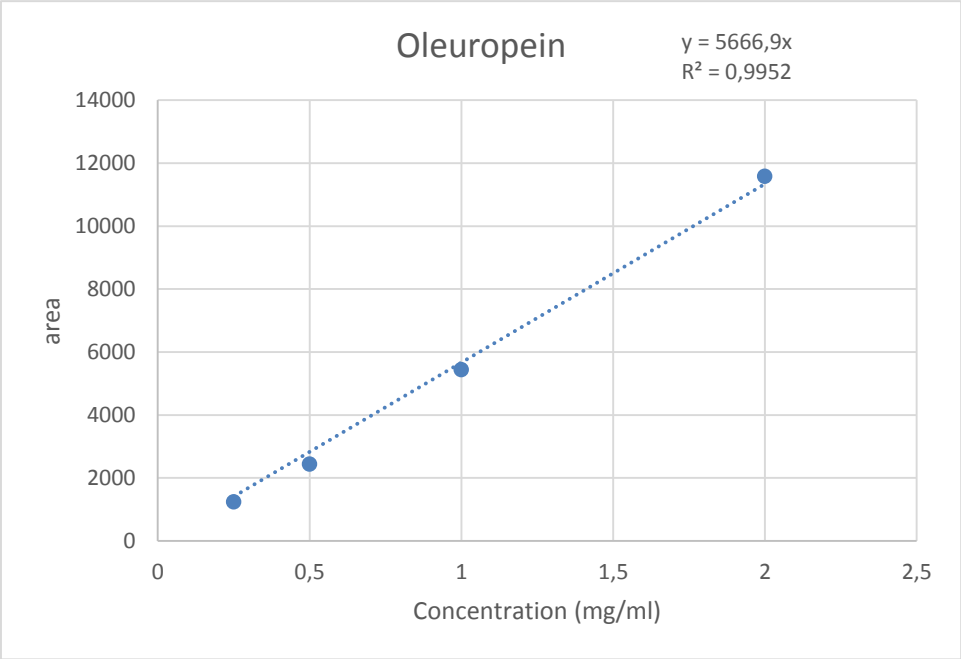

Figure A3. Oleuropein calibration curve

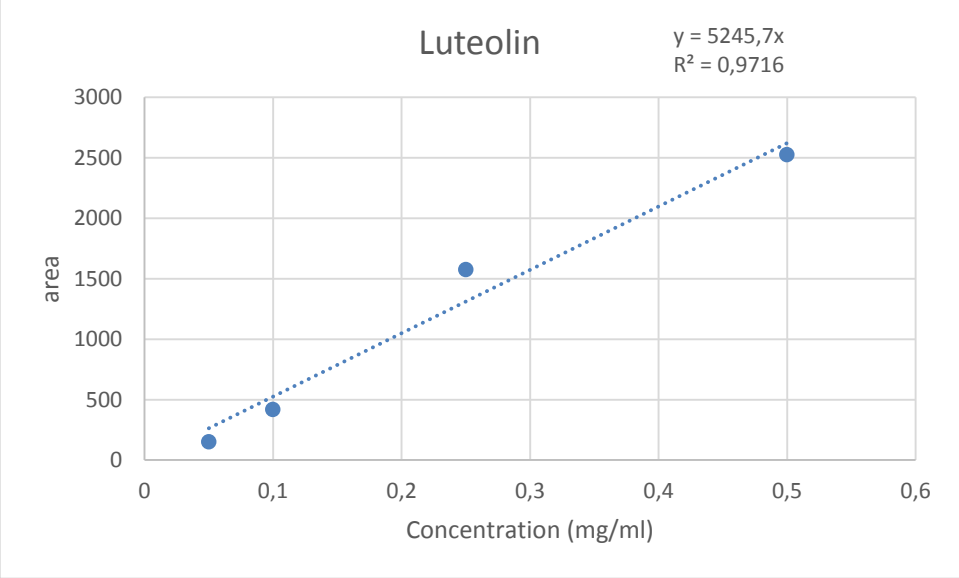

Figure A4. Luteolin calibration curve

APPENDIX B

CALIBRATION CURVE OF GALLIC ACID

Calibration curve of gallic acid standard

0.5 mg/ml stock standard of gallic acid was prepared by firstly dissolving 250 mg of dry gallic acid in 10 ml of ethanol and then diluting to 500 ml with distilled water. The solution were kept in the 4°C. Final concetrations for calibration curve of gallic acid were 0.001-0.002-0.004-0.006 and 0.01 mg/ml.

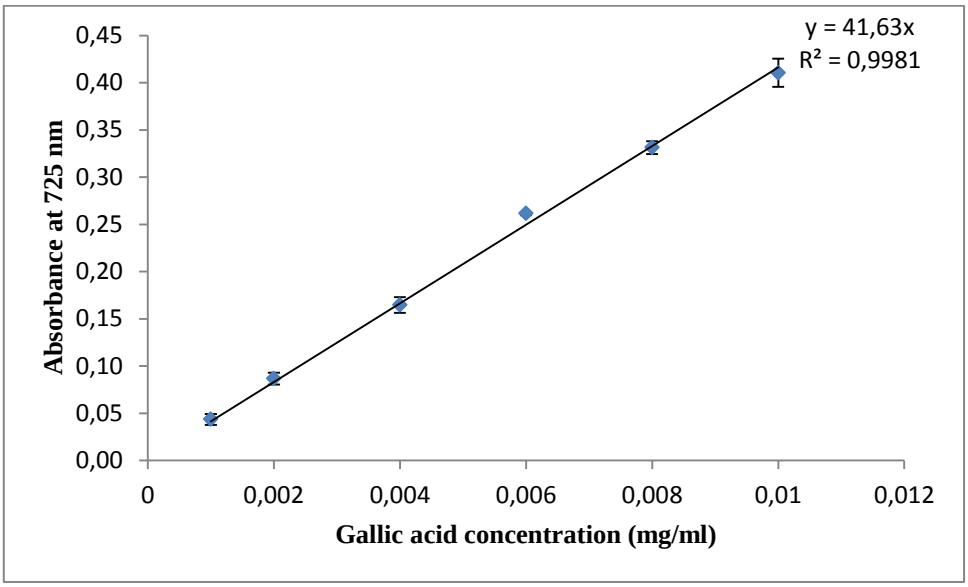

Figure B1. Gallic acid calibration curve

APPENDIX C

CALIBRATION CURVE OF TROLOX

Calibration curve of trolox standard

Scavenging activity of olive leaf extract and its fractions were determined by inhibition of ABTS radical cations, which can be observed as a decrease in the absorbance values at 734 nm in UV-Visible Spectrophotometer. Firstly, the absorbance of ABTS radical cation solutions was measured. It was adjusted to absorbance of 0.7 ± 0.02 by diluting with absolute ethanol. Afterwards 200 µl of ABTS solution was dispensed on 10 µl of samples. Samples were subjected to spectrophotometric measurement at 734 nm for 30 minutes, kinetic data were collected every 30 seconds. Inhibition percentage was calculated as follows;

$$\text{ABTS Inhibition (\%)} = (1-(A_f/A_0))*100$$

Inhibition percentages were calculated as Trolox Equivalent Antioxidant Capacity in µM by Trolox calibration curve given below.

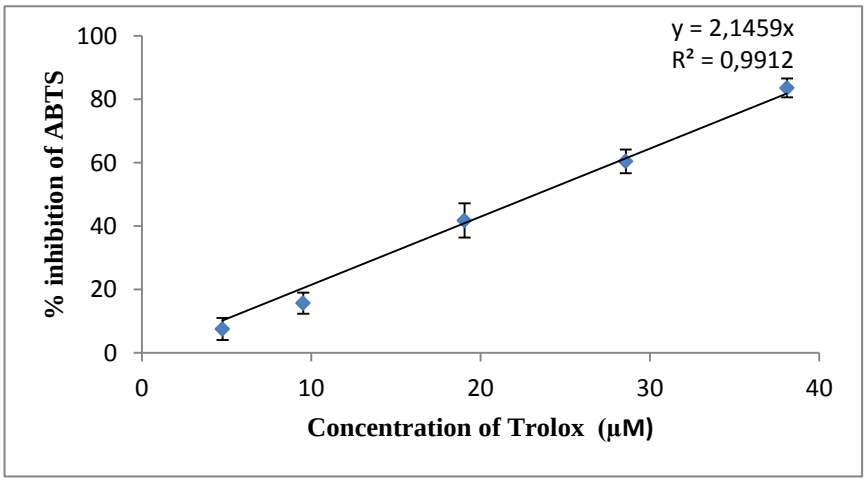

Figure C1. Trolox calibration curve

APPENDIX D

WOUND CLOSURE PERCENTAGES

Table D1. Diameters of wound area under oxidative stress generated by exogenous H_2O_2 (mm).

Day	1	3	5
H_2O_2 concentration(μM)			
1	4387.93	4281.14	3780.505
	4312.31	3771.175	3672.66
	4526.62	3953.485	3734.615
10	3744.225	3649.595	3427.065
	3879.21	3705.03	3552.68
	4397.375	4111.085	4015.33
50	3745.59	3274.645	3219.275
	4310.935	3972.355	3886.225
	4529.43	4147.54	3910
100	4366.52	3664.55	3562.135
	5017.88	N/A	N/A
	4700.725	N/A	N/A

Wound closure percentages were calculated by using the formula below

Wound closure percentage (%) = $((D_0-D_x)/D_0)*100$

D_0: diameter of wound on the first day of assay

D_x: diameter of wound on determined time points.

X denotes 1st, 3rd and 5th day of the assay in the calculations.

Diameter of the first day was measured as 5309.9 mm.

Wound closure percentage of the 1st day in the presence of 1 μM H_2O_2 can be calculated as,

((5309.9-4387.93)/5309.9)*100 = 17.36 %

Table D2. Wound closure percentages of under oxidative stress generated by exogenous H_2O_2 (%).

H_2O_2 concentration (μM)	Day 1	Day 3	Day 5
1	17.36±2.16	24.63±4.87	31.44±5.32
10	25.22±5.48	28.49±4.16	37.97±8.65
50	20.99±7.62	28.47±8.70	30.85±7.38
100	12.45±8.19	N/A	N/A

Table D3. Wound closure percentages under effect of OLE (%).

OLE concentration (μg/ml)	Day 1	Day 3	Day 5
0	28.33±6.15	41.13±2.71	90.53±13.40
1	31.7±10.46	45.6±8.83	100.00
10	28.93±1.90	39.67±6.54	100.00
50	26.2±3.84	43.12±6.27	73.54±6.81
250	12.96±3.25	14.43±2.77	N/A

APPENDIX E

WOUND SCRATCH ASSAY MICROGRAPHS

Table E1. Micrographs of wound scratch assay under different parameters
(cont. on next page)

	Days		
H_2O_2 1 µM	1	3	5
Fr 2 1 µg/ml			
Fr 2 10 µg/ml			
Fr 2 50 µg/ml			
Fr 4 1 µg/ml	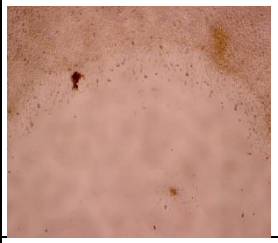		
Fr 4 10 µg/ml			

Table E1. (cont)

	Days		
H_2O_2 1 µM	1	3	5
Fr 4 50 µg/ml		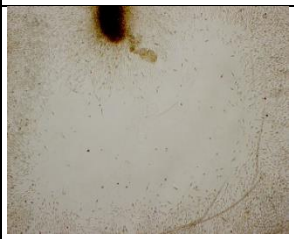	
Fr 5 1 µg/ml			
Fr 5 10 µg/ml			
Fr 5 50 µg/ml			
Fr 6 1 µg/ml			
Fr 6 10 µg/ml			

Table E1. (cont.)

	Days		
H_2O_2 1 µM	1	3	5
Fr6 50 µg/ml	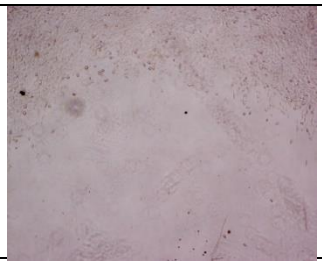	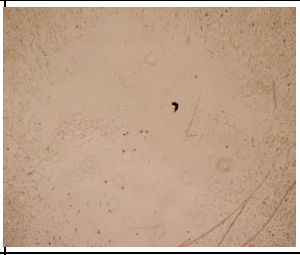	
H_2O_2 10 µM			
Fr 2 1 µg/ml	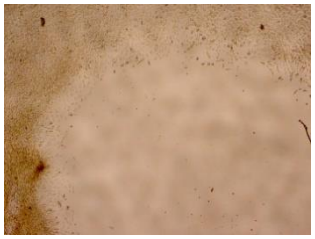		
Fr 2 10 µg/ml		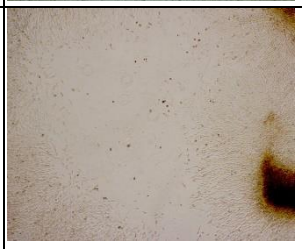	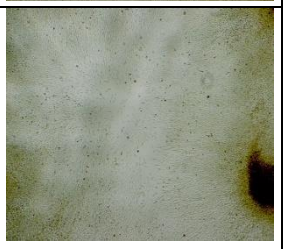
Fr 2 50 µg/ml			
Fr 4 1 µg/ml	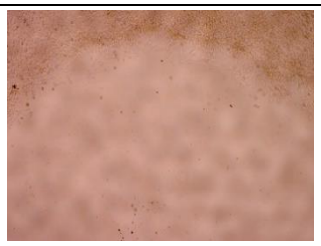		
Fr 4 10 µg/ml		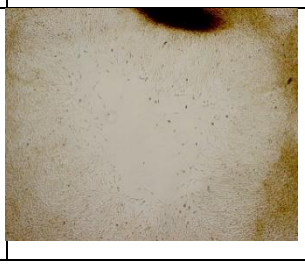	

Table E1. (cont.)

	Days		
H_2O_2 10 µM	1	3	5
Fr 6 50 µg/ml			
Fr 5 1 µg/ml			
Fr 5 10 µg/ml	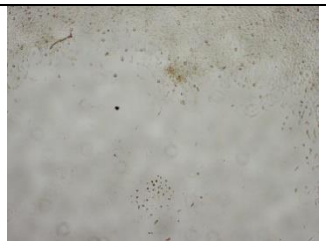	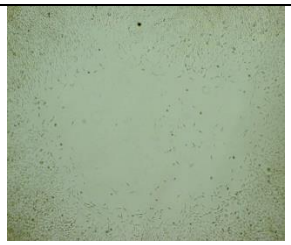	
Fr 5 50 µg/ml			
Fr 6 1 µg/ml	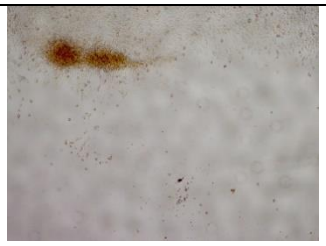	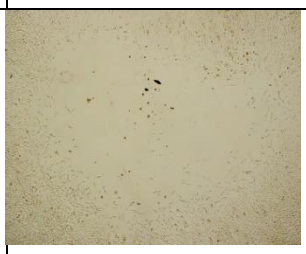	
Fr 6 10 µg/ml			

Table E1. (cont.)

	Days		
H2O2 50 µM	1	3	5
Fr 2 1 µg/ml			
Fr 2 10 µg/ml	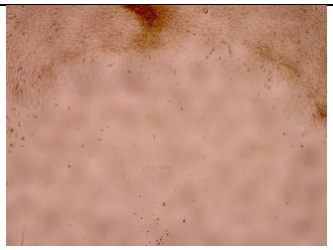		
Fr 2 50 µg/ml	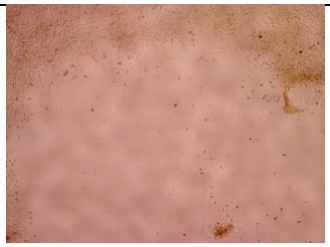	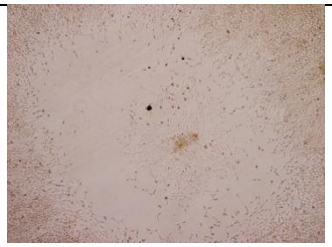	
Fr 4 1 µg/ml			
Fr 4 10 µg/ml		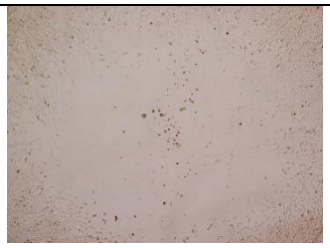	
Fr 4 50 µg/ml			

Table E1. (cont.)

	Days		
H2O2 50 µM	1	3	5
Fr 5 1 µg/ml		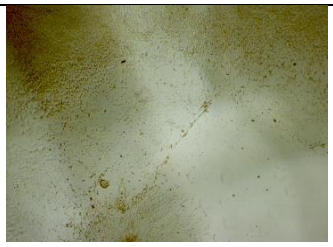	
Fr 5 10 µg/ml		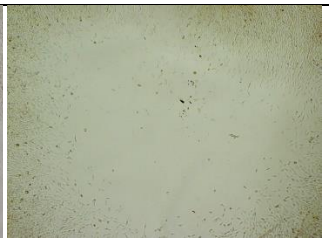	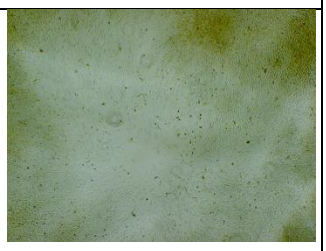
Fr 5 50 µg/ml		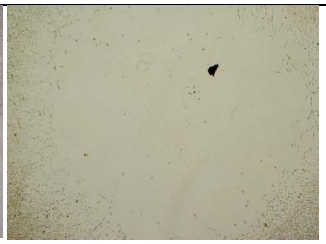	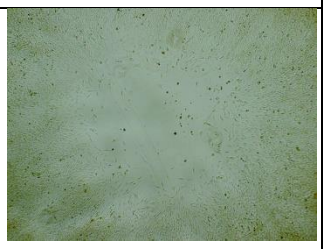
Fr 6 1 µg/ml	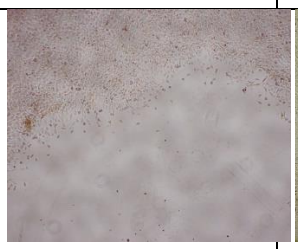		
Fr 6 10 µg/ml	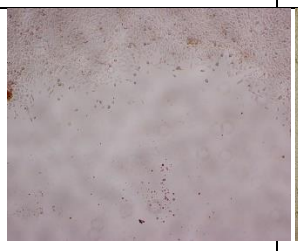		
Fr 6 50 µg/ml		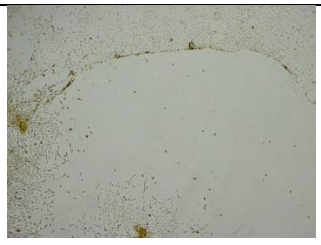	

Table E1. (cont.)

	Days		
H2O2 100 µM	1	3	5
Fr 2 1 µg/ml		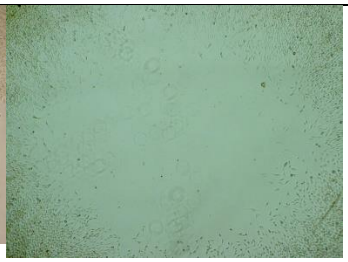	
Fr 2 10 µg/ml	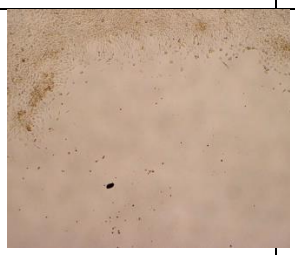		
Fr 2 50 µg/ml			
Fr 4 1 µg/ml			
Fr 4 10 µg/ml	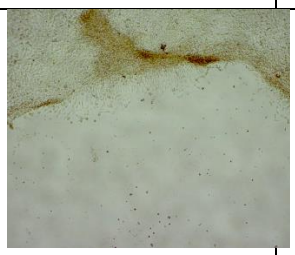		
Fr 4 50 µg/ml	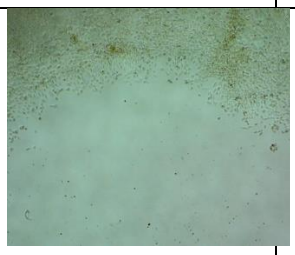		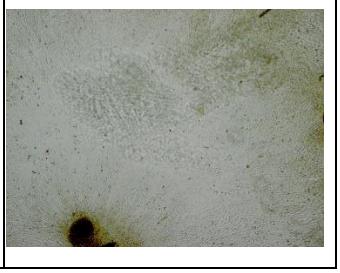

Table E1. (cont.)

	Days		
H2O2 100 µM	1	3	5
Fr 5 1 µg/ml		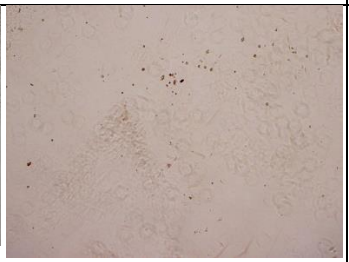	
Fr 5 10 µg/ml		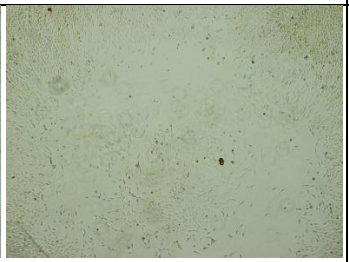	
Fr 5 50 µg/ml			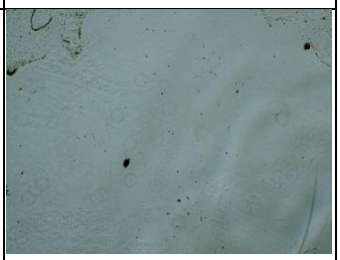
Fr 6 1 µg/ml	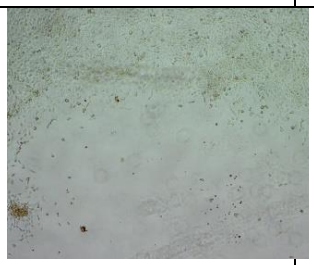	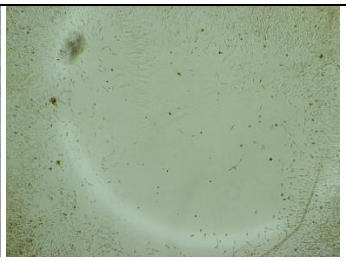	
Fr 6 10 µg/ml			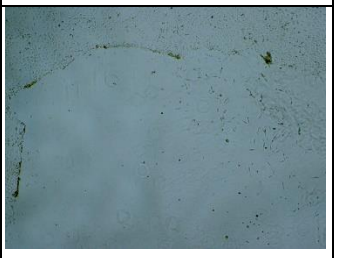

APPENDIX F

WOUND SCRATCH CONFOCAL IMAGES

Table F1. Wound scratch confocal images (cont. on next page)

	Days	
H2O2 100 µM	3	5
Fr 2 1 µg/ml	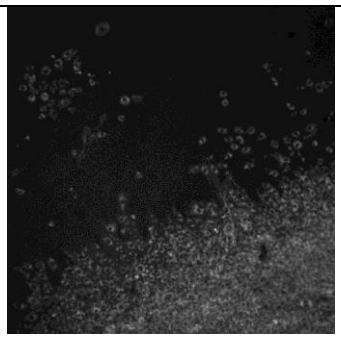	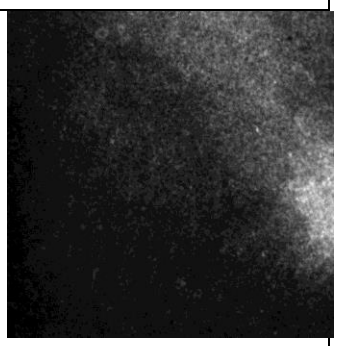
Fr 2 50 µg/ml	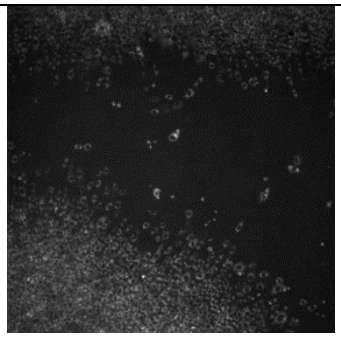	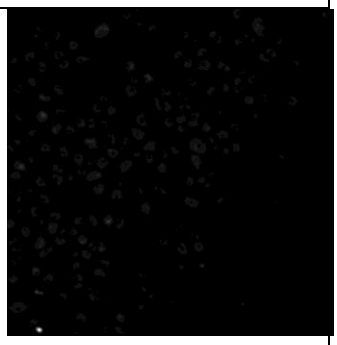
Fr 4 1 µg/ml	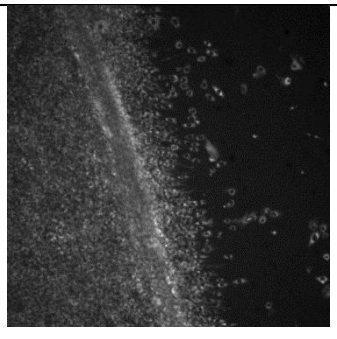	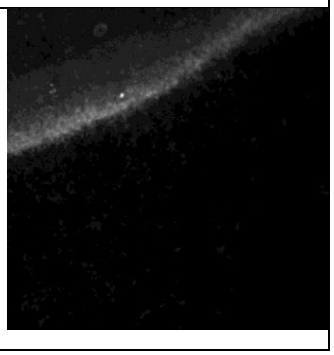

Table F1. (cont.)

	Days	
H2O2 100 µM	3	5
Fr4 50 µg/ml	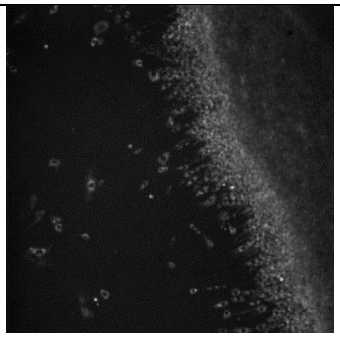	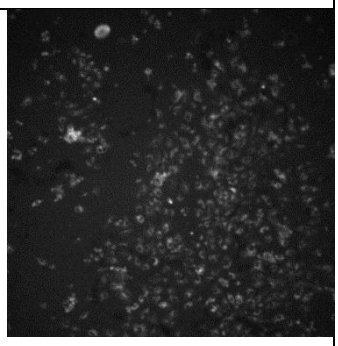
Fr5 1 µg/ml	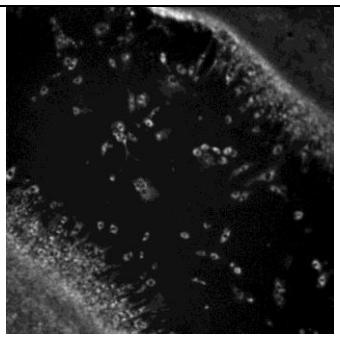	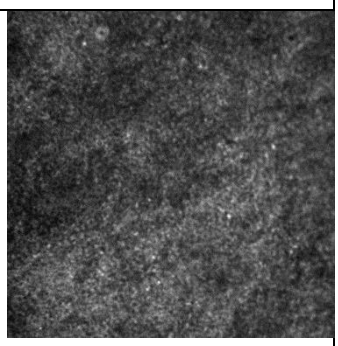
Fr5 50 µg/ml	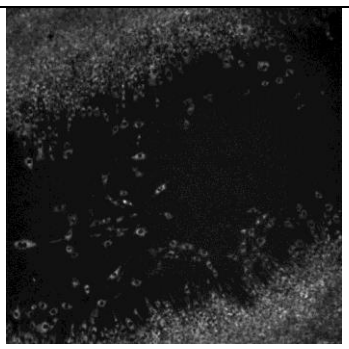	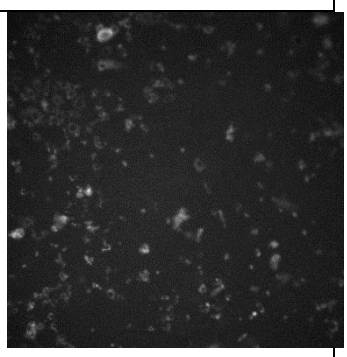
Fr6 1 µg/ml	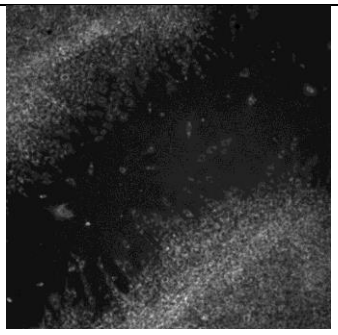	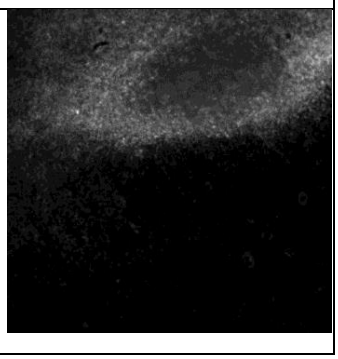

Table F1. (cont.)

	Days	
H2O2 100 µM	3	5
Fr6 50 µg/ml	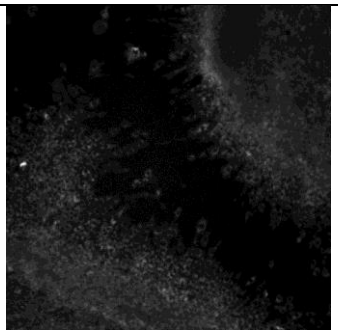	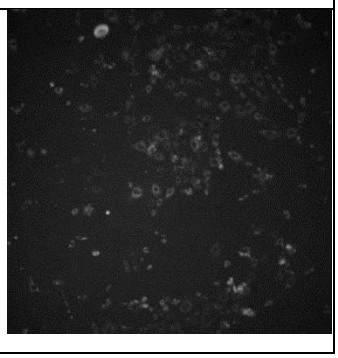

CURRICULUM VITAE

GENERAL INFORMATION
Name: İpek Erdoğan
Telephone: +90 5435412177
E-mail: epackerdogan@gmail.com

EDUCATION:
PhD in Bioengineering 2009-July 2015
Izmir Institute of Technology, Izmir, Turkey
M.S. in Biotechnology 2005-2009
Izmir Institute of Technology, Izmir, Turkey
B.S. in Bioengineering 2001-2005
Ege University, İzmir, Turkey

Research experience:

PhD. Advisor: Oguz Bayraktar Ph.D. Izmir Institute of Technology, Izmir, Turkey
Project Title: Preparation and Characterization of Wound Dressing Contact Layer

M.Sci. Advisor: Bünyamin Akgül Ph.D. Izmir Institute of Technology, Izmir, Turkey
Project Title: Identification of miRNAs Involved in Camptothecin-Induced Apoptosis in Jurkat T Cell Line

Publications:

- Uslu ME, Ceylan C, Bayraktar O. 2014. Kinetic and structural characterization of interaction between trypsin and *Equisetum arvense* extract. *Turkish Journal of Biochemistry* 39(4):463–471
- Erdogan I, Demir M, Bayraktar O. 2015. Electrospun Zein Fibers Using Olive Leaf Extract as a Crosslinking Agent. Journal of Applied Polymer Sciences 132(4)..

Proceedings

- Erdogan I, Sunguc C, Uslu ME, Bayraktar O. 2013. Investigation of anti-tumoral activity of Cistus creticus extract against PC-3 cell line. *European Journal of Pharmaceutical Sciences* 50, 29.
- Sunguc C, Erdogan I, Uslu ME, Bayraktar O. 2013. In vitro antitumor activity of Sarcopoterium spinosum leaf extract with bioactive natural compounds. *European Journal of Pharmaceutical Sciences* 50 (supplement 1), 4.
- Uslu ME, Erdogan I, Bayraktar O. 2013. Incorporation of *Equisetum arvense* extract into silk fibroin–hyaluronic acid sponge matrices for wound dressing applications. *New Biotechnology* 29: 117

Oral presentations:

- Uslu ME, Gonzales Gil A, Erdogan I, Bayraktar O. 2-5 September 2014. Fenolik Bileşiklerin İpek Fibroin Kullanılarak Köpük Fraksiyonlama Yöntemi ile Ayrılması. 11. Ulusal Kimya Müh. Kongresi
- Uslu ME, Erdogan I, Bayraktar O. 25-26 September 2014. Preparation and Characterization of Silk Fibroin-Chitosan- Clinoptilolite Composite Films with Olive Leaf Extract for Wound Dressing Applications. 2nd International Congress On Healthcare And Medical Textiles.
- Erdogan I, Uslu ME, Bayraktar O. 27-31 August 2014. "Effects of Some Selected Plant Extracts on 3T3 Fibroblast Cell Line Wound Model. 6th International Conference on Oxidative Stress in Skin Biology and Medicine.
- Uslu ME, Erdogan I, Bayraktar O. 27-31 August 2014. Effect Of Phenolics On Blood Coagulation. 6th International Conference on Oxidative Stress in Skin Biology and Medicine.
- Uslu ME, Erdogan I, Bayraktar O. 7-9 November 2013. Development of Active Carrier Systems for Lycopene. International Cleaning and Personal Care Products and Production Technologies Symposium and Exhibition-İzmir.
- Erdogan I, Uslu ME, Karagönlü S, Bayraktar O. 7-9 November 2013. Microencapsulation of Ozonated Olive Oil for Cosmetic Applications. International Cleaning and Personal Care Products and Production Technologies Symposium and Exhibition-İzmir.
- Sunguc C, Erdogan I, Uslu ME, Bayraktar O. 26-28 September 2013. In Vitro Antitumour Activity of Sarcopoterium Spinosum Leaf Extract with Bioactive Natural Compounds. 5th BBBB International Conference-Athens, Greece
- Sunguc C, Tutuncu C, Erdogan I, Uslu ME, Bayraktar O. 16-19 September 2013. Encapsulation of Trans-Resveratrol Using Electrospray Method for Enhanced Stability. Advanced Materials World Congress- Çeşme, Izmir
- Erdogan I, Balcı B, Sunguc C, Uslu ME, Bayraktar O. 9-11 May 2013. Olive Leaf Extract and Clinoptilolite Loaded Silk Fibroin Chitosan Blend Films as a Potential Coating on Packaging Materials. 7th International Packaging Congress-Izmir.